Structural and Functional Studies of Virulence Factor Homologs EspG and VirA

By

Katherine L. Germane

Dissertation

Submitted to the Faculty of the

Graduate School of Vanderbilt University

in partial fulfillment of the requirements

for the degree of

DOCTOR OF PHILOSOPHY

in

Pathology, Microbiology and Immunology

December, 2011

Nashville, Tennessee

Approved:

Professor Earl Ruley

Professor Benjamin Spiller

Professor Eric Skaar

Professor Timothy Cover

Professor Ryoma Ohi

“A tutte le dame….To all the dames.” - Dominic Germane

ACKNOWLEDGEMENTS

First and for most, I would like to thank my advisor Dr. Benjamin Spiller. I feel honored to be able to have worked with him. He is one of the most intelligent people I have had the privilege to meet. His enthusiasm and biting sarcasm towards science made every day interesting. He was always open to whatever project or experiment I was interested in attempting. Whenever I was stumped he was always available with suggestions for a new direction. During the two times I cam back with a google search and thought I was about to get scooped he took charged and made sure I was able to get my research published. I can say, with out a doubt, that I would not have wanted any other advisor or lab to work with, nor would I have changed my graduate experience for the world and he is the one to thank. I was also fortunate to work with Borden Lacy's lab and gain the support and guidance of Borden who was a calming influence in a wild storm.

As to my lab, they are my second family and great friends. I could not have asked for a better group of women. We have laughed, we have cried and we have floated down a river together. Lisa, with her beautiful singing voice and caring and supportive attitude, is our rock. I will miss her infectious laughter, especially when it comes out of nowhere in the middle of a silent lab, and her wonderful baked goods (the mixer was one of the best investments I have ever made). Whenever I was in a jam she was always there to help me. Michele, thanks for joining the lab, no seriously, thanks. Also, I will miss your mother's cookie trays and if I dwell on this fact I will start crying from withdrawal. Tara, my climbing buddy and pudding

partner in crime, your sarcasm and biting remarks made each and everyone of my days (especially the shitty glares). However, you still haven't made me Indian food and you know I never forget when it comes to food. As to Katie Winarski or K-2 or New Katie, my replacement and evil blonde twin, you suck but I will forgive you for your hostile take over and all the nail polish colors I was forced to witness. Last but not least, Oswald, you are a prickly thing and a bit quiet but the best friend a girl could ask for.

I would like to thank my committee- Dr. Timothy Cover, Dr. Ryoma Ohi, Dr. Earl Ruley and Dr. Eric Skaar. I appreciate their time, support and constructive criticism as I progressed through my graduate career. I would especially like to thank my chair Earl Ruley who never stopped questioning and always provided a useful philosophical approach to my work. I have received an amazing training experience with the Microbiology & Immunology Department and the Molecular Biophysics Training Program. I was fortunate to have the excellent support of both programs, faculty and personnel.

I owe my friends for my sanity. Thuy, Jess, Amy, Swathi, Lynn and Jessie are my angels. The laughter and support they have provided is un-parallel. I could never get through a conversation with any of them with out smiling. I may not have been able to see them often, but they were always there for me. I love you guys.

Lastly, I am in debt to my family for everything they have provided me. My family has always been behind me in every endeavor I have under-took. I can safely say I would not have made it through graduate school with out them. My mother listened to my histrionics and always did her best to placate me by telling me

random hilarious stories. My father would always tell me that “I could still go to medical school/dental school”, which served as a poke for me to get back to work so I would not have to suffer through more years of school. I also appreciate my sister for never asking when I would be finished and what I wanted to do in the future, which was refreshing. As to the rest of my family, past and present, their influence and support has meant the world to me. They have provided me with experiences and opportunities to explore life and the world. I will be forever grateful.

These studies were supported by the DDRC (Grant DK058404) and NCRR (ULIRR024975). I was supported by the Molecular Biophysics training program (T32 GM08320) and provided with a travel grant from the graduate school to attend the Gordon Research Conference on “Microbial Adhesion & Signal Transduction”.

TABLE OF CONTENTS

LIST OF TABLES

LIST OF FIGURES

LIST OF ABBREVIATIONS

ADP	adenosine diphosphate
ADPRT	adenosine diposphate transferase
AJ	adherens junction
Arf	ADP-ribosylation factor
ATP	adenosine triphosphate
Bp	base pair
Cif	cell cycle inhibition virulence factors
Cfu	colony forming unit
CT	C-terminus
DMSO	dimethyl sulfoxide
DTT	dithiothreitol
EGTA	ethylene glycol tetraacetic acid
EHEC	enterohemorrhagic *Escherichia coli*
EPEC	enteropathogenic *Escherichia coli*
FBS	fetal bovine serum
FERM	F for 4.1 protein, E for ezrin, R for radixin and M for moesin domain
GAP	GTPase activating protein
GBD	GTPase binding domain
GDI	GDP-dissociation inhibitor
GEF	guanine nucleotide exchange factor

GMPCPP	moderately promotive, completely suppresses dynamic instability
GST	glutathione s-transferase
GTPase	guanosine triphosphate hydrolase enzyme
HM	host membrane
IM	inner membrane
kDa	kilodalton
LEE	Locus of Enterocyte Effacement plasmid
LPS	lipopolysaccharide
MEM	modified Eagles medium
MIRAS	Multiple Isomorphous Replacement with Anomalous Scattering
Natpro	native promoter
NE-CAT	northeastern collaborative access team
NT	N-terminus
OM	outer membrane
PAMPS	pathogen-associated molecular patterns
PBD	p21 binding domain
PDB	protein data base
PEG	polyethylene glycol
Pen/strep	penicillin/streptomycin
PGN	peptidoglycan
PIP_2	Phosphatidylinositol 4,5-bisphosphate

PMSF	phenylmethylsulfonyl fluoride
PMN	polymorphonuclear leukocytes
Rms	root mean square
Se-Met	selenomethionine
Spp	species
T3SS	type three-secretion system
T3SA	type three-secretion apparatus
TLS	translation/libration/screw
WT	wild type

CHAPTER I

INTRODUCTION

Bacterial Type III Secretion Virulence Factors

In order to persist and spread within the host, many animal gram-negative bacterial pathogens have evolved to effect a well-orchestrated attack on host cell signaling pathways in order to persist and spread within the host. The bacteria use these pathways to block or hide from immune responses by directly altering immune response pathways or other signaling pathways to colonize within or on the cell. In order to control the spatial and temporal dynamics of such pathways, various species of bacteria secrete virulence factors, via a type three-secretion system (T3SS), directly into the host cell (Table 1, Figure 1) [1-5]. These factors mimic or alter host cell proteins in order to redirect signaling for the bacterium's benefit [1, 3, 6].

Colonization and spread can be viewed as discrete, required steps in bacterial pathogenesis that require different bacterial effectors. Colonization allows the bacteria to establish a niche, usually within a tissue that comes into contact with the external environment. Even within this niche, bacteria must survive host efforts to clear the infection, both clearance by polymorphonuclear leukocytes (PMN) before bacterial attachment to the host cell, and subsequent host efforts to clear the infection. Once the bacteria reach the host cell, they either maintain their

environment at the cell surface or induce cell engulfment to replicate and maintain a niche inside the host cell. Host cell entry occurs when the bacterium induces a dynamic cytoskeleton rearrangement that results in the endocytosis of the bacterium. The bacteria can live and replicate inside the endosome, retrieving nutrients from the host, or be released, replicate in the cytoplasm, and move from cell to cell using actin based motility to spread. Both attached and intracellular bacteria inhibit cytotoxicity, autophagy, and cytokine release to maintain their environment and prevent removal by host cell death and a subsequent innate immune response [4, 5, 7]. To disseminate within the host and infect new tissues, the bacteria must get past host cell barriers. Thus, at some point during infection, most species of bacteria induce cytotoxicity or tight junction disruption to cause tissue damage, which results in inflammation [4]. The resulting damage allows for dissemination to new tissues by providing space between host cells so the bacteria can pass the barrier. Each of these steps of pathogenesis requires specific subsets of virulence factors, some of which have multiple functions for both steps of pathogenesis, to interact with host proteins to divert pathways to help the bacteria maintain their niche and spread.

Bacterial Species	Disease	Characterized Effectors
Pseudomonas aeruginosa	Opportunist pathogenic; can cause pneumonia	ExoU, ExoY, ExoS, ExoT
EPEC	Diarrhea (EPEC) or hemorrhagic colitis (EHEC; Cattle commensal (EHEC)	Tir, Map, EspF, EspB, EspZ, EspH, EspG, NleA, NleB, NleC, NleD, NleE, NleF, NleG, NleH, NleK, NleL, EspJ, EspL, EspM, EspFu, Ibe, cif
Salmonella enterica serovars	Gastroenteritis; typhoid fever	AvrA, SipA, SipB, SipC, SopA, SopB, SopE, SopE2, SptP, SlrP, SopD, SspH1, SteA, SteB, PipB, SifA, SpiC, SseF, SseG, SseL, SseJ, SspH, SteC, SpvB, SpvC
Shigella spp.	Bacillary dysentery; shigellosis	IpaA, IpaB, IpaC, IpaD, IpaJ, IpgD, IpgB, IcsB, OspC, OspZ, OspF, VirA, OspE, OspG, IpaH family
Y*ersinia* spp.	Bubonic plague (pestis); Gastrointestinal disease (enterocolitica)	YopE, YopH, YopP/J, YopM, YopT, YpkA/YopO
Yersinia enterolytica biovar 1B	Severe gastrointestinal disease	YspP, YspF, Cif
Photorhabdus spp.	Opportunistic pathogen (asymbiotica); insect pathogen (luminescens)	LopT
Chlamydia spp.	Obligate intracellular parasites, sexually transmitted disease; can cause blindness	CADD, CT847, tarp, IncA, IncG, CT229, Cpn0585
Burkholderia spp.	Melioidosis (B. pseudomallei); glanders (B. mallei)	CHBP, BopE
Vibrio spp.	Gastroenteritis, wound infections (parahaemolyticus); secretory diarrhea (cholera)	VopL, VopA, VPA450, VopT, VopF, VopS, VopQ
Bordetella spp.	Whooping cough	BopC/BteA, BopN
Aeromonas spp.	Opportunistic pathogen; fish/humans	AexT AexU

Table 1: Gram-negative bacteria target a number of different tissues, which result in a varying set of disease states. They are able to effect these diseases by secreting type three secretion effectors, which target different host cell processes. Here the best-characterized effectors are listed, which seem to have overlapping functions important for bacterial infection. Table adapted from Dean et al. 2011 [1].

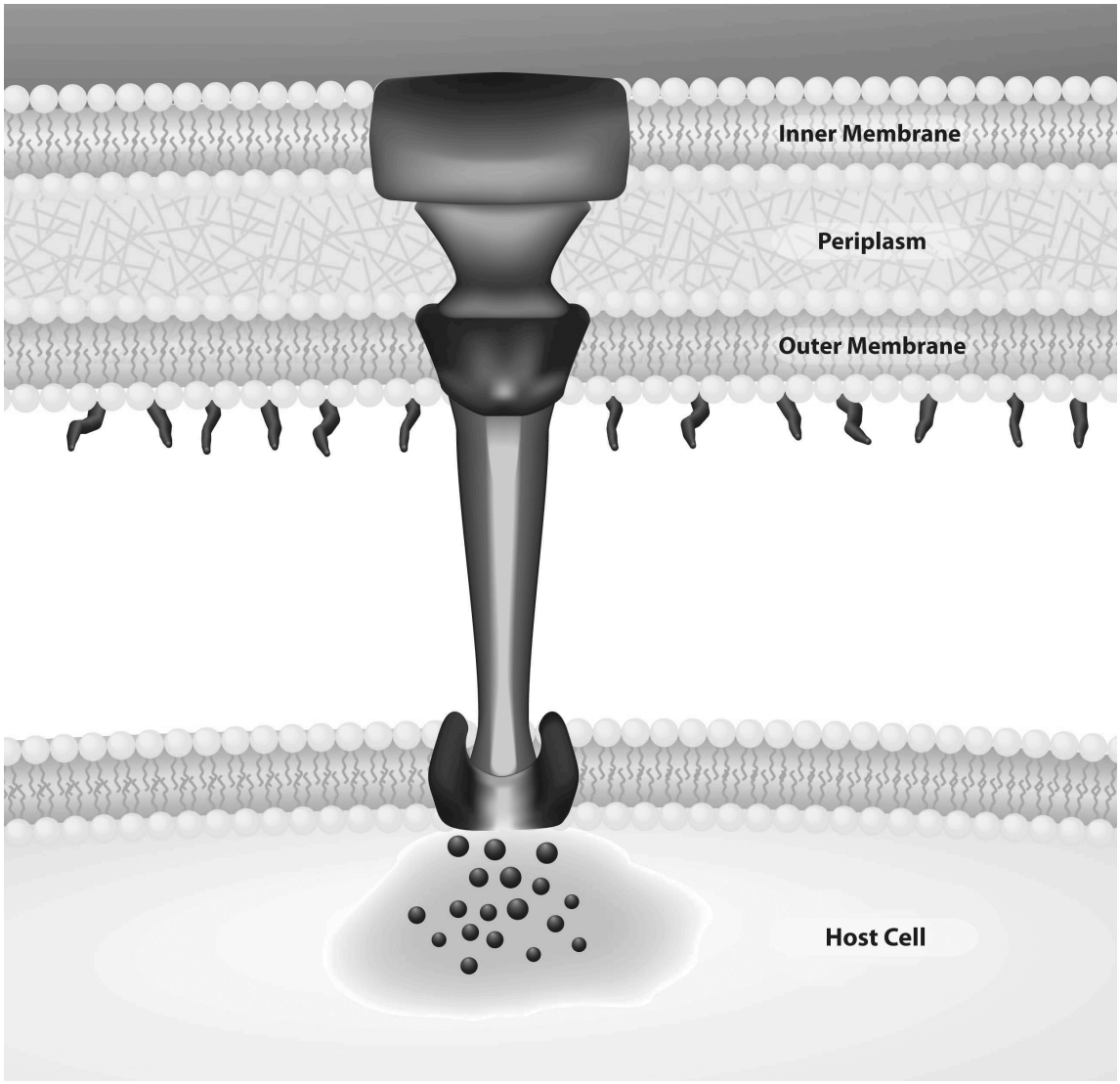

Figure 1: Type III Secretion Systems are used to secrete virulence effectors into host cell. Gram-negative bacteria require a means by which to secrete effectors across the outer and inner bacterial plasma membranes, peptidoglycan wall and host membrane. The type three secretion apparatus is a needle that forms a pore in the host membrane by which virulence effectors can be directly released into the host cell cytoplasm. The type three secretion apparatus (T3SA) is a highly regulated specific secretion apparatus, which uses ATP to translocate the effectors. The effectors have an unknown N-terminal secretion sequence which may or may not require a chaperone for T3SA recognition. Adapted from Coburn et al. by Dan Dorset [4].

Colonization

Macrophage Evasion

Macrophages work to destroy bacteria and other foreign debris in the extracellular milieu and recruit other immune cells to the site of infection. The macrophages engulf the foreign matter into a phagosome. The phagosome then merges with a lysosome, where enzymes and peroxides destroy the foreign matter. Before host cell colonization and during dissemination to new tissues, bacteria in the extracellular milieu are susceptible to macrophage attack [8]. As shown in table 2, many virulence effectors can prevent phagocytosis by the macrophages. These effectors tend to have multiple functions and inhibit phagocytosis by affecting the cytoskeleton of the macrophage. Several of these effectors are GTPase regulators. YpkA/YopO act as a GDP disassociation inhibitor (GDI) and EspH acts as a guanine exchange factor (GEF) [9, 10]. In addition, YopH acts as a tyrosine phosphatase of Fyb, which alters actins during phagocytosis [11]. ExoU acts as a phospholipase to lyse the phagosome and prevents caspase 1 cytokine production [12]. *Salmonella* and *Shigella* prevent macrophage attack by inducing apoptosis, which releases the bacteria back into the extracellular matrix. Their virulence effectors, IpaB and SipB, bind and activate caspase-1, which in turn induces cytokine production and recruitment of polymorphonuclear leukocytes (PMN) [13, 14]. The PMNs make the epithelial cell lining leaky and thus allow further dissemination of the bacteria [15-17]. At this point the bacteria are available to bind and colonize the host non-immune cells.

Effector	Target/ mechanism	Function	Bacteria	
ExoU	Phospholipase A2 of unknown targets	Possible phagosome lysis or cell lysis tissue damage for infection; kills inflammatory cells; Inhibits caspase 1 cytokine production	*Pseudomonas aeruginosa*	[12]
YpkA/ YopO	Serine/threonine kinase of Gαq, Rac GDI, binds monomeric actin	Blocks phagocytosis; induces cytotoxicity	*Yersinia* spp.	[9, 10]
YopH	Tyrosine phosphatase of Fyb and p130Cas	Inhibits phagocytosis of macrophages and neutrophils; disrupts tight junctions	*Yersinia* spp.	[11]
SipB	Binds and activates caspase-1	Induce macrophage apoptosis	*Salmonella enterica*	[14]
IpaB	Caspase 1 , CD44 and cholesterol	Phagosome escape and macrophage apoptosis	*Shigella* spp.	[13]
EspZ	Targets CD98	Inhibits cytotoxicity and inhibit phagocytosis	EPEC/EHEC	[18]
EspH	DH-PH RhoGEFs	Blocks phagocytosis and promotes actin remodeling and pedestal formation	EPEC/EHEC	[19, 20]
LopT	Modifies Rho GTPases	Prevents phagocytosis by macrophages	*Photorhabdus* spp	[21]

Table 2: Virulence factors important for macrophage evasion.

Pedestal Formation and Cell Entry

Once the bacterium avoids macrophage removal, it can either colonize the cell surface or inside the cell. EPEC binds to the cell surface and forms a pedestal out of the plasma membrane of microvilli. *Shigella, Salmonella, Burkholderia, Chlamydia* and *Aeromonas* are intracellular bacteria and require the host cell to endocytose the bacterium [4]. Endocytosis and pedestal formation require a localized cytoskeleton rearrangement at the site of bacterial attachment, which is controlled by virulence factors [16, 22, 23]. Virulence factors can control the cytoskeleton through the regulation of small GTPases, actin and focal adhesion proteins [24]. Activation of the GTPases can induce fillipodia, lamelapodia, actin stress fiber formation, cell migration and cell rounding [25, 26]. Common functions of virulence factors are mimicking or binding GAPs and GEFs. GAP and GEF mimics or regulators are the most common GTPase regulating virulence effectors. Host GAP proteins mediate the inactivation of GTPases by binding the GTPase and inducing the hydrolysis of GTP to GDP. GEF proteins reverse this process to activate the GTPase. Only active GTPases can induce a signal cascade and actin rearrangement. Ibe acts as a GAP to promote pedestal formation by EPEC during infection [27]. SopE1/2, IpaA, IpgB, tarp and BopE act as Rho GEFs to induce actin stress fiber formation and membrane ruffling for bacterial host cell entry for intracellular bacteria [28-35]; while MAP, EspH and EspM, EPEC GEF effectors, are involved in pedestal formation [19, 28, 36-38].

While GTPase regulation is the major target for actin rearrangement for entry and pedestal formation, other effectors have been found to regulate actin dynamics either directly or through host proteins. This group of effectors, found in *Table 3*, have a much more diverse set of targets but they all are involved in regulation of actin in some manner. They can be generally grouped into those proteins that promote actin polymerization, reorganization of actin at the host cell membrane and actin destruction. A few virulence proteins can directly nucleate and induce polymerization, SipA, SipC and IpaC, while EspFu acts through N-WASP to induce actin stress fiber formation at the site of T3S [39-45]. The effectors also directly act on focal adhesion proteins- vinculin, filamin, actinin, β-catenin, and talin- to localize actin bundles to specific areas of the cell membrane for host cell entry, pedestal formation and cell-to-cell spread [31, 32, 39, 40, 45-48]. The effects of these proteins, in a concerted effort with GTPase regulators, allow for a fine tuned approach to induce membrane rearrangement at a specific site for cell entry and pedestal formation.

Effector	target/mechanism	Function	Bacteria	
Map	Binds EBP50 (NHERF1), NHERF2,and acts as a GEF for Cdc42	Induces filopodia formation, mitochondrial disruption, SGLT-1 inactivation, TJ disruption	EPEC/EHEC	[28, 36, 37]
EspH	DH-PH RhoGEFs activity	Blocks phagocytosis and promotes actin remodeling and pedestal formation	EPEC/EHEC	[19, 20]
EspM	RhoAGEF activity	Induces stress fiber formation	EPEC/EHEC	[38]
Ibe	IQGAP1 activity	Pedestal formation	EPEC/EHEC	[27]
SopE	Acts as a GEF for Cdc42 and Rac1	Membrane ruffling, cell entry	*Salmonella enterica*	[29, 30]
SopE2	Acts as a GEF for Cdc42 and Rac1	Membrane ruffling, cell entry	*Salmonella enterica*	[29, 30]
IpaA	Vinculin , Rho signaling β1-integrins	Activates vinculin, actin rearrangement for invasion	*Shigella* spp.	[31, 32]
IpgB	RhoGEF binds rho ligands	Membrane ruffling, filipodia and actin stress fiber formation	*Shigella* spp.	[28]
tarp	Binds GEFs	Actin remodeling promotes cell entry	*Chlamydia* spp.	[33]
BopE	GEF for Cdc42 and Rac1	Facilitates entry	*Burkholderia* spp.	[34, 35]
Tir	14-3-3tau, α-actinin, cortactin, CK18, IQGAP1, IRTKS, IRSp53, Nck, PI3K, Talin, Vinculin	Adhesion of bacteria and actin polymerization	EPEC/EHEC	[46-52]
EspG	ARF6, PAK1	cytoskeleton regulation for pedestal formation	EPEC/EHEC	[53, 54]
EspL	annexin 2	enhances actin bundling	EPEC/EHEC	[55]
EspO	Integrin-linked kinase	unknown	EPEC/EHEC	[56]
EspFu	N-WASP	relieves N-WASP inhibition for pedestal formation	EPEC/EHEC	[39, 40]
SipA	Binds actin to induce polymerization	helps host cell entry	*Salmonella enterica*	[41]
SipC	Acts with SipA, induces actin nucleation	helps host cell entry	*Salmonella enterica*	[42]
IpaC	Actin, β-catenin	filipodia formation, disrupt tight junction, phagosome escape	*Shigella* spp.	[34,36]

Table 3: Virulence factors important for pedestal formation or host cell entry.

Survival Mechanisms- non-innate immunity

Once inside the cell, intracellular survival is a priority for the bacteria. The bacteria must avoid cell recognition and prevent host cell growth and division (Table 4). Host cells can recognize foreign bodies within the cell and induce autophagy to destroy the foreign matter. *Salmonella* and *Chlamydia* replicate within endosomes and in order to prevent recognition and a lysosome response, the bacteria secrete virulence factors that alter membrane trafficking [57, 58]. The alteration of membrane trafficking and the endosome architecture prevents the recognition of the endosomes as foreign. *Chlamydia* alters trafficking through a number of virulence factors, in particular IncA and IncG, by altering Rab GTPase activity and mimicking SNARE proteins [59-61]. *Salmonella* virulence factors, SteA, PipB, SpiC and SSeG, alter membrane trafficking and location of the endosome by activating ERK1/2, Hook3, Kinesin and other unknown targets [62-66]. Much like the *Salmonella* and *Chlamydia, Shigella* can induce a strong autophagy response [67-69]. IcsA, a *Shigella* protein important for actin-based spread, induces autophagy, which *Shigella* reduces by secreting IcsB, which binds IcsA [70].

Host cell growth and apoptosis are another targets of infectious bacteria. Bacteria that infect the gut are subject to removal due to the regular endothelial cell lining turnover, which would effectively remove the bacteria from the host. Many bacteria can inhibit turnover through the secretion of cell cycle inhibition virulence factors (Cif), which act as cysteine proteases or bind and alter cell cycle proteins such as GCIP to stop the cell at different growth phases [71, 72]. The bacteria further

promote intracellular survival by preventing apoptosis of the host cell after bacteria recognition, which in turn prevents an inflammatory response. SopB, SlrP and AvrA of Salmonella act as inositol phosphatases, E3-ligases and acetyl-transferase of different pathways to collectively inhibit apoptosis [73-77]. EPEC targets CD98, Bax-inhibitor-1 NHERF2, and RPS3 [18, 78]. Collectively, inhibiting host cell recognition, cell growth and cell death effectively inhibits direct removal from the host.

Survival Mechanisms-Immune System Regulation of NF-kappaB

Non-immune cells use cytokines to recruit PMNs to the site of infection. The host cells recognize PAMPs of the bacteria such as LPS and flagellin, which in turn activate cytokine transcription-factor NF-kappaB. Cytokines are secreted to recruit PMNs and natural killer cells to the site of infection. NF-kappaB is the major target of virulence factors of T3SS gram-negative bacteria. Virulence effectors inhibit NF-kappaB induced transcription of cytokines by targeting different parts of the signaling pathway (table 7). The virulence effectors can target upstream of NF-kappaB by de-ubiquitinating NF-kappaB inhibitor I-kappaB or preventing ubiquitination of I-kappaB. The acetyltransferase activity of AvrA/YopJ/SSeL removes ubiquitin from I-kappaB and YspK/ospG kinase activity inactivates the ubiquitin machinery [73, 79-84]. Other effectors can inhibit MAPK, ERK, and P38 activation of NF-kappaB by removing phosphates through lyase activity and acetyltransferase activity [65, 80, 81, 85-87]. NleB and NleD cleave upstream regulators JNK, RelA, C-Rel and I-kappaB [88, 89]. Several species of bacteria have

effectors that inhibit downstream activity of NF-kappaB. OspZ, BopN and AopP prevent nuclear trafficking of the transcription factor by an unknown mechanism[49, 90, 91]. In addition, there are many other virulence effectors that inhibit NF-kappaB activity, but their function and target are not well understood [88-91]. Each species of bacteria have several virulence factors that inhibit NF-kappaB. The redundant virulence effectors ensure a tight inhibition of NF-kappaB. However, even with severe inhibition of NF-kappaB activity, low levels of cytokine expression and PMN recruitment still occurs [92] .

Effector	Target/mechanism	Function	Bacteria	
SteA	unknown	Hijack membrane vesicle trafficking	*Salmonella enterica*	[62]
PipB	kinesin motor protein	Transport along microtubules, recruit kinesin to SCV for Sif Extension	*Salmonella enterica*	[63, 64]
SpiC	binds Hook3 , activates ERK1/2	Disrupts golgi morphology, SOCS-3 expression in macrophages to inhibit cytokine signaling	*Salmonella enterica*	[65]
IncA	SNAREs	membrane trafficking	*Chlamydia* spp.	[59, 60]
IncG	14-3-3beta, Rab protein recruiter	Alter membrane trafficking	*Chlamydia* spp.	[61]
CT229	binds Rab4	Alter membrane trafficking	*Chlamydia* spp.	[93]
Cpn0585	binds Rabs	Alter membrane trafficking	*Chlamydia* spp.	[94]
SseF	binds TIP60 increases histone acetylation	Promote intracellular replication	*Salmonella enterica*	[95]
SseG	unknown	Brings SCV at the MTOC and promotes intracellular replication	*Salmonella enterica*	[66]
IpgD	Phosphoinositide 4-phosphatase of unknown protein	Intracellular survival	*Shigella* spp.	[78]
EspZ	targets CD98	Inhibits cytotoxicity and inhibit phagocytosis	EPEC/EHEC	[18]
NleH	targets Bax-inhibitor 1, NHERF2, RPS3	Blocks apoptosis, inhibits NF-KappaB signaling	EPEC/EHEC	[96, 97]
AvrA	acetyltransferases/ protease removal of ubiquitin of I-KappaB and β-catenin	Inhibits apoptosis and inflammatory response by NF-KappaB activation	*Salmonella enterica*	[73, 74]
SopB	inositol phosphatase	Inhibits apoptosis, invasion, Akt activation, fluid secretion and SCV formation/ biogenesis /positioning	*Salmonella enterica*	[75]
SlrP	E3 ubiquitin ligase of thioredoxin and ERdj3	Inhibit apoptosis	*Salmonella enterica*	[76, 77]
IcsB	Binds Atg5	Protects against autophagy	*Shigella* spp.	[70]
cif	cysteine protease	Cell cycle inhibitor	EPEC/EHEC	[71]
cif	cysteine protease	Cell cycle inhibitor	*Yersinia* spp.	[71]
cif	cysteine protease	Cell cycle inhibitor	*Photorhabdus* spp	[71]
CT847	binds GCIP/MAID	Induce cells to enter S growth phase	*Chlamydia* spp.	[72]

Table 4: Non-immunosuppressant virulence factors important for intracellular survival.

Effector	target/mechanism	Function	Bacteria	
NleB	Unknown	Inhibits TNF induced NF-kappaB activation	EPEC/EHEC	[88]
NleC	protease of RelA, p50, c-Rel, I-KappaB	Inactivates NF-KappaB signaling	EPEC/EHEC	[89]
NleE	unknown	Blocks I-KappaB degradation to inhibit NF-kappaB activation	EPEC/EHEC	[98]
NleG	UBE2D2 U-box E3 ubiquitin ligase	Inhibits NF-KappaB signaling	EPEC/EHEC	[99]
NleH	Bax-inhibitor 1, NHERF2, RPS3	Blocks apoptosis, inhibits NF-κB signaling	EPEC/EHEC	[100, 101]
AvrA	acetyltransferases/ protease removal of ubiquitin of I-kappaB and β-catenin	Inhibits apoptosis and inflammatory response by NF-KappaB activation	*Salmonella enterica*	[74, 79]
SpiC	binds Hook3, activates ERK1/2	Disrupts golgi morphology, SOCS-3 expression in macrophages to inhibit cytokine signaling	*Salmonella enterica*	[65]
SspH1	targets and activates PKN1	Inhibits NF-kappaB induced gene expression	*Salmonella enterica*	[102]
SpvC	phosphothreonine lyase of MAPK, JNK, Erk1/2, p38	Intracellular survival and inhibition of inflammatory response	*Salmonella enterica*	[86]
SseL	deubiquitinase	Functions up stream of I-KappaB kinase, affect unknown	*Salmonella enterica*	[82]
OspZ	unknown	Blocks nuclear translocation of NF-Kappa B, prevents transcription, recruits PMN	*Shigella* spp.	[88]
OspF	Phosphothreonine Lyase of MAPK, Erk and P38	Inhibits histone phosphorylation and prevents NF-KappaB dependent transcription	*Shigella* spp.	[85]
IpaH9.8	E3 ubiquitin ligase of N-WASP, MAPKK, U2AF, vinculin	Regulates transcriptome, reduces inflammatory response	Shigella spp.	[103]
OspG	kinase inhibits ubiquitin conjugating enzymes	Down regulates NF-KappaB	Shigella spp.	[84]
YopP/J	acetyltransferase, inhibits activation of MAPKK and IKK	Inhibits MAPK and NF-KappaB, inhibits inflammation and induces apoptosis of immune cells	*Yersinia* spp.	[80, 81]
YopM	possible E3 ligase and TRL4 LRR mimic,	Inhibits MAPK, NF-KappaB signaling and reduces innate	*Yersinia* spp.	[104-

	prevents dephosphorylation of PKN2 and RSK1	immune surveillance of Yersinia (mitigates immunogenicity)		106]
YspK	serine/threonine kinase of ubiquitin conjugating proteins	Inhibits NF-KappaB activation	*Yersinia* spp.	[83]
VopA	acetyltransferase of MKKs	Inhibits mapk pathway and NF-KappaB activation	*Vibrio* spp.	[87]
VopF	binds filamin A/B, BCA3, COMMD1	Induce membrane protrusions/actin rearrangement and disrupt tight junctions, inhibits NF-KappaB	*Vibrio* spp.	[107]
BopN	unknown	Induces IL-10, blocks nuclear trafficking of NF-kappaBp65, promotes trafficking of NF-kappaBp50	*Bordatella* spp.	[90]
AopP	unknown	Interferes with NF-KappaB nuclear trafficking	*Aeromonas* spp.	[91]
NleD	protease of JNK	Inhibits AP-1 activation	EPEC/EHEC	[108]
SopA	E3 ubiquitin-ligase	Reduces PMN migration by inhibiting NF-kappaB	*Salmonella enterica*	[109]

Table 5: Immunosuppressant virulence factors important for intracellular survival.

Tissue Dissemination

Cytotoxicity and Disruption of Tight Junctions

Unlike colonization and intracellular survival, the bacteria target cytoskeleton stability, cell death pathway and membrane tight junction proteins to promote acute inflammation and dissemination of the bacteria to other host tissues (table 5). Epithelial cells provide a strong barrier against secretion of foreign matter into other tissues. The tight junctions anchor each cell together forming a seal between the cells, which maintains the cell shape and polarity. Bacteria that have infected these epithelial cells can induce cytotoxicity and various cell death pathways.

Cytotoxicity causes cell rounding, and both processes perturb the association of the cells. In contrast to GEFs, GAP mimics such as ExoS/T, YopE, AexT/U induce actin disruption causing cell rounding [110-115]. Other, more non-traditional, regulators of GTPases have functions that have only been found as bacteria virulence effectors. These effectors are capable of permanently modifying GTPases and destroying the actin cytoskeleton. YopT is the only known cysteine protease that cleaves Rho proteins and inhibits their activity [116]. Vibrio has two virulence factors that ADP-rybosylates (VopT) and AMPylates (VopS) Rho GTPases, while SpvB ADP-ribosylates actin to produce the same result [117-119]. Other virulence effectors can induce autophagy (VopQ), necrosis (BopC), cell lysis (VPA450) and apoptosis (CADD) [120-124].

Tight junction disruption provides a channel between cells, which results in cell rounding and in some cases cell death [125].Tight junction disrupting virulence factors are the most common effectors- Map, EspF, NleA, IpaC, YopH, and VopF[11, 28, 36, 37, 39, 40, 45, 107, 126-134]. They rarely target the same proteins, and several effectors have multiple targets – profilin, SNX9, catenin, p130Cas, filamin, and Fas. The effectors can control localization and activation of these proteins. Tight junction disruption, along with cell rounding and cell death, is integral to the dissemination of bacteria to new tissues and the establishment of infection.

Effector	target/mechanism	Function	Bacteria	
Map	EBP50 (NHERF1), NHERF2, GEF for Cdc42	Induces filopodia formation, mitochondrial disruption, SGLT-1 inactivation, TJ disruption	EPEC/EHEC	[28, 36, 37]
EspF	14-3-3zeta, ABCF2, actin, Arp2, CK18, N-WASP, Profilin, SNX9, ZO-1/ZO-2	Mitochondrial disruption, NHE3 inactivation, SGLT-1 inactivation, TJ disruption, disrupts nucleolus, disrupts intermediate filaments, induce membrane remodeling, binds and activates N-WASP, inhibits PI3K-dependent phagocytosis	EPEC/EHEC	[39, 40] [126-131]
EspB	α1-antitrypsin, α-catenin, Myosin-1c	AJ disruption, inhibit phagocytosis	EPEC/EHEC	[135-137]
NleA	Syntrophin, Sec23/24, MALS3, PDZK11, SNX27, TCOF1, EBP50 (NHERF1), NHERF2, MAGI-3, SAP97, SAP102, PSD-95	Tight Junction disruption	EPEC/EHEC	[132-134]
SspH	ubiquitin E3 ligase	Possible target of tight junctions and actin	*Salmonella enterica*	[138]
IpaC	Actin, β-catenin	Filipodia formation, disrupt tight junction, phagosome escape	*Shigella* spp.	[34,36]
YopH	tyrosine phosphatase of Fyb and p130Cas	Inhibits phagocytosis of macrophages and neutrophils, disrupts tight junctions	*Yersinia* spp.	[11]
VopF	binds filamin A/B, BCA3, COMMD1	Induce membrane protrusions/actin rearrangement and disrupt tight junctions, inhibits NF-KappaB	*Vibrio* spp.	[107]
SpvB	ADP-ribosylates actin	Destabilizes cytoskeleton for cell cytotoxicity	*Salmonella enterica*	[118]
YpkA/YopO	serine/threonine kinase of Gαq, Rac GDI, binds monomeric actin	Blocks phagocytosis, induces cytotoxicity	*Yersinia* spp.	[9, 10]
CADD	binds Fas, TNFR1, DR4 and DR5	Induces apoptosis	*Chlamydia* spp.	[121]
VPA450	inositol polyphosphate 5-phosphatase	Induces membrane blebbing and cell lysis	*Vibrio* spp.	[139]

VopT	ADP-ribosyltransferase of Ras	Cell cytotoxicity and loss of membrane integrity	*Vibrio* spp.	[117]
VopS	AMPylate Rho GTPases	Blocks actin assembly, induces autophagy	*Vibrio* spp.	[119]
VopQ	unknown	Induce autophagy and inhibits phagocytosis	*Vibrio* spp.	[122]
BopC/BteA	unknown	Necrotic cell death	*Bordatella* spp.	[123, 124]
AexT	ADP rybosylator of Actin and GAP of Rho, Rac, Cdc42	Actin de-polymerization, cell cytotoxicity	*Aeromonas* spp.	[110, 111]
AexU	RhoGAP, ADP-ribosyltransferase of NF-KappaB	Host cell apoptosis and disruption of actin filaments	*Aeromonas* spp	[114]
ExoY	adenylate cyclase	Possibly disrupts actin	*Pseudomonas aeruginosa*	[140]
YopE	Rho GAP (targets Rho, Rac, Cdc42)	Reduce phagocytosis by macrophages, actin disruption	*Yersinia* spp.	[115]
YopT	cysteine protease of Rho proteins	Disrupts actin cytoskeleton	*Yersinia* spp.	[116]
ExoS	RhoGAP activity, ADP-ribosylation	ADPRT activity, golgi trafficking actin disruption; GAP activity against Rho Rac Cdc42. Inhibits cytokinesis	*Pseudomonas aeruginosa*	[112]
ExoT	RhoGAP activity	Actin disruption. GAP activity against Rho Rac Cdc42	*Pseudomonas aeruginosa*	[113]

Table 6: Virulence factors important for dissemination of bacteria to new tissues.

Shigella Pathogenesis

S*higella* species are gram-negative facultative anaerobes responsible for 5-15% of the world's diarrheal episodes. 99% of *Shigella* infections, shigellosis, occur in developing countries and are particularly prevalent in children under the age of 5 [141]. The bacteria, which spread through an oral-fecal route, cause severe inflammation and destruction of the lower intestinal tract [142]. The mortality levels of shigellosis are highest among children in developing countries due to poor sanitation and lack of access to antibiotics [143]. An emerging concern is that *Shigella* strains are becoming resistant to recently developed antibiotics, fluoroquinones, and therefore new vaccine and antibiotic development is necessary [144].

The pathway of infection has been comprehensively mapped for *S. flexneri*. Once in the large intestines, *S. flexneri* bacteria cross the epithelium through microfold-cells and are subsequently engulfed by macrophages [145, 146]. The bacteria lyse the phagosome through an unknown function of virulence factors IpaH7.8 and IpaC, induce apoptosis of the macrophage through activation of caspase-1 by IpaB, and are released into the sub-mucosa (figure 2) [13, 45, 147-152]. Before apoptosis, caspase-1 activation leads to cleavage and secretion of IL-1β, which recruits polymorphonuclear cells, resulting in loss of integrity of the epithelial cell lining [151, 153]. The leakiness of the cell lining allows for further dissemination of bacteria across the barrier.

Once in the sub-mucosa, the bacteria bind the baso-lateral side of the epithelial cell through an interaction between the Mxi/spa type-three secretion apparatus and surface receptors [2, 154]. This interaction occurs between virulence proteins IpaB/C of the apparatus and CD44 and β1-integrins [155, 156]. The T3SA forms a pore in the membrane and secretes virulence factors into the host cell. These virulence factors target cytoskeleton regulators and induce actin stress fibers and filipodia formation, which wrap around the bacterium and bring it into the cell via an endosome. This process is performed by a concerted effort between virulence factors IpgB1, IpgB2, IpaC, IpaA, IpgD1 and VirA. Recently, however, VirA's function during entry has been disputed [157-160]. IpgB1 and IpgB2 mimic RhoG and RhoB, while IpaA targets vinculin for actin tethering and IpaC induces actin polymerization [28, 31, 32, 45, 152]. IpgD1 seems to be important for entry and intracellular survival, as it acts as a phosphoinositide 4-phosphotase to activate the PI-3 kinase/Akt pathway, which is important to protect the cell from apoptosis [78]. The virulence factors IpaB/C/D can induce rapid lysis of the endosome to release the bacterium into the cytoplasm [13, 45, 152, 161]. Inside the cells the bacteria replicate and spread from cell to cell using actin-based motility performed by IcsA recruitment of N-WASP, thus avoiding an extracellular immune response [162-164].

Once inside the cell, the bacteria are protected from patrolling immune cells. However, the intracellular surveillance systems can recognize the bacteria and activate the expression of chemokines and chemo-attractants to target immune cells to the infected host cell. OspF, a phosphothreonine lyase, irreversibly inactivates

MAPK and prevents histone phosphorylation and transcription factor NF-kappaB targeting to chemokine and other immune signaling genes [85]. This decreases the secretion of IL-8 and further polymorphonuclear infiltration of the epithelial cell lining. IpAH9.8, an E3 ubiquitin ligase, further reduces levels of MAPK kinase and splicing factor U2AF that affect expression levels of IL-8 and IL-B1 [113]. However, the low levels of cytokines still generate a strong inflammation response, recruiting PMNs and activating Natural Killer cells, which is the cause of the damage to the intestines and diarrhea. While not perfect, control of the immune response allows the bacteria time to spread from cell to cell. Eventually the PMNs recruited to the site of infection kill the bacteria [92].

The virulence factors and the Mxi/spa T3SA essential for invasion and intracellular survival are encoded on the virulence plasmid of *Shigella* [165, 166]. The virulence plasmid is highly diverse among species of *Shigella*, with a core-conserved set of genes necessary and sufficient to provide virulence [167-170]. These proteins are clustered on the plasmid by function, with the T3SA proteins, "entry" proteins and proteins important for actin nucleation and spread grouped together [171, 172]. There are several genes that have yet to be identified or characterized and while many of the virulence factors function are well characterized, several do not have a known target or molecular mechanism [173].

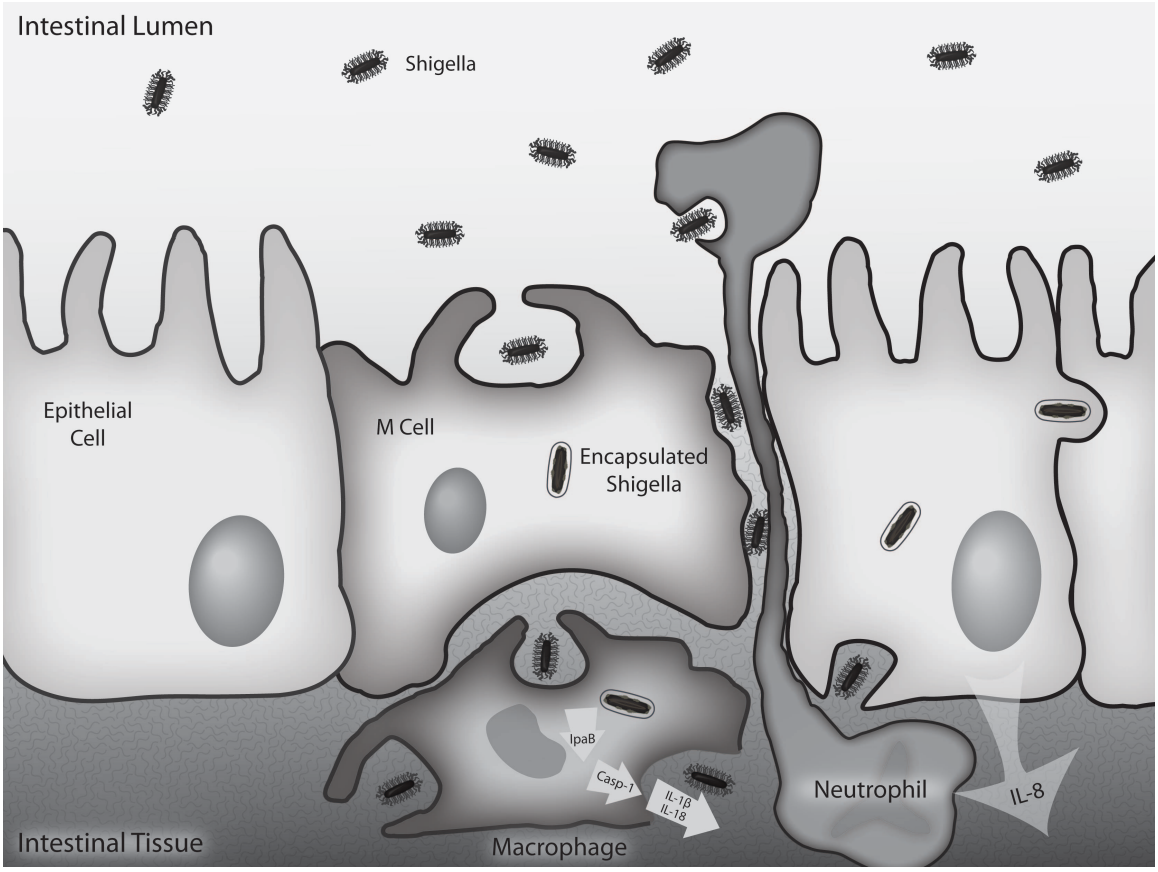

Figure 2: Pathway of *Shigella* infection. The bacteria cross the intestinal barrier by transcytosis through the M cell. The macrophages engulf the bacteria causing cytokine release due to macrophage apoptosis, which recruits PMN and promotes leakiness of the cell lining for further infection. The bacteria bind to the baso-lateral side of the cell to induce engulfment for colonization. Adapted from LaBrec *et al*. by Dan Dorset [174].

EPEC Pathogenesis

Much like *S. flexneri*, EPEC is a facultative anaerobe that spreads through an oral fecal route and is a causative agent of diarrhea in children in third world countries and recent diarrheal outbreaks in Europe due to contaminated vegetables [175, 176]. However, the mode of infection is completely different. *E. coli* are usually avirulent, commensal bacteria in the gut, but they are able to pick up virulence plasmids and genes resulting in various strains of virulent *E. coli [177]*. While the bacteria mainly colonize the surface of the intestinal lining, the infection can spread and cause urinary tract infection or sepsis/meningitis [175]. EPEC was first incriminated as the cause of diarrheal outbreaks in the 1940s and has continued to be the cause of approximately 30% of infant diarrhea in Brazil, Mexico, South Africa and Bangladesh resulting in the death hundreds of thousands of children a year [175, 178-189].

EPEC infection results in 'attaching-and-effacing' lesions in the small bowel, affecting the length and number of microvilli and structure of the enterocyte borders. The lesions are the site of destruction of the absorptive surface, villus atrophy and thinning of the mucosal lining [190]. The destruction indicates adherence as an important step in EPEC infection. Much like *Shigella*, EPEC contain a LEE virulence plasmid which codes for a filamentous Esp /Esc T3SA and virulence proteins necessary and sufficient for forming attachment and effacing lesions on the epithelial cell lining [191]. Non-virulent *E. coli* can be transformed into pathogenic

bacteria by solely adding the LEE plasmid [192]. However, many of the virulence proteins and genes found on the plasmid are not well characterized [193].

Once the bacteria reach the gut, the initial attachment occurs through binding by pili on the apical side of the epithelial cell (figure 3) [194] . The T3SA can then bind and form a pore in the host membrane by the tip proteins EspB and EspD [195]. The initial virulence factor secreted through the T3SA is Tir. Tir inserts in the membrane where it can bind the outer membrane protein Intimin on EPEC, which allows for tight attachment of the bacteria to the host [52]. Next, actin pedestal formation occurs, destroying the surrounding microvilli and creating a niche on which the bacteria can colonize and prevent removal from the gut [196]. The pedestal is formed by a concerted effort between the virulence factors to induce a dynamic cytoskeletal rearrangement. Besides attachment, Tir can induce cell signaling in the host through the NCK pathway to recruit N-WASP for actin polymerization at the site of bacteria attachment [46-51]. The genomic virulence effector $EspF_u$ amplifies this effect by binding N-WASP, relieving auto-inhibition, and increasing actin polymerization [39, 40]. EspM and Map act as GEFs for Cdc42 and RhoA which induces stress fibers and filipodia, which is controlled by continued signaling from Tir [28, 36-38]. At the same time EspT acts to activate these Cdc42 and RhoA to induce membrane ruffling and lamellipodia [55]. The functions of these virulence effectors, combined with EspH that prevents Rho inhibition, and EspG, the activity of which is described in the body of this thesis, induce the formation of a pedestal [19, 20, 53, 54]. To prevent the cytotoxicity of this event,

NleH and NleD inhibit apoptosis of the host cell and EspZ maintains the focal adhesion sites between the epithelial cells [18, 37, 96, 108].

EPEC has several mechanisms to inhibit a host immune response. EPEC can prevent phagocytosis by macrophages and targets NF-KappaB inactivation, which responds to signaling from TOLL-like receptors recognizing pathogen-associated molecular patterns (PAMPs) due to EPEC flagellin [197, 198]. EPEC infected macrophages can inhibit phagocytosis of non-opsonized bacteria and IgG by secreting virulence factors EspB, EspF and EspJ [193, 199-201]. EspB targets and inhibits myosin, which is involved in actin movement required to engulf the bacteria [135]. EspH's ability to inhibit GEF proteins and prevent cytoskeleton rearrangement play an important role in preventing stress fiber formation and the initial membrane ruffling required for phagocytosis [19, 20]. While the function of EspJ is unknown, knocking out either protein abolishes the ability to prevent phagocytosis of opsonized bacteria [201].

While EPEC infection ultimately results in activation of an inflammatory response, the bacterium works hard to prevent immune system response. The flagellin PAMP recognition induces activation of NF-KappaB, which in turn activates TLR signaling, cytokine expression and PMN recruitment [202]. The bacteria inhibit this response by secreting the Nle family of virulence factors into the host cell [88, 203]. These proteins reduce the activation of NF-KappaB and the subsequent inflammatory response [88, 203]. NleE inhibits translocation of NF-KappaB into the nucleus, which lowers the expression of IL-8 [98]. In addition, NleB inhibits

activation of NF-KappaB in response to TNF but not IL-1β [88]. The target and mechanism in which both NleE and NleB are unknown, whereas NleC has been found to be a protease that cleaves inactive NF-KappaB [89]. NleD cleaves JNK and p38 MAP kinase, which inhibits another AP-1 transcription factor [108]. This particular transcription factor is involved in the inflammatory response and other cell processes [204]. The function of all the virulence factors underscores the extent at which EPEC attempts to survive and thrive in its environment; however, the low levels of cytokine expression and signaling induces a strong inflammatory response which removes the infection [193].

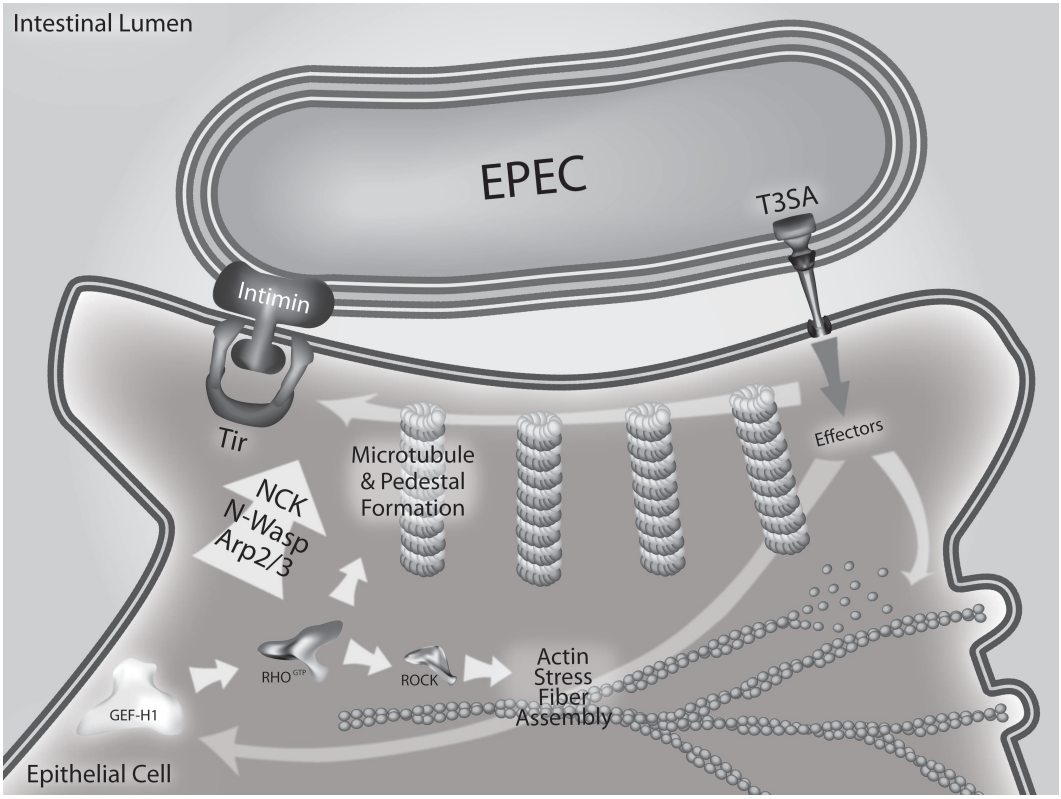

Figure 3: EPEC attachment and effacement of gut epithelial cell[205]. The bacterium attaches to the apical side of the host epithelial cell and secretes virulence effectors through a type-three secretion needle. Once secreted into the host cell, Tir inserts into the membrane and tethers the bacteria to the cell surface through binding of intimin on the cell surface. Other virulence factors induce a local rearrangement of the cytoskeleton to form a pedestal under the bacterium. Adapted from Matsuzawa et al. by Dan Dorset[205].

VirA and EspG

VirA is an essential virulence factor for cell-to-cell spread of *S. flexneri* [158, 206] VirA is a 44.7 kDa protein expressed under Mxi-Spa control from the large virulence plasmid and secreted through the Mxi-Spa T3SS [207]. VirA was reported to proteolyze α-tubulin, inducing destruction of microtubules for membrane ruffling for entry and bacterial tunneling through the cell [158]. VirA null bacteria exhibit a 50% decrease in spread, distinguishing VirA as an important protein in the dissemination of disease [208, 209].

VirA is distantly related to two *E. coli* proteins, EspG and EspG2, respectively having 20% and 13% amino acid sequence identity respectively to VirA [210]. EspG has been found on the virulence plasmids of both enteropathogenic *E. coli* (EPEC) and the rodent pathogen *Citrobacter rodentium,* while EspG2 is chromosomal and only found in EPEC [211-213]. EspG and EspG2 seem to play similar roles to VirA in that the proteins can functionally substitute for each other [206, 212]. This is particularly interesting because EPEC does not enter the cell, but adheres to the apical side of the intestinal epithelium, forming pedestals [214]. EspG/EspG2 have been proposed to induce microtubule destruction during pedestal formation in vivo and it has been postulated that the proteins induce Gef-H1 activation of the Rho pathway, resulting in the nucleation of actin for pedestal formation to prevent the phagocytosis of the bacteria [205]. VirA has been shown to complement an EspG/EspG2 null EPEC and regain wild type adherence and pedestal formation,

while both EspG and EspG2 were shown to complement a VirA null bacterium and eliminate their entry defect [206, 212].

Research Objective

Herein, I describe structural and functional analyses used to determine the different mechanisms by which homologs VirA and EspG alter the cytoskeleton. I determined the structure of VirA by x-ray crystallography and found that the protein has a unique fold, which does not resemble a cysteine protease (Chapter II). Further studies of VirA's ability to degrade microtubules show VirA does not proteolyze α-tubulin, nor does it directly or indirectly induce microtubules as previously proposed (Chapter II). Efforts to determine functional domains of VirA led me to determine the x-ray crystallography structure of EspG (Chapter III). A structural comparison showed that the two proteins contain a surface conserved patch and specific residues important for function. To test the importance of the conserved region I created wild type and mutant EspG expressing inducible HEK293 cell lines, which revealed a novel binding partner of EspG. Further studies show that VirA has a different host cell target than EspG (Chapter III). Moreover, functional assays revealed biologically relevant and important functional domains and residues. Studies of actin regulating host proteins during Shigella infection led me to identify ezrin activation as a downstream target of VirA (Chapter IV). Collectively, my studies provide a better understanding of how EspG and VirA

complement each other and reveal a mechanism by which they regulate actin rearrangement during infection.

CHAPTER II

STRUCTURAL AND FUNCTIONAL STUDIES INDICATE THAT *SHIGELLA* VIRA IS NOT A PROTEASE AND DOES NOT DIRECTLY DESTABILIZE MICROTUBULES

Introduction

VirA is a conserved virulence factor with important roles in spread and perhaps entry. At the beginning of my studies, a model existed in which VirA principally acted to destroy the microtubule network by proteolysis of tubulin in a similar manner as papain [1,2]. VirA's homolog, EspG, has been shown to have a similar effect on microtubules and can complement for VirA during *Shigella* infection, which suggests the proteins likely have similar mechanistic properties [206, 211, 212, 215]. To gain insight into how VirA might function during *Shigella* infection, we determined the structure of VirA for a comparative analysis against papain and EspG. Furthermore, we performed tubulin proteolysis assays to study VirA's action and importance during infection.

In this study, I have determined the structure of VirAΔ44 to a resolution of 2.4 Å. The structure reveals a novel fold, not yet found in the PDB, with a N-terminal 4-stranded anti-parallel β-sheet, a central core anti-parallel 6-stranded β-sheet and a c-terminal helical bundle. Functional studies indicate VirA does not target tubulin as previously reported and the effector is important for *Shigella* host cell entry.

Methods

Expression and purification of VirA: Full length and N-terminal truncation mutants of VirA (Δ44, Δ86) from *S. flexneri* 2a strain 301 were expressed from pET28 in *E.coli* BL21(DE3) for 16 hours at 20°C. Cells were harvested by centrifugation, lysed with a French Press in the presence of 0.5 mg/mL lysozyme, 5 mg/mL Dnase,10 mg/mL leupeptin, 1mM PMSF, 7 mg/mL pepstatin, and purified by metal affinity chromatography. The N-terminal His-tag was removed by thrombin and VirA was further purified by gel filtration. Se-Met incorporated VirAΔ44 was purified in essentially the same way using *E. coli* B834(DE3) auxotrophic cells grown in M9 media supplemented with standard amino acids and selenomethionine, in a modification of the Van Duyne protocol [216].

Limited proteolysis of VirA: 11 μg of full length his-tagged VirA was incubated with varying concentrations of chymotrypsin in pbs. Samples were incubated for 16 hours at 4°C. Samples were visualized on bis-tris 4-12% gradient gels using SDS-PAGE.

Gentamicin protection assays: Assays were perfumed essentially as described by Elsinghorst [217]. Triplicate samples of semi- confluent HeLa cells in 12 well plates were infected with ~105 *Shigella*, or a VirA null *Shigella* strain [218] centrifuged at 1000xg for 10 minutes, washed 3 times with MEM, incubated for 2 hours with MEM + 100 μg/mL gentamicin, washed 5 times with MEM, and lysed with 0.1 deoxycholate in pbs. 40% of the lysed solution was plated onto congo red plates.

The inoculum was quantified by plating serial dilutions.

Tubulin degradation assays: To test tubulin degradation by VirA, full length VirA (purified without PMSF or leupeptin) was incubated with twice-cycled tubulin [219] (CytoSkeleton, Denver, CO) and visualized by SDS-PAGE. 25 μg of VirA and 25 μg of tubulin were incubated in 100 mM KCl, 10 mM K-Hepes pH 7.7, 2 mM DTT for 2 hours at 37 C. Similar experiments were performed with addition of protease inhibitors (0.1 mg/mL leupeptin and/or 10mM PMSF). Experiments were performed four times. Duplicate samples were visualized on bis-tris 4-12% gradient gels using SDS-P AGE and quantified using NIH Image.

Microtubule disassembly by VirA: Microtubule disassembly was assayed essentially as described[220, 221]. Surfaces of double- stick tape flow cells were sequentially coated with 1 mg/ml biotinylated BSA and 0.1 mg/ml streptavidin. 1 μM fluorescent (1:9 rhodamine-labeled:unlabeled), biotinylated (1:100 biotinylated:unmodified) GMPCPP-microtubules were then allowed to attach to the flow cell surface, and washed with 3 volumes of Flow Cell Buffer (FCB; 80mM Pipes, pH 6.8, 0.5mM MgCl2, 1mM EGTA containing 1 mM MgATP, 500 mg/ml casein, 50 mM KCl, and 1X Oxygen Scavenging Mix[222]. VirA was diluted to 5 mM in FCB and introduced into the flow cell. Microtubule disassembly was monitored by time lapse fluorescence microscopy using a Nikon 90i epifluorescence microscope equipped with a 100X 1.4 NA Nikon objective and a CoolSNAP HQ2 cooled CCD camera. Microtubule lengths were measured at 0 and 30 minutes.

Microtubule assembly in the presence of VirA and Cell extract: 1mg/mL fluorescent

(1:9 rhodamine-labeled:unlabeled) microtubules were added to Xenopus egg extract (100mg protein/mL) and polymerization was induced by the addition of 5% DMSO, essentially as described [223, 224]. Assembly was visualized using a Nikon 90i epifluorescence microscope equipped with a 20X 1.4 NA Nikon objective and a CoolSNAP HQ2 cooled CCD camera. Assembly was visualized after 30 minutes, for VirA quantities of 0 (buffer), 25μg, 50μg, 100μg, 250μg, and 500μg, in a 200μL reaction volume.

Crystallization and preparation of heavy atom derivatives: Full-length VirA crystals were grown by vapor diffusion from a reservoir of 10% PEG 3350, 100 mM bis-tris pH 5.0, and 1M NaCl (figure 4B). Chymotrypsin treated VirA crystals were grown by vapor diffusion from a reservoir of 10% PEG 3350, 100 mM bis-tris pH 5.0, and 1M and NaCl (figure 4C). Δ44 VirA crystals were grown by vapor diffusion from a reservoir of 1.9-2.0 M ammonium sulfate, 100 mM bis-tris pH 5.25-5.35, and 0-2% glycerol (figure 6A). The CH3HgCl derivative was prepared by transferring crystals to fresh drops of their own mother liquor containing 1mM CH3HgCl and soaking for 48 hours. Native and derivative crystals were cryoprotected with 20% glycerol and flash cooled in liquid nitrogen.

Data collection and structure determination: Diffraction data were collected from single crystals at 100K on the NE-CAT beam line at the Advance Photon Source (Argonne, IL). Data were, processed with HKL2000 [225] (table 7). Heavy atom positions were located with SHELX [226] using the derivatives with the isomorphous native, native 27, and refined using SHARP [227]. Electron density was

improved by solvent flipping[228]. The structure was traced in O [229] and refined with iterative rounds of manual rebuilding in O and COOT [230] and refinement in CNS [231] and Phenix [232] against the higher resolution native 45. TLS refinement and B-group refinement was done in Phenix for the final rounds of refinement. TLS groups were identified using the tlsmd website [233, 234]. The refined model consists of amino acids 53-326, 340-399 in molecule A and amino acids 52-327, 340-399 in molecule B, and 91 water molecules.

Structural analysis: DALI, SSM, and VAST were used to search the Protein Data Base for protein fold similarities to VirA [235-238].

Figure preparation: PyMol [239] was used to prepare structure figures. The sequence alignment was performed with ClustalW and ESPript [240, 241]. The topology diagram was made with TopDraw [242].

Results and Discussion

X-ray Crystal Structure of VirA

To investigate the biochemistry underlying VirA function, we have expressed and crystallized full-length and N-terminally truncated VirA from *Shigella flexneri.* Full-length VirA crystals diffracted to 8 Å and limited proteolysis by chymotrypsin revealed the N-terminus of VirA was unstructured. While chymotrypsin treated VirA crystallized and diffracted to ~3 Å, the diffraction patterns contained twinning due to a heterogeneous cleavage at the N-terminus (figure 4A). Since limited proteolysis and mass spectrometry revealed the first ~44 amino acids to be disordered, several constructs of truncated VirA were tested for expression and stability as judged by analytical gel filtration (figure 5).

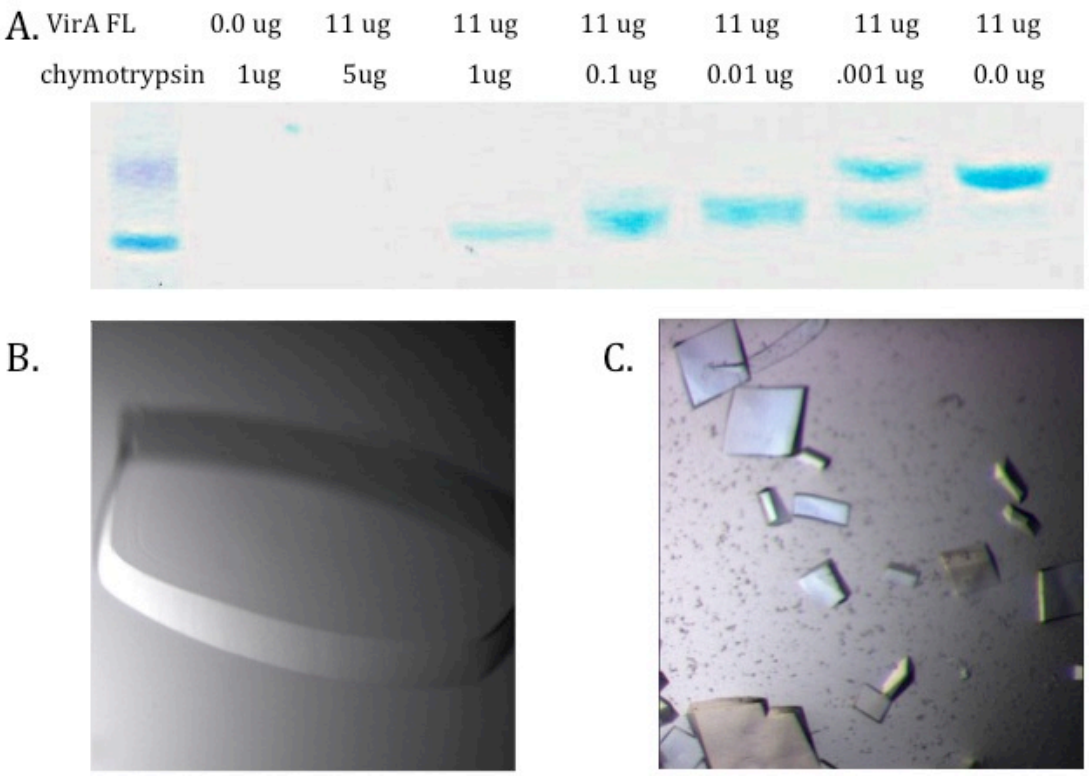

Figure 4: Full-length and chymotrypsin treated crystals made from limited proteolysis of full-length protein. (A) Limited proteolysis of full length VirA visualized by Coomassie. Proteolysis by chymotrypsin revealed a single cleavage species approximately 5 kd smaller than full length VirA. (B) Full-length VirA crystals in grown in 10% PEG 3350, 100 mM bis-tris pH 5.0, and 1M NaCl diffracted to 8 Å. (C) Chymotrypsin treated VirA grown in 10% PEG 3350, 100 mM bis-tris pH 5.0, and 1M and NaCl diffracted to ~3 Å.

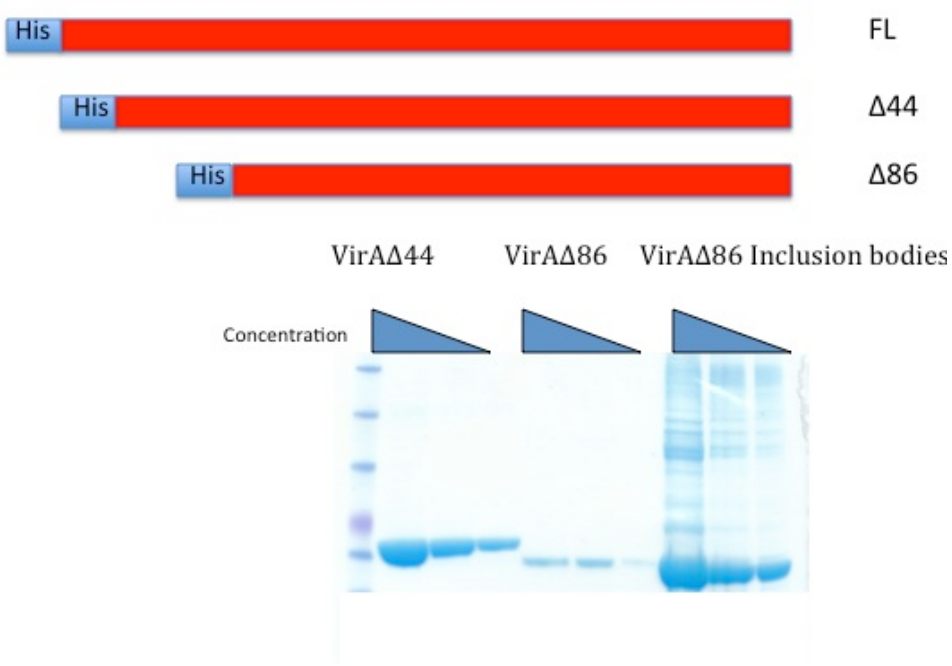

Figure 5: New constructs of VirA were made for a homogeneous sample of truncated VirA. Constructs contained an N-terminal His tag with either 44 or 86 residues removed. VirAΔ44 expressed well, whereas VirAΔ86 went mostly to inclusion bodies.

Removal of the first 44 amino acids resulted in a dramatic improvement in crystal quality. The Δ44 construct crystallized and diffracted to 2.4 Å (figure 6). The structure was determined by MIRAS using a mercury derivative and crystals of Se-methionine-substituted VirA. There are two molecules in the asymmetric unit, and the structure includes residues 53–326 and 340–399 of molecule A and residues 52–326 and 339–399 of molecule B. The N-terminus and residues 327–339 are not visible and presumed to be disordered. The two molecules are very similar to each other. The individual domains align with rms differences of 0.03 Å for the N-terminal domain, 0.38 Å for the central sheet, and 0.54 Å for the C-terminal helical subdomain. Additionally, there is an ~5° rotation between the N-terminal domain and the rest of the molecule, resulting in an overall rms difference of 1.95 Å for all main chain atoms. Data collection and refinement statistics are given in Table 7.

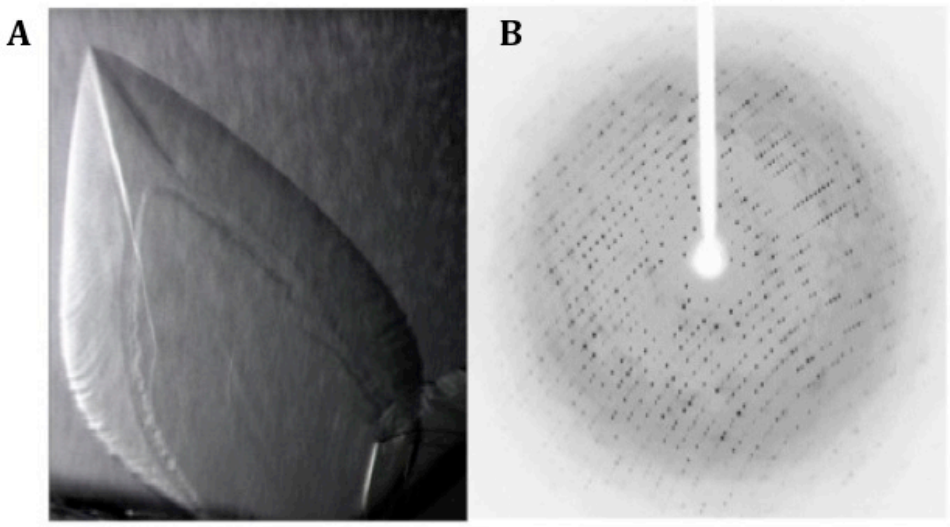

Figure 6: Crystals of VirAΔ44 diffract to 2.4 Å. (A) Crystals of VirAΔ44 can be grown by hanging drop vapor diffusion in 1.9-2.0 M ammonium sulfate, 100 mM bis-tris pH 5.25-5.35, and 0-2% glycerol after 7 days. (B) The crystals diffracted to 2.4 Å resolution at the APS synchrotron X-ray Source.

Table 7: Data Collection and Refinement Statistics

	Native 27	Native 45	SeMet	Mercury
Data collection				
Space group	$P4_12_12$	P41212	P41212	P41212
Cell dimensions				
a=*b*, *c* (Å)	92.101, 200.374	91.29, 198.29	92.264, 200.739	92.412, 201.226
Wavelength	0.97919	0.97919	0.97919	0.97919
Resolution (Å)	50-2.8	50-2.4	50-3.2	50-2.7
Completeness (%)	97.8(98.8)	99.5 (98.0)	96.5 (97.5)	97.5 (82.5)
Redundancy	8.9 (9.6)	6.3 (5.0)	4.1 (3.7)	6.6 (4.3)
Figure of merit Centric/accentric	0.53/0.39			
Refinement				
Resolution (Å)		2.4		
No. reflections		33386		
R_{work} / R_{free} %		21.73% / 26.68%		
R.m.s. deviations				
Bond lengths (Å)		0.008		
Bond angles (°)		1.136		
Ramachandran Plot		98.5% of residues in allowed regions		

The crystal structure reveals VirA to be a V-shaped molecule with a prominent cleft between the N- and C-terminal domains (figure 7). Ten α-helices and 10 β-strands, in the form of two β-sheets, comprise VirA. The N-terminal domain is a flat four-stranded sheet, with helices at the N- and C-termini. This domain is connected to the rest of VirA by its C-terminal helix and a loop.

Consistent with a lack of mobility between these domains, the packing between the N-terminal domain and the rest of VirA appears to be quite tight, as judged by the low *B*-factors (relative to the rest of VirA) of the packing interface and the lack of solvent accessibility between the domains (figure 8). The first helix, α1, protrudes from the rest of VirA, making no contacts with the rest of the protein until residue 60, consistent with a lack of structure in the extreme N-terminus. The central structure of VirA is a six-stranded sheet buttressed by eight helices and represents a large portion of the C-terminal domain. The sheet is curved, forming a convex surface between the N- and C-terminal domains. Helix α3 lies on the convex surface, partially filling the convex face. However, a prominent cleft still exists between the N-terminal domain and the rest of VirA with dimensions ~20 Å (depth) × 15 Å (width) × 20 Å (length). The C-terminal domain also contains a three-helix bundle formed by residues 208–267, which extends the face of the interdomain cleft formed by the N-terminal and central domains.

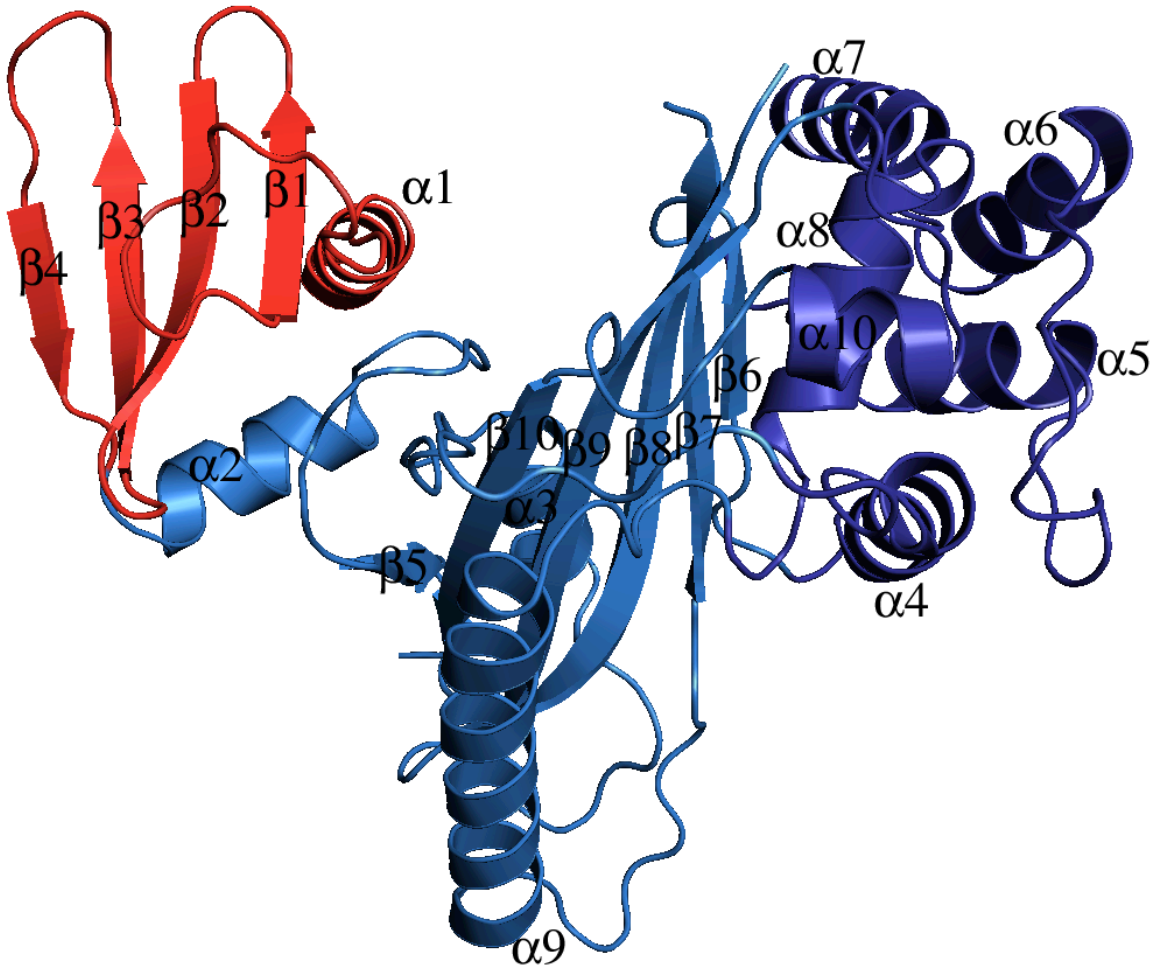

Figure 7: Ribbon diagram of VirA. The N-terminal domain is colored red and the C-terminal domain blue. The helical C-terminal subdomain is colored dark blue.

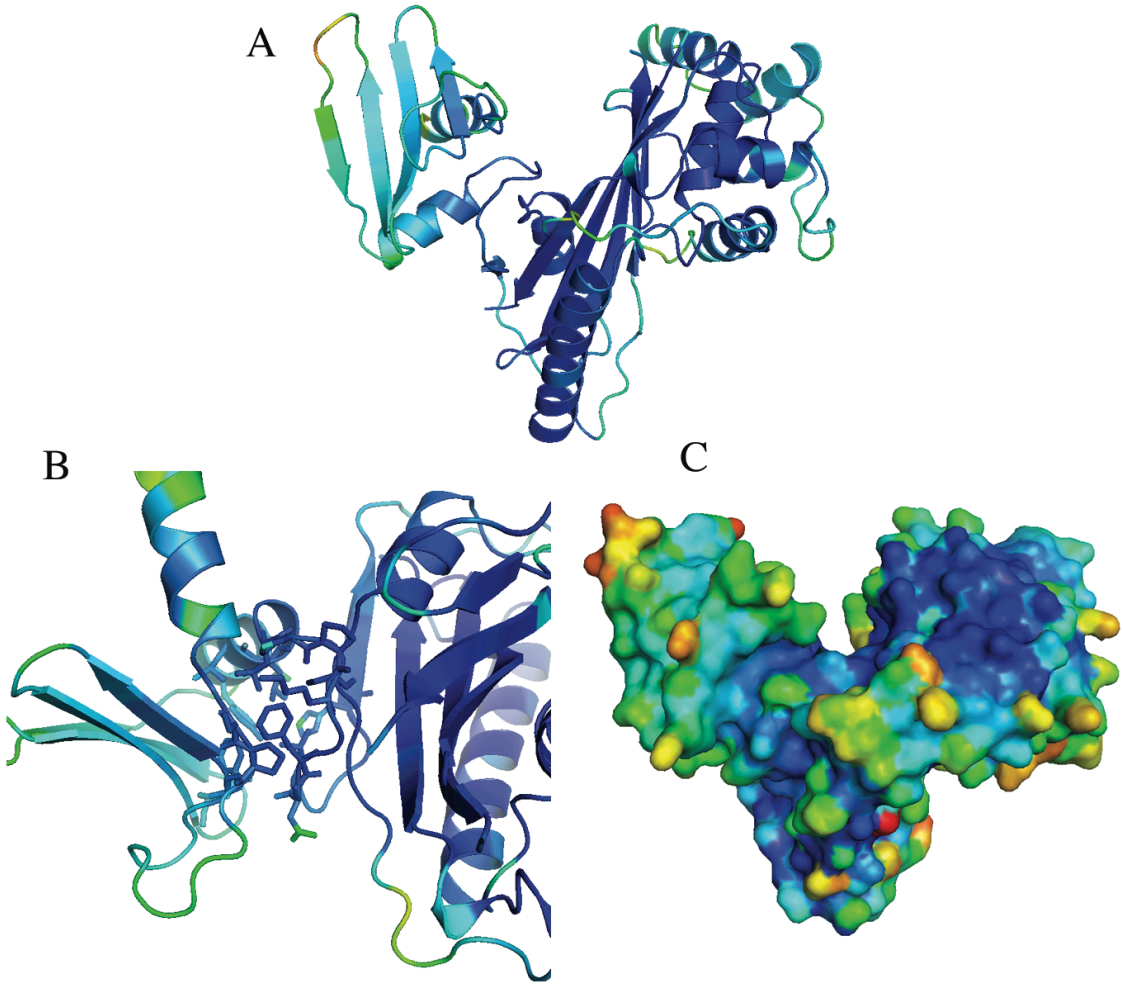

Figure 8: VirA structure colored by B-factor. All panels are colored by B-factors, with dark blue being low and red being high B-factors. (a) a ribbon diagram (b) a close up of the interaction between the N-terminal domain and the rest of VirA. The residues involved in the interaction all have low B-factors, consistent with a lack of motion between these domains. (c) The solvent accessible surface area of VirA shows the interface between the domains excludes solvent, indicating tight association.

VirA has a Novel Protein Fold

To assess VirA's structural homology to other proteins, the VirA coordinates were submitted to the DALI, VAST, and SSM webservers [235, 236, 243, 244]. The results indicate only very short regions of structural similarity, two secondary structural elements and a loop, which matched a small portion of a protease scaffold. The elements are located at the core of the protein and are not functionally important to either VirA or the scaffold. The lack of structural homology indicates that VirA represents a novel fold, without substantial structural or sequence homology to any previously determined structure. The N-terminal domain, which on the basis of biochemical assays, has been reported to be a papain-like protease [158], lacks structural homology to papain (figure 9). Further, the putative active site nucleophile (Cys34) is in an unstructured region of VirA and is not conserved in EspG (figure 9 and 12).

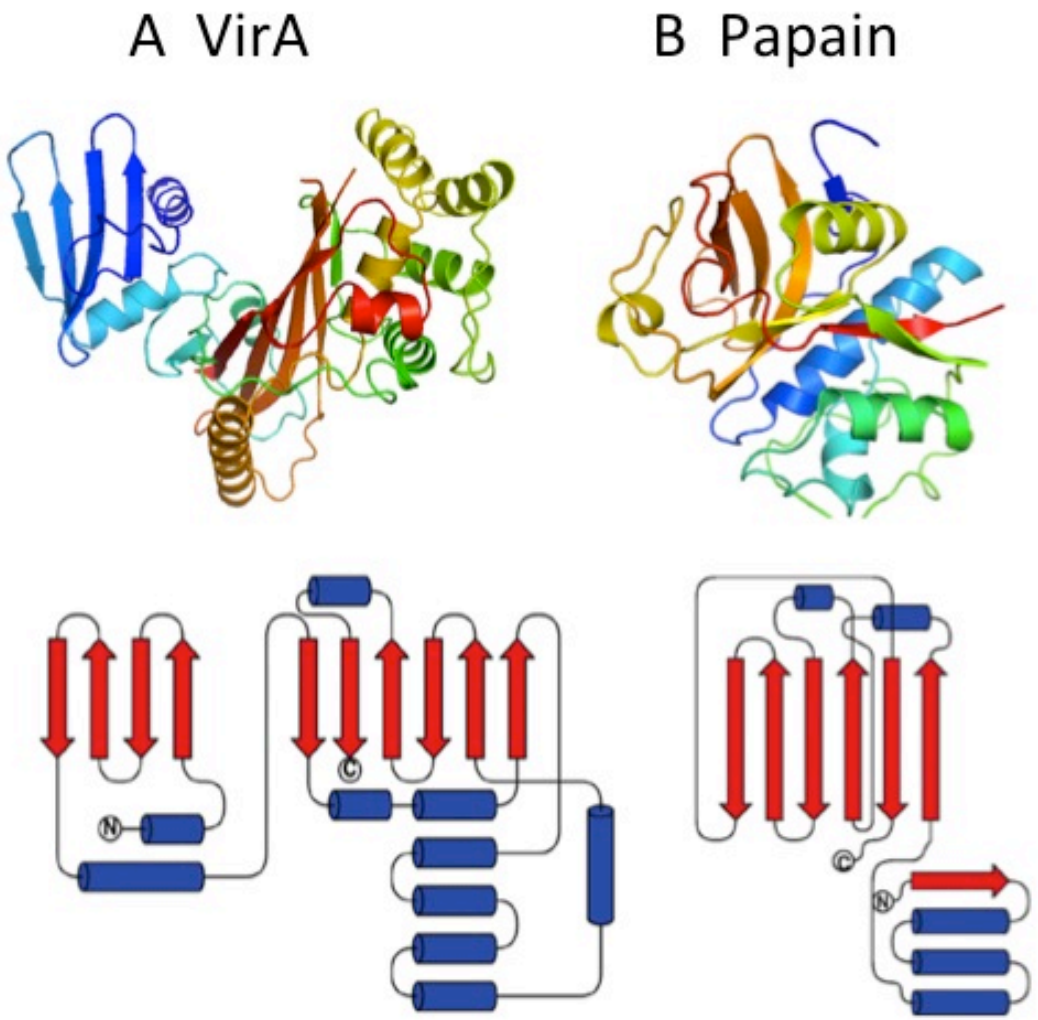

Figure 9: Comparison of VirA and papain structures. Ribbon diagrams of VirA (left) and papain [245] and topology diagrams of VirA (left) and papain [245]. The VirA N-terminal domain and papain both contain four-stranded antiparallel sheets; however, the sheet in VirA is flat, and the sheet in papain is highly curved and is alternatively described as a part of a β-barrel or as a sheet [246, 247].

VirA Does Not Proteolyze Microtubules

The lack of structural evidence to support the protease function of VirA led me to directly test VirA's ability to degrade tubulin. As shown in figure 10A, purified VirA does not cleave tubulin. These experiments were performed in quadruplicate using roughly stoichiometric quantities of presumed catalyst and substrate. VirA is also unable to promote the disassembly of fluorescently labeled microtubules assembled from the nonhydrolyzable GTP analogue GMPCPP (figure 10B). Rhodamine microtubules were incubated with either buffer or a 5-fold molar excess of VirA and imaged every 30 s for 30 min. The average rate of depolymerization was 0.037 μ/min for VirA (n = 15, standard deviation of 0.015) and 0.039 μ/min for the control (n = 17, standard deviation of 0.018). These values are in agreement with the published spontaneous depolymerization rate of 0.03 μ/min for GMPCPP microtubules [220] and are inconsistent with a model in which VirA directly depolymerizes microtubules.

To rule out indirect modulation of microtubule proteolysis or destruction through a host protein, VirA was incubated in the presence of tubulin and xenopus oocyte extract. DMSO was added to the samples with varying concentrations of VirA to induce polymerization of microtubules. Figure 11 shows representative images of a buffer control and a 250 μg (12.5mg/mL) experiment. VirA did not inhibit polymerization or induce destruction of microtubules in the presence of oocyte extract at high concentrations. This data further indicate that VirA does not modulate tubulin as an intended target during infection.

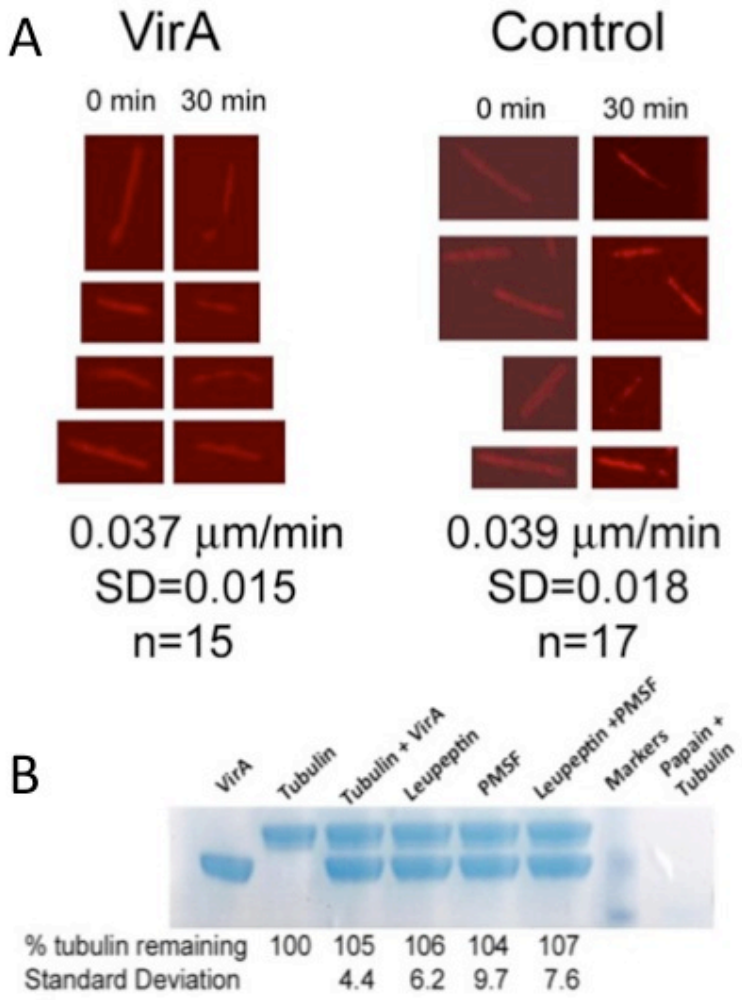

Figure 10: Destabilization and proteolysis assay of microtubules and tubulin by VirA. (A) Representative examples of microtubules treated with either an ~5-fold molar excess of VirA or buffer. Samples were imaged every 30 s for 30 min. Significant photobleaching is evident, but the depolymerization rate is unaffected by VirA. (B) Coomassie-stained SDS–PAGE showing VirA's inability to digest tubulin. VirA and tubulin were incubated at 37 °C for 2 h. Gels from four experiments were quantified by densitometry and averaged. In addition to the proteins, PMSF (10 mM) and/or leupeptin (0.1 mg/mL) was added. No digestion is discernible. The last lane shows complete digestion of tubulin by papain under similar conditions.

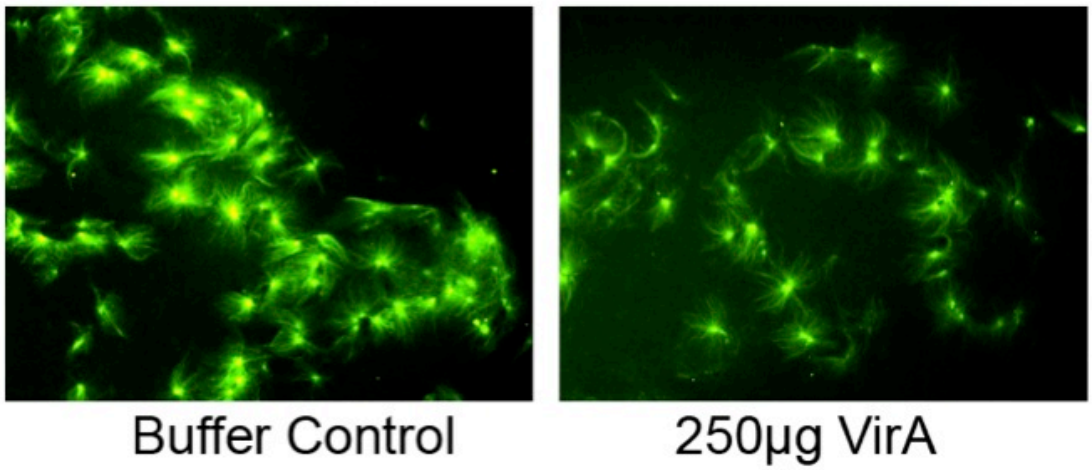

Figure 11: Representative images of fluorescent microtubules samples incubated with VirA. Buffer control and VirA samples have similar amounts of polymerized tubulin, indicating that VirA is not acting through a host factor to destroy microtubules.

Sequence Comparison of VirA and EspG/EspG2

VirA is a member of the EspG gene family, composed of EspG1 and EspG2 from *E. coli*, EspG from *C. rodentium*, and VirA from *Shigella* species. Conservation within each species is nearly perfect, while conservation between families is quite limited (figure 12). VirA is only ~20% identical to EspG from *E. coli* or *C. rodentium.* The two EspG families within *E. coli* are ~43% identical, although functionally redundant [211, 212], and the *C. rodentium* EspG is ~75% identical to EspG1 from *E. coli*. The level of pairwise identity between VirA and EspG2 is only 13%. There are insertions of five, six, and seven amino acids in VirA relative to EspG. Two of these insertions occur within β-strands, removing five of ten amino acids from β7 and four of thirteen amino acids from β8. An unstructured loop connects β7 and β8 in VirA such that the central sheet of the C-terminal domain of EspG may well be intact, albeit with a shortened loop between β7 and β8. EspG also contains conserved glycines in putative helices α4 and α6. The VirA structure combined with sequence alignment indicates that some structural differences are possible between VirA and EspG. However, the lack of numerous insertions within secondary structural elements is consistent with similar folds.

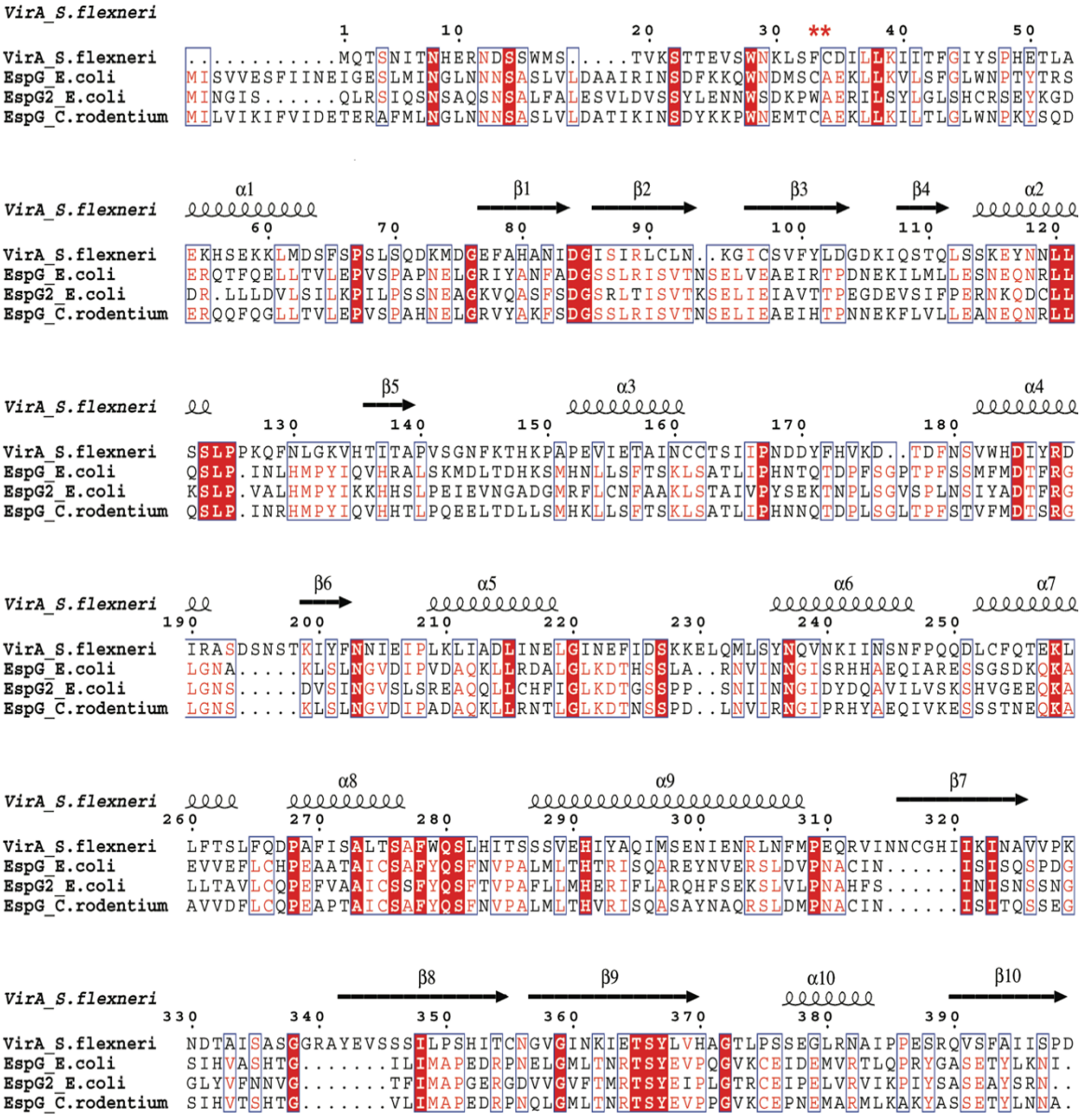

Figure 12: A multiple sequence alignment showing secondary structural elements as coils (helices) and arrows (sheets). Red asterisks denote the putative active site cysteine, conserved in VirA and EspG, but not EspG2. Regions of high conservation are boxed. Strictly conserved residues are colored white on a red background. Residues conserved in 3 of the proteins are colored red on a white background. Prepared with ESPript[241].

The VirA structure and accompanying functional studies indicate that VirA is not a protease. Further, we are unable to detect microtubule severing or depolymerization by VirA. We conclude that such activity in cells is not due to direct or indirect interactions between VirA and microtubules or microtubule regulating host proteins. Studies have shown that homolog EspG induces actin stress fiber formation when transfected into Caco-2 cells, which would suggest VirA induced microtubule destruction is a result of this process [205]. However, additional studies are necessary to reconcile the low level of sequence conservation among EspG family members with the observation that homologs can functionally substitute for each other [206, 212].

CHAPTER III

STRUCTURAL AND FUNCTIONAL STUDIES INDICATE THAT THE EPEC EFFECTOR, ESPG, DIRECTLY BINDS P21-ACTIVATED KINASE

Introduction

VirA's homolog EspG can successfully complement VirA's function during Shigella infection [206, 212]. This phenomenon is surprising considering the low sequence conservation and substantially different modes of infection for EPEC and *Shigella* [174, 248]. Sequence alignments suggest that secondary structural elements are conserved with the exceptions of a few extensions and loop insertions in the VirA sequences [159]. When the sequence alignment is mapped on the surface of the VirA structure, two patches of conserved surface exposed residues can be identified. To further understand the function of VirA, a goal for this study was to determine which if either of these surface exposed features was conserved in EspG and to gain insight into how these effectors modulate the host cytoskeleton. Prior to beginning this work I had ruled out the proposed role for EspG and VirA in tubulin proteolysis, and there was not a known target or pathway by which these proteins alter the cytoskeleton.

In this study, I have determined the structure of EspGΔ43 to 1.6 Å resolution. The structure is homologous to VirA, although the N-terminal domain is rotated and translated relative to its position in VirA. Functional studies indicate EspG, but not VirA, binds p21 activated kinase1 (PAK1). This provides a novel target of EspG and further understanding of how EPEC reorganizes the cytoskeleton.

Methods

Expression and purification of EspG: The 355 C-terminal residues of EspG were amplified from Enteropathogenic *E. coli* strain E2348/69 (accession FM180568) by PCR and cloned into pET-28a, incorporating a vector encoded N- terminal hexahistidine tag and thrombin site. This construct, Δ43EspG, was transformed into *E. coli* BL21 (DE3) and grown in Luria Bertani broth containing 50 μg/ml kanamycin. Overnight cultures were diluted (1:50) and grown to an optical density of 0.6 (600 nm) at 37˚C. Cultures were moved to 20˚C, and protein expression was induced with a final concentration of 100 uM isopropyl Beta-D-1-thiogalactopyranoside for 16 h. Cells were harvested by centrifugation and lysed with a French Press in the presence of chicken egg white lysozyme, bovine pancreatic deoxyribonuclease I, 10 μg/mL leupeptin, 1 mM PMSF, 7 μg/mL pepstatin, and 1 mM tris(2-carboxyethyl)phosphine. EspG was purified by metal affinity chromatography and size exclusion chromatography.

Expression and purification of GST and PBD-GST constructs: GST and PBD-GST (a kind

gift from Gary M. Bokoch [249]) vectors were transformed into BL21 cells and grown in Luria Bertani broth containing 50 μg/ml ampicillin. Cultures were harvested and lysed following the protocol described above for EspG. GST and PBD-GST were purified using Glutathione sepharose 4 fast flow (GE Life Sciences).

Crystallization and preparation of heavy atom derivatives: EspGΔ43 crystals were grown by vapor diffusion from a reservoir of 2.0-11.0% PEG 8000 and 100 mM bis-Tris pH 6.25-7.5 (figure 13A). The NaBr derivative was prepared by quickly soaking (~30s) crystals in fresh drops of mother liquor containing 1M NaBr. Native and derivative crystals were cryoprotected with step-wise soaks in 10, 15, and 20% glycerol.

Data collection and structure determination: Diffraction data were collected from single crystals at 100K at sector 24- IC-C at the Advance Photon Source (Argonne, IL). Data were indexed, integrated and scaled with HKL2000 [225]. Data collection statistics are given in supplemental Table 1. Heavy atom positions were located and refined using the Phenix program suite [232]. Electron density was improved by automated density modification including solvent flipping and histogram matching as implemented in Phenix [232]. The structure was traced with a combination of automated and manual tracing in Phenix and COOT [230, 232]. Refinement was done using Phenix [232]. TLS refinement was incorporated in the final rounds of refinement using TLS groups identified using the tlsmd webserver. The refined model consists of amino acids 44-158, 161-316, 321-395, and 427 water molecules.

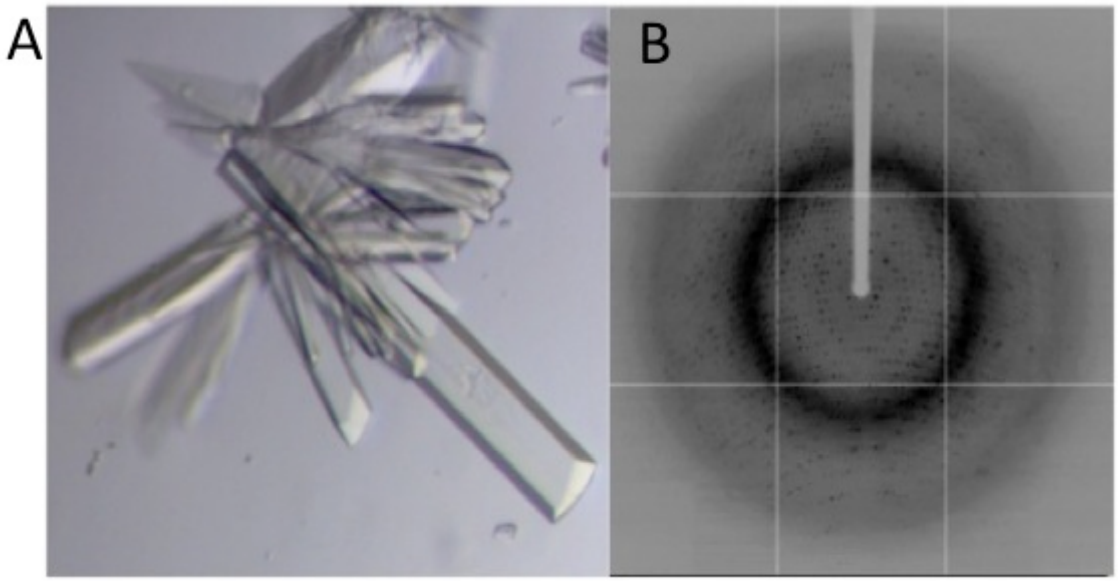

Figure 13: EspG Crystals Diffract to 1.6 Å. (A) Crystals of EpsGΔ43 can be grown by hanging drop vapor diffusion in 2.0-11.0% PEG8000 and 100 mM bis-tris pH 6.25-7.5. (B) Diffraction data from native EspGΔ43crystals. The crystals diffracted to 1.6 Å resolution at the APS synchrotron X-ray Source.

Stable cell lines expressing EspG: EspG was amplified with a Flag tag from a pET28 vector encoding full-length EspG and cloned into the pcDNA5/FRT/TO vector (Invitrogen). This vector was subsequently mutated to create the DR-AA mutant. Inducible Flag-EspG and Flag-EspG_DR-AA HEK293 FlpIn T-Rex cell lines were produced by co-transfection of the pcDNA5/FRT/TO vectors with the recombinase expression plasmid pOG44 and selected with 150 μg/ml hygromycin according to the manufacturers instructions (FlpIn system, Invitrogen). Clones were verified by western blots and PCR. EspG and EspG_DR-AA expression was induced with 0.1 μg/ml of doxycycline 24 hours before each experiment. Cell lines were maintained in Dulbecco's modified Eagles medium (GIBCO) supplemented with 10% fetal bovine serum and 1% pen/strep. HEK293 FlpIn T-Rex (Invitrogen) cell medium was supplemented with 100 μg/ml zeocin and 15 μg/ml blasticidin.

EspG-PBD binding assay using cellular lysates: EspG and EspG_DR-AA stable cell lines were induced 24 hours prior to an experiment. Un-induced and induced cells were lysed with a non-denaturing PBS/triton based buffer from Cell Signaling (product 9803), supplemented with 10 μg/mL leupeptin, 1mM PMSF, and 7 μg/ml pepstatin. The lysate was clarified by centrifugation at 12,000 rpm for 5 minutes, and normalized for total protein level by densitometry of coomassie stained SDS-PAGE gels. Purified PBD-GST and GST were added at 1.5 mg/ml to glutathione sepharose and bound for 1 hour at 4 °C prior to the experiment. The sepharose was washed 3 times with lysis buffer. Equal amounts of un-induced and induced lysates were added to a 35 μL slurry of 50% sepharose and incubated for 1 hour at 4 °C. The

sepharose was washed 3 times with lysis buffer and boiled in SDS-PAGE buffer. The samples were subjected to SDS-PAGE and Western blotting with anti-flag (M2) antibody (Sigma) primary and goat anti-mouse secondary antibody (LI-COR Biosciences). Blots were developed with an Odyssey fluorescent scanner.

PAK1 activation/phosphoylation assay: Cells were prepared and lysed as was done for the PBD binding assay, above. Extracts were probed for PAK1 phosphorylation by western blotting using a phospho-specific antibody that recognizing T423 of PAK1, the critical activation loop phosphorylation site. The primary antibody was from Cell Signaling, and the secondary antibody was from LI-COR Biosciences. Blots were developed with an Odyssey fluorescent scanner.

EspG-PBD direct binding assay: Purified His-tagged Δ43EspG was added to 35 µL of 50% slurry of GST or PBD-GST bound sepharose in the presence of PBS buffer with 1% triton-X100. The samples were incubated for 1 hour at 4°C. The agarose was washed 3 times with PBS/triton buffer and boiled in SDS-PAGE buffer and DTT. The samples were subjected to SDS-PAGE and Western blotting with an anti-hexahistidine primary antibody (Santa Cruz Biotechnology) and goat anti-rabbit secondary (LI-COR).

Structural analysis and figure preparation: Pymol and COOT were used for structural analysis [230]. PyMol was used for figure preparation. The sequence alignment was performed with ClustalW and ESPript [240, 241]. Mapping of sequence conservation onto the structure was done using consurf [250] using an alignment of 19 sequences prepared in ClustalW [240].

Table 8: Data Collection and Refinement Statistics

	Native	NaBr
Data collection		
Space group	$P2_12_12_1$	$P2_12_12_1$
Cell dimensions		
a, *b*, *c* (Å)	71.15, 74.38, 93.92	71.26, 74.6, 93.0
Wavelength	0.9795	0.9195
Resolution (Å)	50-1.6	50-2.2
Completeness (%)	50-1.6Å: 89.8(51.8) 50-1.8Å: 98.6(98.2)	99.5(99.3)
Redundancy	50-1.6Å: 4.8(4.2)	5.4(5.4)
I/sigmaI	50-1.6Å: 32.4(3.0)	16.8(3.7)
Figure of merit		Experimental: 0.37 DM: 0.66
Refinement		
Resolution (Å)	1.6Å	
No. reflections	58,526	
No. reflections free set	1,959	
R_{work} / R_{free} %	16.1/18.8	
R.m.s. deviations		
Bond lengths (Å)	0.006	
Bond angles (°)	1.004	
Ramachandran Plot	99.7% of residues in allowed regions	

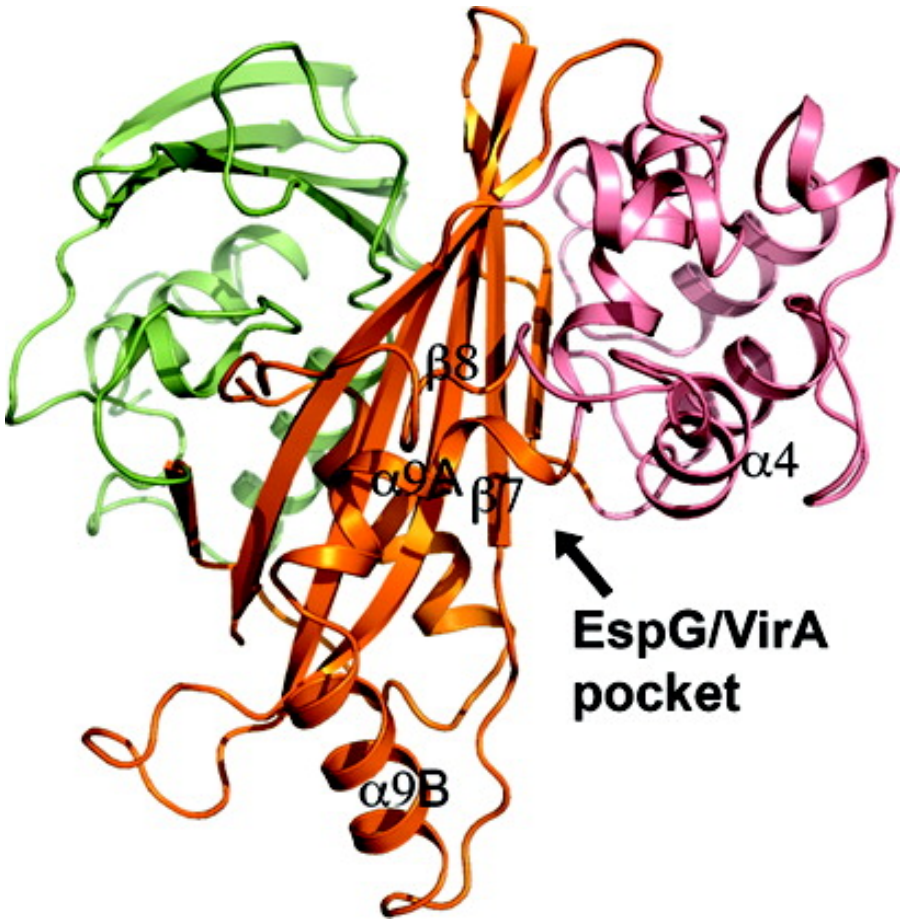

Figure 14: The X-ray crystallography structure of EspGΔ43. The structure, solved at 1.65 Å, is shown as a ribbon diagram with the NT domain colored green, the central sheet orange, and the helical domain salmon.

Results and Discussion

X-ray Crystal Structure of EspG

We have determined the X-ray crystal structure of EspG [Protein Data Bank (PDB) entry 3Q1C] and compared it to that of VirA (PDB entry 3EB8). As with VirA and other T3SS effectors, the amino terminus of EspG is likely disordered [159, 160, 251]. While we were unable to obtain crystals of full-length EspG, crystals of Δ43EspG diffracted to 1.6 Å (figure 13B). The EspG structure was determined by single-wavelength anomalous scattering, using data from a NaBr derivative, and density modification [252]. The final structure was refined to 1.8 Å and includes residues 44–158, 161–316, and 321–395 (figure 14). Data collection and refinement details are given in Table 8.

Despite having ~17% identical sequences (figure 12), EspG and VirA are structurally similar (figure 15 and 16). Both proteins contain a central six-strand sheet, flanked by an amino-terminal domain, composed of a four-strand β-sheet, and a helical domain. The individual domains of the two proteins are fairly similar, with root-mean-square [253] differences of 2.3 Å for the amino-terminal domain (EspG residues 70–141), 4.6 Å for the central sheet (EspG residues 153–187, 213–220, 294–371, and 386–395), and 3.3 Å for the helical domain (EspG residues 194–212, 221–292, and 374–384). The principal differences are a ~60° rotation of the amino-terminal domain between EspG and VirA and a ~90° kink in helix 9 (figure 16).

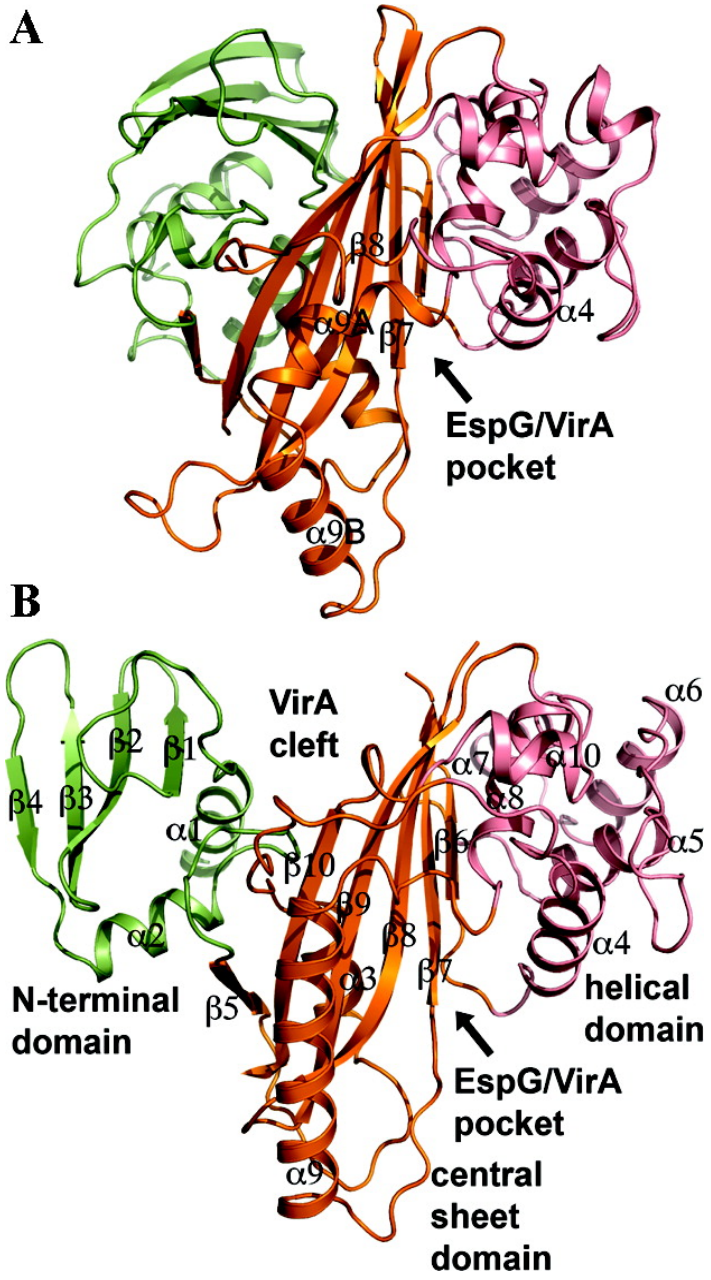

Figure 15: EspG (A) and VirA (B) shown as ribbon diagrams with the NT domain colored green, the central sheet orange, and the helical domain salmon. The structures are oriented so that the central sheet and helical domain align, and the rotation of the N-terminal domain is visible. Secondary structural elements and domains are labeled in panel B. Features of EspG described in the text are labeled in panel A.

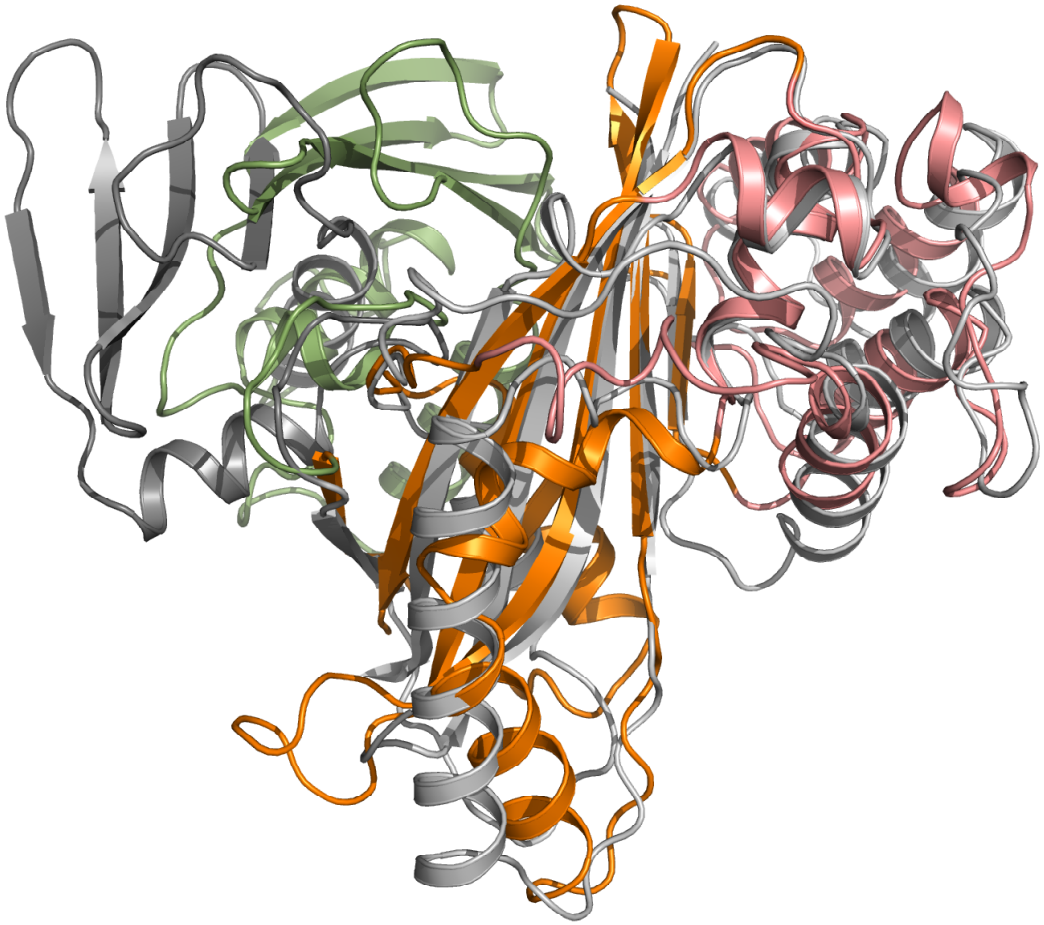

Figure 16: Alignment of EspG and VirA. Both structures are oriented as in figure 15, with EspG colored by domain and VirA colored gray.

Structural Comparison of EspG and VirA

The structural analysis of VirA revealed a prominent interdomain cleft (figure 15B) [159]. The alternate position of the amino-terminal domain observed in EspG largely fills this cleft (Figure 15A). Although this could represent the closed conformation of a mobile domain, the lack of sequence conservation indicates that this cleft is not required for EspG function (Figure 12). There is, however, a deep pocket revealed in the structure of EspG (Figure 15A) that appears to be highly conserved between EspG and VirA (Figure 16). This pocket is ~18 Å long, ~11 Å wide, and ~20 Å deep, and the residues surrounding it are well conserved among all EspG, EspG2, and VirA sequences.

The rim of the ~20 Å deep pocket is lined by 12 well-conserved residues, primarily from helix 4, helix 9, and the loop preceding strand 7 (figure 17 and 18). Two isoleucines, 328 and 330, from strand 7 and two hydrophilic residues, S342 and T344, from strand 8 form the base of the pocket (figure 17). Helix 4, which forms one rim of the pocket as shown in Figure 18, uses conserved hydrophilic and charged residues: S201, D205, and R208. An orthogonal rim of the pocket is formed by residues from kinked helix 9: Q293, S294, and V297. D205 and R208 are notable because they are the only conserved charges that line the entrance to the pocket. To evaluate the importance of D205 and R208, we mutated them to alanine, and the double mutant (EspG_DR-AA) was stably expressed in Hek cells.

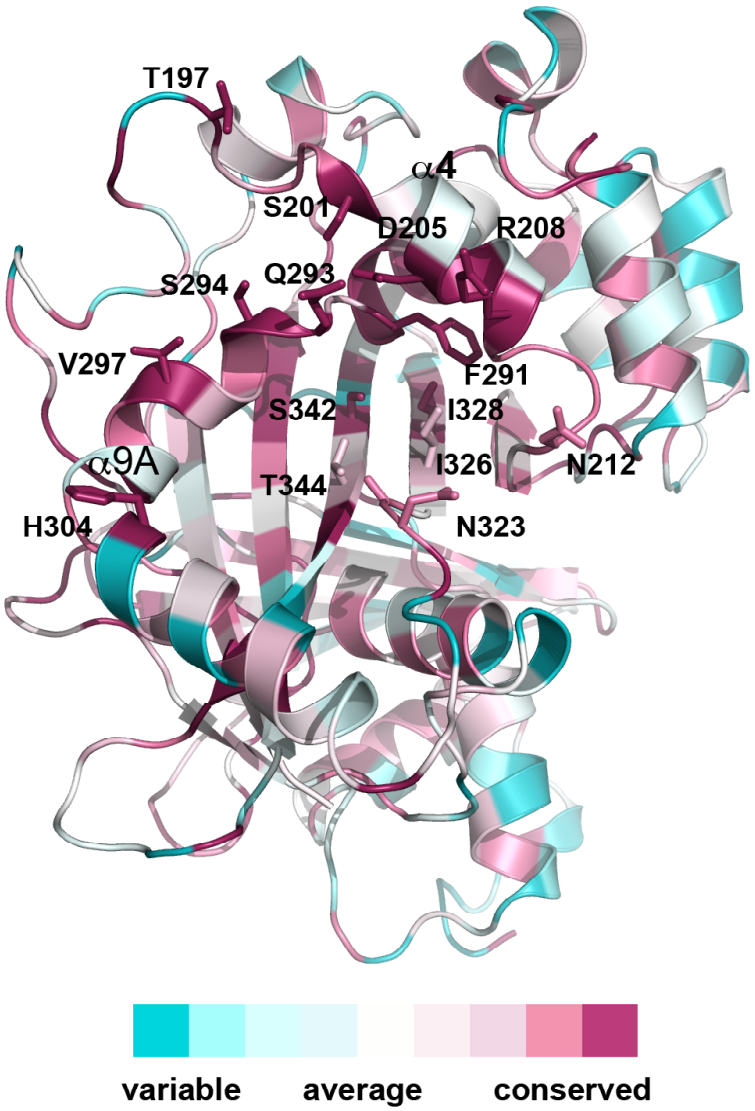

Figure 17: Secondary structure representation of EspG, oriented as in figure 18B, and colored by residue conservation. Secondary structural elements and conserved residues forming the pocket are highlighted.

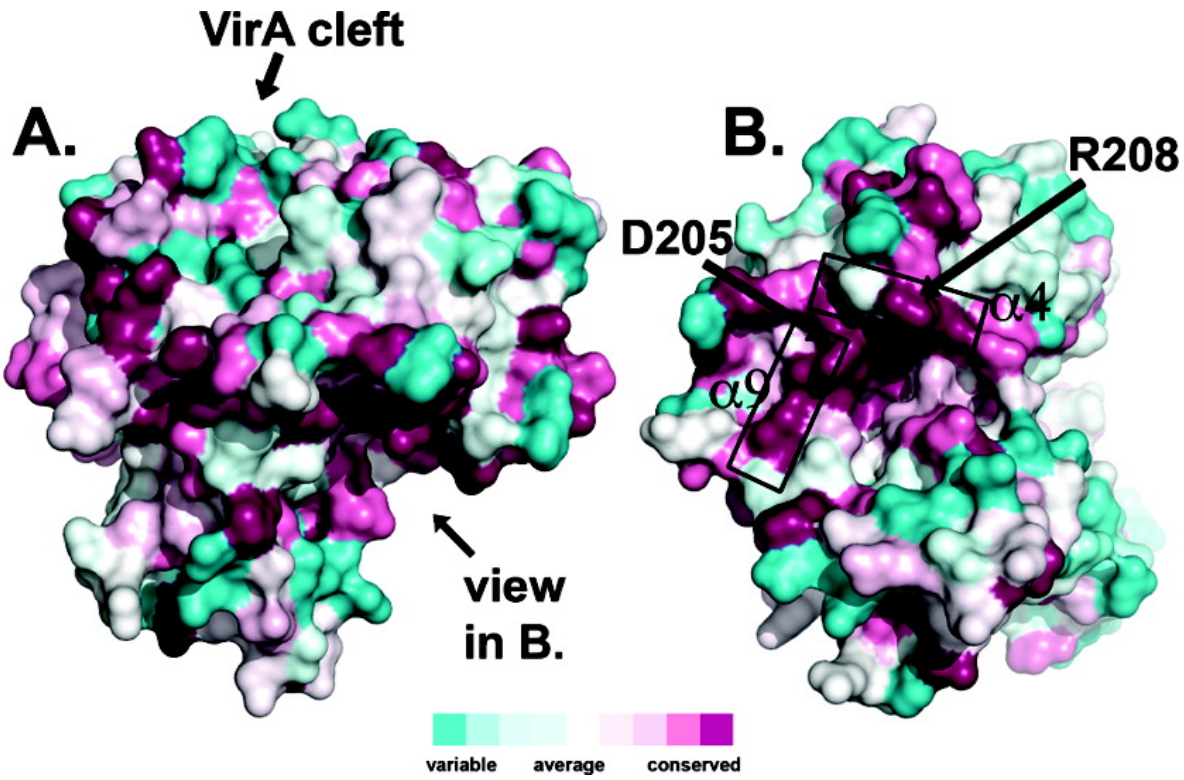

Figure 18: Surface rendering of EspG, colored by residue conservation. (A) EspG oriented as in figure 17. The residues that align with the VirA cleft are highly variable among EspG, EspG2, and VirA family members. (B) EspG viewed along the arrow in panel A. A continuous stripe of highly conserved residues is observed in panel A and continued into panel B. A deep, highly conserved pocket, the rim of which is formed by residues from R4 and R9, is seen in panel B. Residues D205 and R208 form much of the entrance to the pocket and are strictly conserved

EspG binds PAK1

Although the functional roles of EspG and VirA in EPEC and *Shigella* infection may be different, the common need to modulate cytoskeletal structure at the membrane led us to investigate the activation of small G-proteins. Activation of Rho, Rac, and Cdc42 is important in regulation of the cytoskeleton [254], and EspG and VirA have been reported to modulate these proteins [205, 255]. Using inducible cell lines expressing flag-tagged EspG and the EspG_DR-AA mutant, we assessed Rho, Rac, and Cdc42 activation by the pocket mutant [256, 257]. In brief, binding domains for GTP-bound states of Rho and Rac/Cdc42 (from rhotekin and p21 activated kinase-1, PAK1, respectively) [256, 257] were incubated with induced and noninduced EspG-containing cells. While we did not observe significant levels of G-protein activation (data not shown), we were surprised to observe EspG bound directly to beads containing the Rac/Cdc42 (p21) binding domain of PAK1 (PBD beads) (figure 19A, 19C). EspG_DR-AA bound substantially more weakly to the beads (figure 19B), consistent with a role in binding for the large conserved patch. EspG and EspG_DR-AA are expressed at similar levels, indicating that the failure of EspG_DR-AA to bind PBD is not caused by gross changes in EspG stability. Paradoxically, EspG expression results in a loss of active (phosphorylated) PAK1 (figure 19D), presumably because of degradation or trafficking to an insoluble cellular compartment.

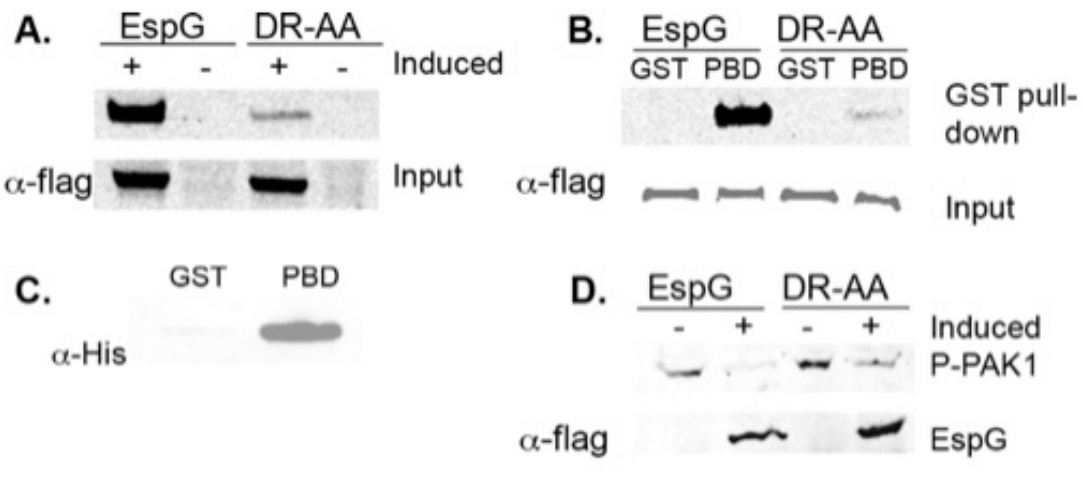

Figure 19: EspG binds PAK-PBD during pull-down assay. (A) Cells expressing equivalent amounts of flag-tagged EspG and EspG_DR-AA were incubated with PBD beads. EspG remained bound to PBD after three washes, whereas EspG_DR-AA was predominately washed off. (B) Neither EspG nor EspG_DR-AA binds to GST beads. (C) Direct binding between purified EspG and the GST-PBD fusion protein indicates that no other cellular proteins are involved in mediating the EspG-PBD interaction. (D) Expression of EspG, and to a lesser extent EspG_DR-AA, results in the loss of active (phosphorylated) PAK1.

PAK1 is a Ser/Thr kinase with a two-lobed catalytic subunit and an activation loop that is phosphorylated in the active form [258, 259]. Additionally, PAK1 contains an amino-terminal inhibitory domain that binds GTP-bound Rac or Cdc42 [257]. Binding to Rac or Cdc42 reorganizes the inhibitory domain, such that it no longer binds the catalytic subunit, at which point phosphorylation of the activation loop is sufficient to activate PAK [258]. The inhibitory domain includes the PBD, and binding to the PBD is sufficient to release the PBD from the catalytic subunit and relieve inhibition. Subsequently, activated PAK1 auto-phosphorylates the inhibitory domain, which prevents future inactivation. Thus, PAK1 can be considered fully active when phosphorylated both on the activation loop and on the inhibitory domain [258].

The specific functional roles played by EspG, EspG2, and VirA during infections have been controversial. Our results show that EspG is structurally similar to VirA and contains a functionally important conserved surface patch that binds the PBD of PAK1. These results support a role in infection in which EspG simultaneously recruits PAK to the sites of EPEC attachment and obviates the requirement for G-protein activation. PAK principally regulates the actin cytoskeleton, although there are numerous other targets, and overexpression of active PAK promotes formation of lamellipodia, filopodia, and membrane ruffles [260-262]. The observation that EspG binds directly to the inhibitory domain of PAK, mimicking a small GTPase, implies that EspG's primary role during pathogenesis is to promote actin remodeling. Rather than recruiting a small GTPase,

EPEC circumvent the standard PAK activation mechanism, consistent with a previous finding that inactivation of host small GTPases did not alter EPEC's ability to form actin rich pedestals [263].

CHAPTER IV

VIRA INDUCES EZRIN ACTIVATION DURING SPREAD OF *SHIGELLA.*

Introduction

VirA is a conserved homolog important for cell-to-cell spread and seems to be involved in actin rearrangement during infection by *Shigella* [264]. Our studies indicated VirA is not a tubulin modifier as previously described. Currently, VirA has no known target in the host cell, although its homolog EspG targets ARF and PAK proteins. EspG and VirA are structurally homologous, with the N-terminal beta sheet of EspG rotated and translated toward the central sheet (figure 17). Both proteins contain a conserved patch between the C-terminal helical bundle and the central sheet (figure 18 and 19), which has been implicated in the binding of PAK proteins by EspG.

This study presents the structural and functional differences between EspG and VirA, along with providing an end-point target for VirA's mechanism of function. We illustrate that while a structural analysis shows similarities in the binding pockets of EspG and VirA, VirA does not bind the PBD of PAK or GBD (GTPase binding domain) of NWASP. Further structural analysis indicates VirA would not be able to bind Arf proteins as compared to EspG [54]. Attempts to find host targets

show that VirA indirectly induces ezrin activation and that EspG can complement VirA's function for cell to cell spread.

Methods

Cell lines: HeLa cells were maintained in Dulbecco's modified Eagles medium (GIBCO) supplemented with 10% fetal bovine serum, 1% pen/strep.

VirA direct binding assay: Purified His-tagged Δ44VirA and Δ43EspG were added to 35 µL of 50% slurry of GST, PAK1PBD-GST and N-WASPPBD-GST bound sepharose in the presence of PBS buffer with 1% triton-X100. The samples were incubated for 1 hour at 4°C. The agarose was washed 3 times with PBS/triton buffer and boiled in SDS-PAGE buffer and DTT. The samples were subjected to SDS-PAGE and Western blotting with an anti-hexahistidine primary antibody (Santa Cruz Biotechnology) and goat anti-rabbit secondary (LI-COR).

Structural Analysis and Figure preparation: PyMol was used for figure preparation.

Plasmids and bacterial strains: The native promoter of *virA*, a 263 bp upstream region, was amplified from *S. flexneri* by PCR using primers that introduced a 5'-BamHI site and a 3' XhoI site. This PCR product was then ligated into BglII and XhoI cut pET 21 vector. This process removes the T7 promoter from pET 21a and produces a low copy number, ampicillin resistant, vector that expresses *virA* from its native promoter. An NheI site was then introduced between the promoter and

the native start codon for *virA*. This vector is referred to as *virA*_natpro. *espG* and *espG2* were PCR amplified from EPEC strain 301 using primers introducing 5'-NheI and 3'-XhoI sites and ligated into NheI/XhoI digested *virA*_natpro. *VirA*Δ60, removing the N-terminal 60 residues, and a two-residue point mutant *virA*-R185A/D188A were made in the native promoter vector by mutagenic PCR.

Secretion Assay: Shigella strains were grown to an optical density of 0.25-0.35 at 600nm. Strains were induced with 100 μg/mL Congo Red [209]. Samples were collected at different time points and clarified by centrifugation at 2000xg for 5 minutes. Supernatants and pellets were collected. Pellets were washed 3 times with PBS and collected by centrifugation at 4500 rpm for 5 minutes. Pellets were lysed using Cell lytic B buffer (Sigma Aldrich). Protein concentrations were normalized by densitometry and probed by Western using VirA antiserum obtained from the Marcia Goldberg laboratory (Massachusetts General Hospital, Boston, Mass, USA).

Shigella Infection: Monolayers of HeLa cells in 10 cm plates were infected with $5x10^8$ of wild type or *virA* null *S. flexneri* 2a strain 301. Plates were spun down at 2000xg for 10 minutes. Plates were incubated at 37°C for 15 – 120 minutes. Cells were lysed with a non-denaturing PBS/triton based buffer from Cell Signaling (product 9803), supplemented with 10 μg/mL leupeptin, 1mM PMSF, 7 μg/ml pepstatin and 200 μg/mL gentamicin. Cell lysates were clarified by centrifugation at 15,000xg for 5 minutes. The supernatants were normalized for total protein level by densitometry.

Quantification of Ezrin Localization by Western: Normalized quantities of lysates from infected cells were solubilized with SDS, separated by SDS-PAGE (4–12% BisTris gradient acrylamide gels or 10% Tris/glycine acrylamide gels), and transferred to 0.45-μm nylon-supported nitrocellulose membranes. Membranes were blocked in Odyssey buffer (LI-COR, Lincoln, NE). Ezrin monoclonal rabbit primary antibodies (Cell Signaling Technology) were used at 1:1000 dilution in a 1:1 mixture of Odyssey buffer and Tween/Tris-buffered saline. For detection with the Odyssey infrared imaging system, goat anti-rabbit secondary fluorophore-conjugated antibodies were used at 1:20,000 dilution in a 1:1 mixture of Odyssey blocking buffer and Tween/Tris-buffered saline. Bound antibodies were visualized using the Odyssey infrared imaging system and Odyssey software (LI-COR).

Stable Cell lines Expressing Ezrin: Ezrin stable cell lines were obtained from Monique Arpin (Pasteur Institute, Paris, France). LLC-PK2 stable cell lines constitutively expressing wild type ezrin, dominant-negative ezrin (N-terminal domain), constitutively active ezrin (ezrin T567D) and constitutively inactive ezrin (ezrin T567A). Cells were maintained in Dulbecco's modified Eagles medium (GIBCO) supplemented with 10% fetal bovine serum, 1% pen/strep and 0.7 μg/mL G418.

Plaque Assays: Plaque assays were performed as previously described [265]. HeLa cells were infected with 0.5 mL of $1.0x10^7$ cfu/mL of either wild type, VirA null, VirA null complemented with empty vector, VirA null complemented with VirAΔ60 on a VirA native promoter, VirA null complemented with VirA185/188 and VirA null complemented with either EspG or EspG2 on a VirA native promoter in *S. flexneri* 2a

strain 301 [218]. Ezrin stable cell lines were infected with 0.5 mL of $1.0x10^8$ cfu/mL of wild or VirA null *S. flexneri* 2a strain 301 [218]. Monolayers were infected with bacteria for 2 hours at 37°C. Extra-cellular bacteria were removed and overlaid with Dulbecco's modified Eagles medium (GIBCO) (lacking Phenol Red), 0.5% agarose, 10% FBS and 200 µg/mL gentamicin. Monolayers were incubated at 37°C for 72 h and overlaid with 0.33% Neutral Red, Dulbecco's modified Eagles medium (GIBCO) (lacking Phenol Red), 0.7% agarose and 10% FBS. Images were taken with a versa doc model 4000. Plaque size was determined using imageJ.

Gentamicin protection assays: Assays were performed essentially as described by Elsinghorst [217]. Triplicate samples of semi-confluent cells in 12 well plates were infected with $\sim 10^8$ *Shigella*, or a VirA null *Shigella* strain [218] centrifuged at 1000xg for 10 minutes, washed 3 times with DMEM, incubated for 2 hours with DMEM + 200µg/mL gentamicin, washed 5 times with MEM, and lysed with 0.1 deoxycholate in PBS. 40% of the lysed solution was plated onto congo red plates. The inoculum was quantified by enumerating plated serial dilutions.

Results and Discussion

VirA does Not Bind PBD or GBD

While sequence similarities between VirA and EspG are low at 20%, an alignment of the sequences to a surface representation of the VirA and EspG structures indicate a pocket of conservation between the two proteins, and

biochemical experiments indicate that PAK1 binds to EspG using this pocket [53, 54]. To test whether VirA binds the PBD domain of PAK1, a pull down assay was performed using GST and GST-PBD from PAK1. Excess VirAΔ44 and EspGΔ43 were added to the protein bound to resin and probed for the his-tag on EspG and VirA. The western blot indicates VirA does not bind to the PBD of PAK1 as compared to EspG (figure 20A).

While VirA does not bind the PAK1 PBD, the virulence factor may bind a homologous GBD of another protein due to the similarities in the binding pocket. Due to its role in actin reorganization, we tested VirA for binding to the PBD of N-WASP. A direct pull-down assay by a GST control and N-WASP GBD was performed to test whether VirA bound to the N-WASP GBD. Excess VirA was added to both samples and binding was visualized by probing for His-tagged VirA. The pull down indicates VirA does not bind the N-WASP GBD (figure 20B).

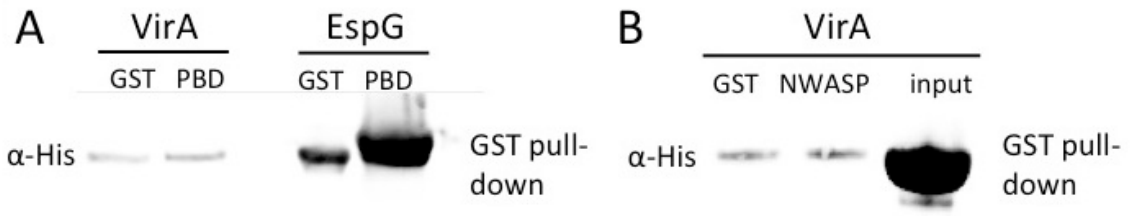

Figure 20: VirA does not bind PBD or GBD during pull-down assays. (A) GST and PAK GST-PBD bound to Nickel-NTA resin did not pull down VirA as compared to EspG. (B) VirA does not bind to the GBD domain of NWASP in a similar assay. Anti-His antibody was used to visualized EspG and VirA from pull-down experiments.

VirA and EspG Binding Site Comparison

The inability of VirA to bind PBDs is a surprising result due to the structural similarities and the area of conservation, which was previously described in chapter III, in the binding pocket between EspG and VirA [53, 54, 159, 160]. The PAK PBD peptide was docked into the VirA binding pocket (figure 21A) and an overlay of the EspG-PBD structure with VirA was made to visualize the difference in residues at the site of protein-protein interaction (figure 21B)[54, 159]. Many of the EspG residues found to be involved in binding PAK are also closely conserved in VirA, with residues N323, Q293, N212, and I307 of EspG matching in residue and location to N315, Q280, N196 and I301/M297 in VirA. Residue V297 of EspG aligns with the structurally similar residue I289 of VirA, which is found on a loop situated in the same location as the helix containing V297. The major differences between the two binding pockets are residues L300 and V346 of EspG that do not match residues Y293 and P350 of VirA, which are located in analogous positions [54]. Differences in binding may also be the result of the difference in helix 9 of VirA and EspG. Helix 9 in EspG is bent, effectively closing the binding pocket, whereas helix 9 is VirA is straight increasing the solvency of the pocket and reducing van der Waal interactions, which can affect binding affinity (figure 21c). The relative conservation of the binding pockets coupled with VirA's inability to bind PAK underscores the importance of using a combination of methods to study effector function.

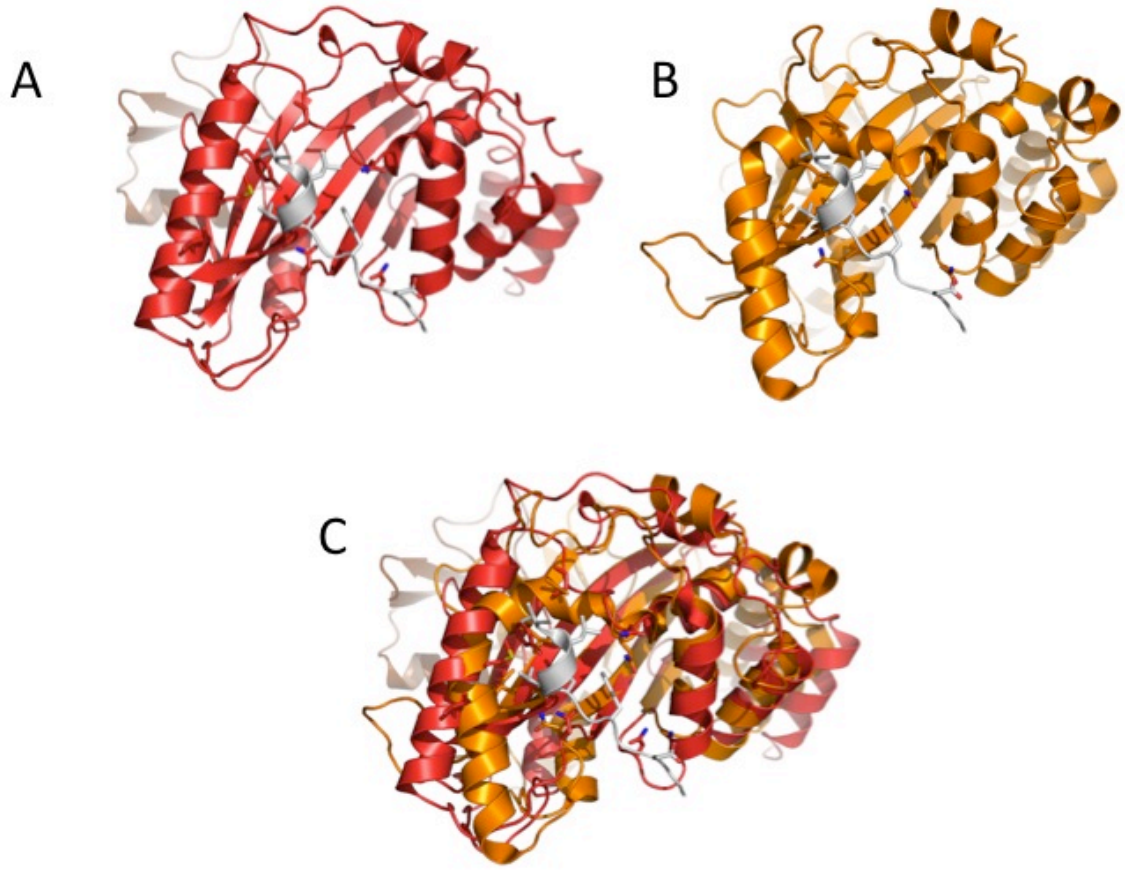

Figure 21: Comparison of PAK PBD binding site of EspG to VirA. The PBD peptide from the EspG-PBD crystal structure (B) was docked in VirA (A). (C) An overlay of both structures reveals similar residue interactions with PBD for both EspG and VirA. VirA is colored in Red, EspG is colored in Orange and PAK peptide is colored in grey. Figure adapted from Seluynin et al. 2011[54].

VirA Lacks the ARF Binding Site

A comparison of the EspG and VirA structures shows that VirA would not be able to bind ARF6, the other host target of EspG. ARF6 binds the opposite face of the long helix (helix 9 or 10, whatever is on the alignment in some previous fig) of EspG that is involved in binding PAK1 (figure 22A) [54]. The two key structural differences between EspG and VirA, destroy the ARF6 binding site. The foremost difference is the orientation of the N-terminal beta sheet of VirA (colored brown) and EspG (colored yellow) (figure 22B). The beta sheet of EspG is rotated and translated away from the ARF6 binding site, while the VirA beta sheet is essentially oriented in a flat position. The upper arrow in figure 22B notes that the position of VirA's beta sheet would prevent ARF6 binding by steric hindrance. In addition, VirA lacks a loop that EspG uses to interact and bind ARF6, which is indicated by the lower arrow (figure 22B).

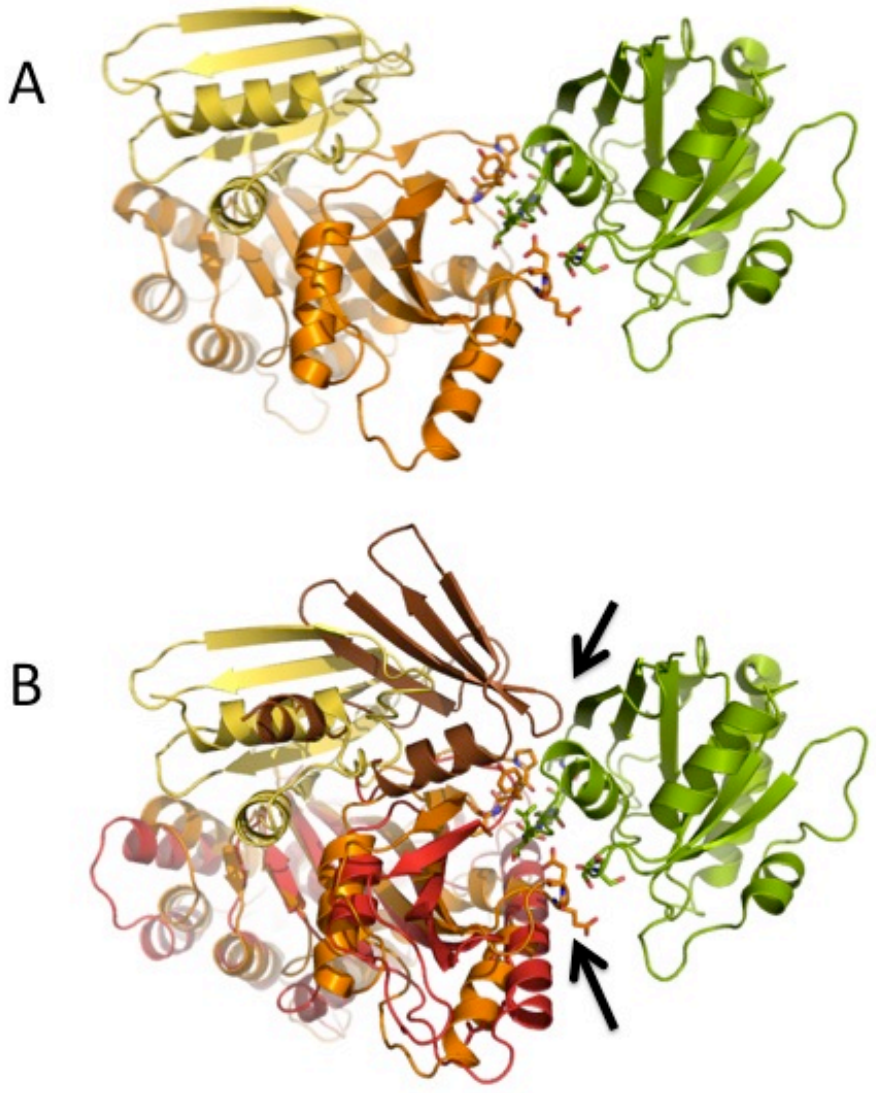

Figure 22: Comparison of ARF binding site of EspG to VirA. (A) Co-crystal structure of EspG bound to ARF6. The N-terminal beta sheet of EspG was colored in yellow, while the rest of the structure is colored in orange. ARF6 is colored in green. (B) An overlay of EspG bound to ARF6 and VirA. The N-terminal beta sheet of VirA is colored in brown, while the rest of the structure is colored in red. The lower arrow indicates a loop on EspG, which VirA lacks, important for interactions with ARF6. The upper arrow indicates the brown beta sheet of VirA would block possible ARF6 binding by steric hindrance. Figure adapted from Seluynin et al. 2011[54].

EspG can Substitute for VirA Function During Infection

Previous studies have shown that VirA is important for cell to cell spread of *Shigella* [264]. To evaluate VirA's roll in cell-to-cell spread and determine whether EspG can function in the same capacity as VirA while having different host targets, spread assays were used to study the effects of homologs and mutants on *Shigella* spread. All proteins were expressed behind a native promoter of *virA* to obtain near native protein levels. As shown in figure 23, use of the native promoter construct produces similar induction kinetics and expression levels to WT *Shigella*, and deletion of the N-terminal 60 residues prevents secretion.

As shown in figure 19, and previously reported using an over-expression system[209], deletion of *virA* severely inhibits cell-to-cell spread as compared to wild-type, and this phenotype can be recovered with wild-type *virA* on a plasmid. In addition, mutation of residues arginine 185 and aspartate 188 of *virA*, which correspond to residues arginine 205 and aspartate 208 of *espG* that are important for PAK1 binding [53], inhibit spread as well (Figure 24). This indicates that the conserved pocket is functionally important for VirA, and may act as a scaffold in a similar manner as EspG. Substitution with *espG*, but not *espG2*, recovers spread of a *virA* null strain (Figure 25). *espG2* has even lower sequence similarity (13%) to *virA* than *espG*, and may be playing a non-redundant roll during EPEC infection as previously indicated [215]. This data suggest EspG may be acting in a similar pathway as VirA due to its ability to fully recover a *virA* null phenotype.

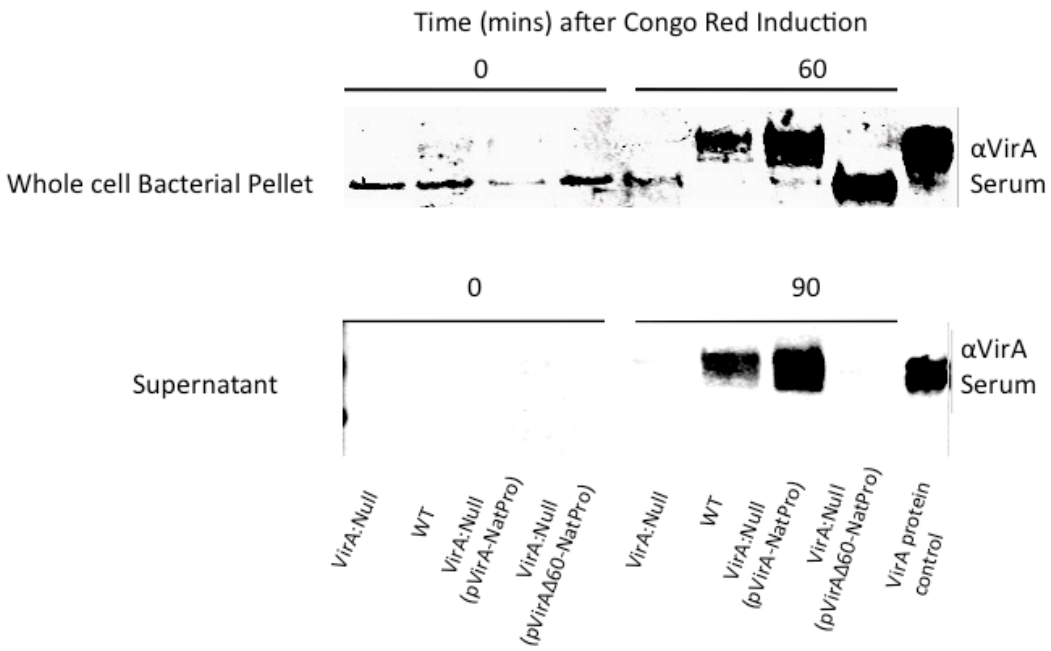

Figure 23: The N-terminus of VirA is required for type three secretion. VirA expression and secretion by *S. flexneri* was tracked over time after induction by Congo Red. Whole cell pellets and supernatants were probed for VirA by anti-VirA Rabbit serum. At time zero, after addition of Congo Red, VirA expression is essentially zero (whole cell pellet). VirA expression peaks after 60 minutes in wild type and *virA* null strains complemented with WT *virA* or a N-terminal mutant. Only full length VirA is secreted into the supernatant through a T3SS after 90 minutes as indicated for WT and *virA* null strains complemented with full length *virA*.

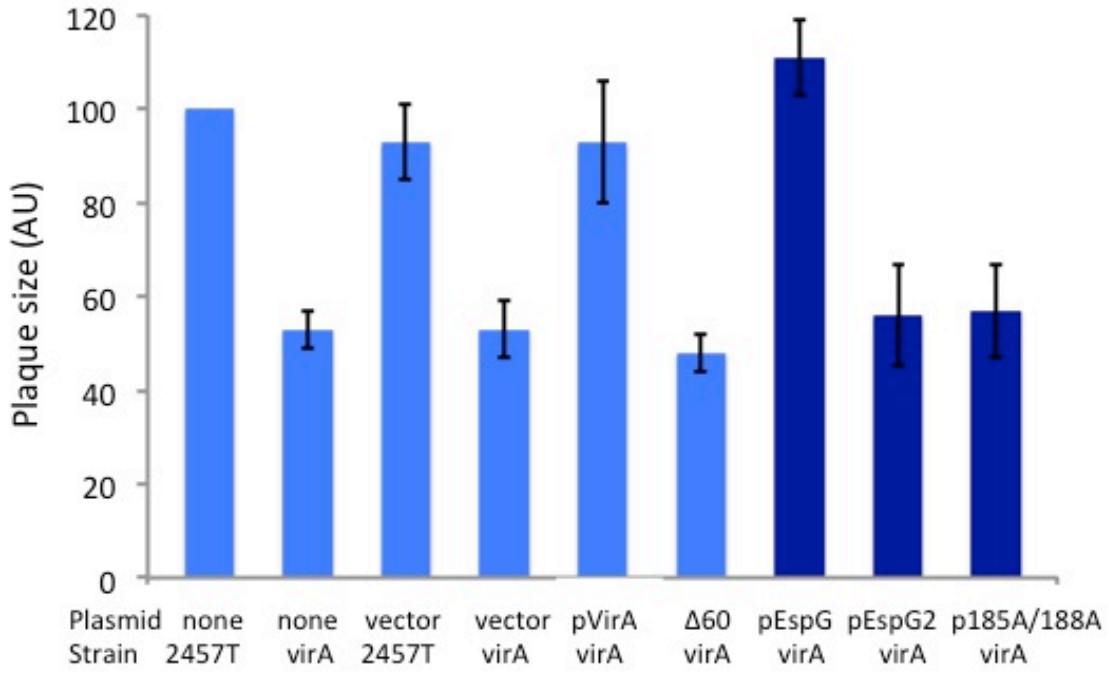

Figure 24: Complement Plaque Assay. HeLa cells were infected with *Shigella* strains and plaque size was measured in arbitrary units. Strains used: Wild type (2457T) and *virA* null (*virA*). Strains contained either empty vector (vector) or vector comprising wild type *virA* (pVirA), virAΔ60 (Δ60), *espG* (pEspG), *espG2* (pEspG2) and *virA*185/188(p185A/188A). Proteins were expressed using the native promoter for *virA*.

Ezrin Activation

To investigate possible targets of VirA, an infection model was used to study differences in protein localization and activation by the protein. Infection by a WT or virA null strain, unlike transfection with virA, allows for a localized spatial and temporal study of VirA's effect on host cell cytoskeletal related proteins. HeLa cells were infected for short time periods to allow for maximal entry and some spread. Infected cell lysate supernatants were probed for differences in soluble protein concentrations and phosphorylation using the cytoskeletal antibody sampler kit (Cell Signaling Technology). While supernatants showed little differences in phosphorylated cytoskeletal proteins (data not shown), *virA* null lysates revealed a 5-fold greater concentration in soluble ezrin as compared to WT lysates. In addition, soluble actin was greater in WT lysates (figure 25). These findings are consistent with other results indicating that VirA induces membrane ruffling during microinjection, which requires changes in actin localization [157]. Ezrin is known to be important for *Shigella* entry and spread and EPEC pedestal formation [266, 267]. Ezrin is soluble in its closed inactive form and can either be activated by either phosphorylation or binding to PIP_2 and a substrate (figure 26) [268-275]. When activated, ezrin tethers actin filaments to the plasma membrane through a membrane bound protein and can control cell polarity and membrane ruffling [276-281]. The active form of ezrin is then found in the insoluble fraction. The observation that lysates from *virA* null infected HeLa cells contain more ezrin than lysates from WT infected cells indicate that VirA plays a role in ezrin activation.

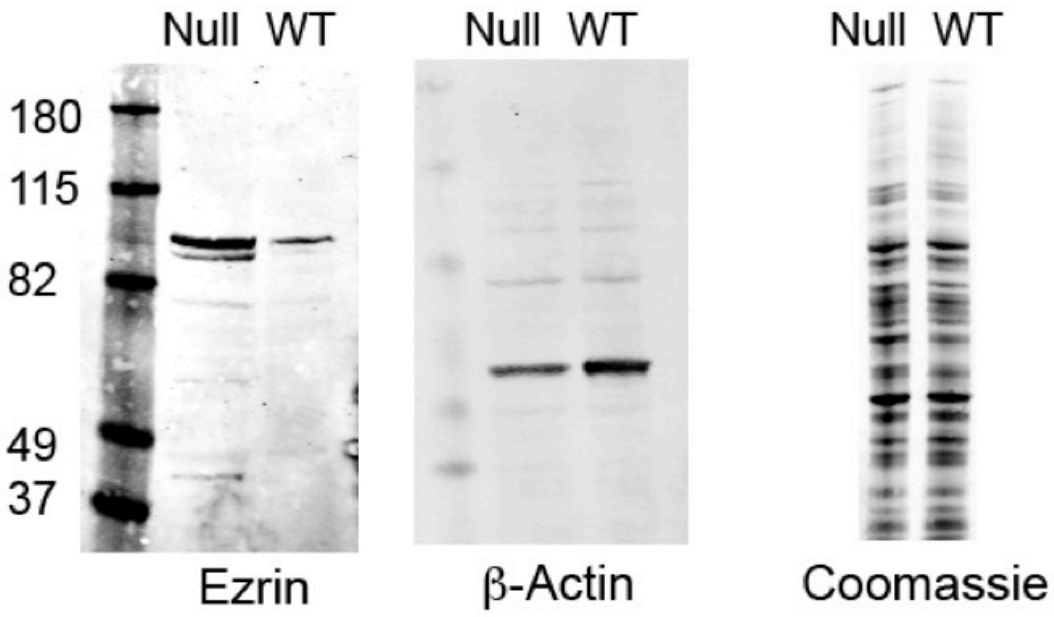

Figure 25: Western analysis of total soluble ezrin during infection. Cell lysate supernatant was probed for total soluble ezrin. Soluble ezrin was 5-fold greater during a VirA null infection as compared to WT *Shigella*. Total soluble Actin was 2-fold greater during WT infection. Cell lysates were stained with coomassie and normalized using densitometry.

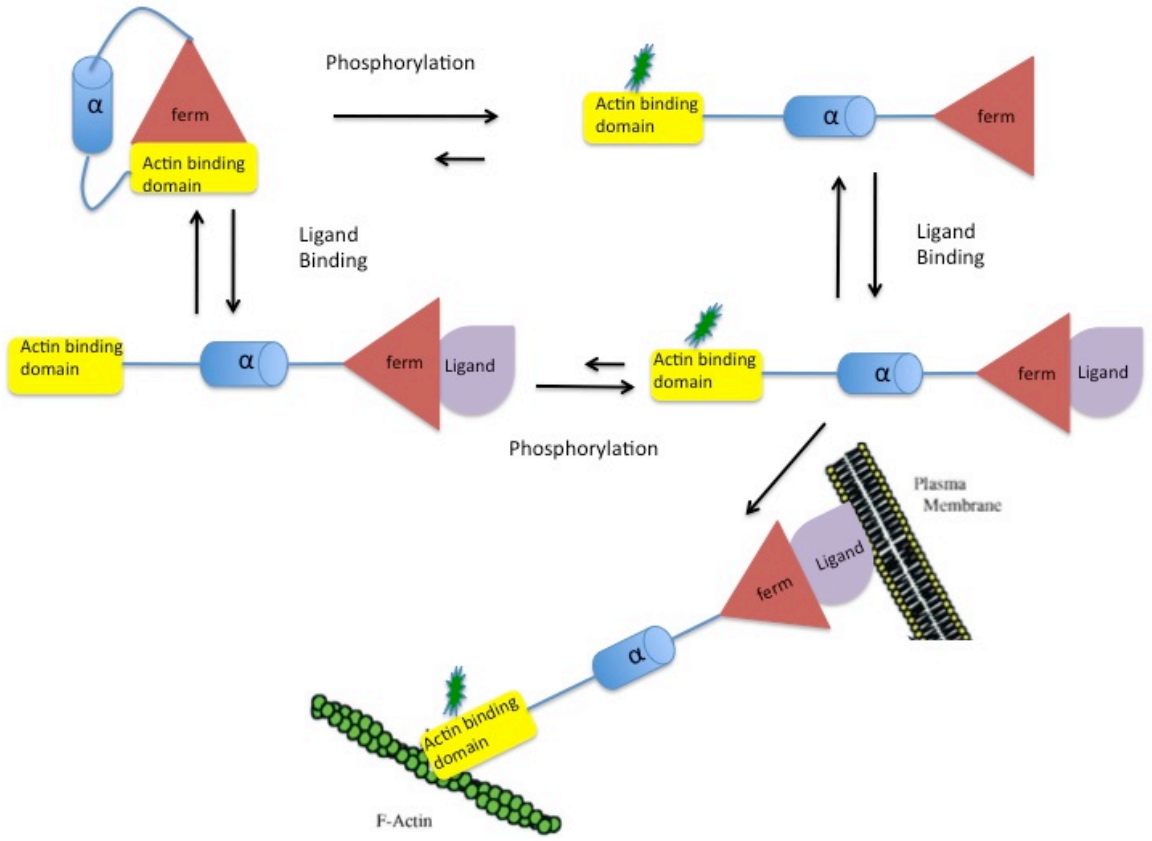

Figure 26: Ezrin activation. Ezrin is found in a closed soluble state when inactivated. Activation occurs through threonine-567 phosphorylation of the tail of ezrin or FERM binding of a membrane bound protein, releases the tail from the FERM domain[269, 270, 273]. The phosphorylated tail binds F-actin, thereby linking F-actin to the Plasma Membrane[273, 280, 281]. Figure adapted from Pearson et al. 2000[282]

Ezrin Activation Required During Shigella Spread

Since VirA does not bind ezrin directly (data not shown), VirA likely acts either through a kinase or by recruiting an ERM domain substrate. To study VirA's effect on ezrin, plaque assays and invasion assays were performed using stable cell lines expressing wild type, dominant-negative, constitutively active, and constitutively inactive ezrin. The dominant-negative mutant consists of the ERM domain expressed alone and is thought to prevent ezrin activation by competing for ERM domain ligand [276, 280]. The constitutively inactive and active lines contain mutations of the T517 phospho site, and are T567A in the inactive mutant and T567D in the constitutively active mutant [283, 284]. The invasion assays indicate that VirA has no effect on entry of the bacteria into any of the cell lines (figure 27A). The plaque assays by contrast indicate that VirA null bacteria produce ~4 fold smaller plaques compared to WT bacteria in WT ezrin expressing cells. The dominant-negative ezrin completely inhibits VirA null spread, while limiting WT spread to 50% of normal spread (figure 27B). Expression of constitutively active ezrin enables VirA null bacteria to form similar plaques to WT *Shigella*, indicating that activation of Ezrin eliminates the need to express VirA during cell-to-cell spread.

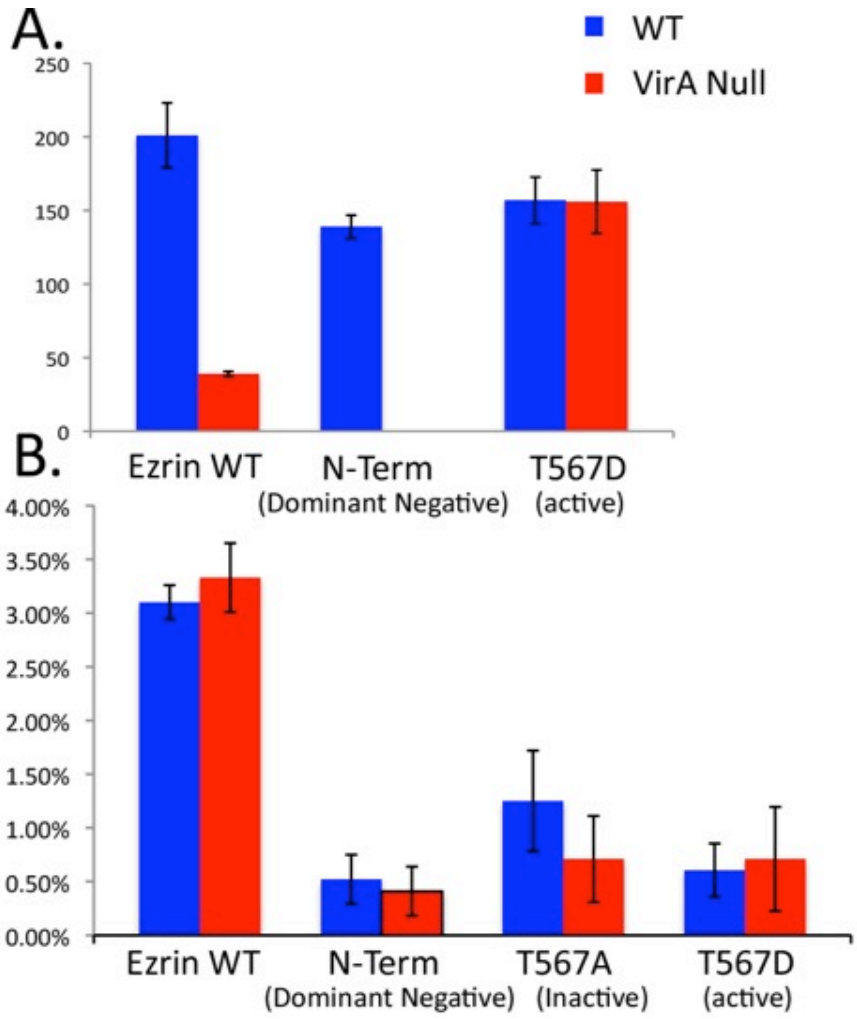

Figure 27: Quantification of WT and VirA Null Shigella differences during spread (A) and invasion (B) of ezrin stable cell lines. (A) A plaque assay measuring spread of wild type (blue) and VirA null [54] *Shigella* measured in arbitrary units (performed in triplicate). (B) Gentamicin protection assay measuring percent entry of wild type (blue) and VirA null [54] *Shigella* into cell. Cell lines used for assays are LLC-pk1 stable constitutively express wild type (ezrin WT), dominant-negative (N-term), constitutively active (T567D) and constitutively inactive (T567A) ezrin.

VirA does not bind the PBD of PAK1 or NWASP, though a structural comparison of residues important for PBD binding indicates most are closely conserved and located in the correct location for binding. Further structural comparisons also indicate steric hindrance and a lack of residue interactions would inhibit ARF6 binding to VirA. While the two virulence proteins do not bind the same targets, a complement study indicates EspG can recover a VirA null phenotype in a spread assay. This indicates that the proteins either function in similar pathways or in different parts of the same pathway. While a direct target of VirA has yet to be determined, downstream ezrin activation by VirA seems to be important for the cell-to-cell spread of *S. flexneri.* The observation of ezrin activation by VirA indicates a requirement for actin re-localization to the plasma membrane cell-to-cell spread of the bacteria.

CHAPTER V

CONCLUSIONS AND FUTURE DIRECTIONS

Summary

Shigella and EPEC are causative agents of gastrointestinal inflammation and diarrhea [174, 188, 285-287]. While they have two different modes of infection, both bacteria use TTS virulence factors to promote infection of host tissues [166, 191]. Virulence factors VirA and EspG are distant homologs found to be important for cell-to-cell spread and pedestal formation [158, 205-208, 212, 288]. Prior to undertaking this project, studies had shown that EspG is capable of substituting for VirA during *Shigella* spread [206, 288]. Additional studies suggested VirA and EspG might promote microtubule destabilization [158, 211, 213, 255].

Chapter two of this thesis describes the structure of VirA determined by x-ray crystallography. VirA's structure is a three-domain protein, a central beta sheet scaffolding an N-terminal beta sheet and a C-terminal helical bundle. VirA has a novel fold, not yet found in the PBD. The structure lacks similarity to papain or other cysteine proteases, contrary to previous suggestions [158]. A sequence alignment of EspG and VirA proteins indicate low conservation, but when mapped onto a surface rendering of VirA's structure, a patch of high conservation can be found in the pocket underneath the helical bundle. The conserved patch highlights a possible

functional region of VirA. Further experiments show that VirA does not proteolyze tubulin or destabilize microtubules through direct or indirect methods.

In chapter III the structure of EspG is described, compared to VirA, and the host target of EspG was identified. The x-ray crystal structure of EspG is structurally similar to VirA, except the N-terminal beta sheet of EspG is rotated and translated towards the central beta sheet. The pocket below the helical bundle is highly conserved between the two structures, with two conserved functionally important residues (R185/D188 of VirA and R205/D208 of EspG) oriented and located on the underside of the helical bundle. Rac activation assays revealed EspG bypasses Rac to directly bind the PBD of PAK1. Mutating the two conserved (R205A and D208A) significantly reduces binding of PBD to EspG. Expression of EspG in cells leads to a decrease, and probable degradation, of phosphorylated (activated) PAK1 protein. The exact mechanism by which PAK activation promotes virulence is unknown. An immediate consequence of EspG expression is an apparent reduction in activated PAK.

Chapter IV reports functional studies of VirA and the identification of a down stream target of VirA, which is likely important during *Shigella* spread. While structurally similar to EspG, VirA did not bind PAK1 PBD or the related N-WASP PBD. Since the virulence factors do not target the same host protein, EspG was evaluated for its ability to complement for VirA during *Shigella* spread and was found to be capable of restoring VirA's function. Although the homologs do not bind the same host protein as the structures may suggest, the complementation data

indicate the virulence factors are targeting the same pathway at different steps or similar pathways. Infection studies revealed that VirA induces ezrin activation in an indirect manner during infection. Ezrin activation by VirA is important for cell-to-cell spread of *Shigella*, which may result in re-organization of actin at the site of protrusions for entry into a new cell.

Future Directions

Short Term Goals

The signaling pathways through which VirA and EspG promote infection must be further elucidated. To achieve this end, the direct target(s) of VirA need to be identified in order to compare signaling pathways of VirA and EspG, and to determine how they functionally substitute for each other. In addition, further studies will be required to understand the relevance of EspG-Arf-PAK mediated membrane trafficking inhibition and whether EPEC uses EspG to inhibit cytokine secretion [289]. Also, we will study whether VirA inhibits membrane trafficking in addition to promoting ezrin activation and enhancing *Shigella* spread. Ezrin activation may be integral to both VirA and EspG activity, but this needs to be determined.

While we know VirA activates ezrin, the pathway by which this process occurs is unknown. Our studies suggest ezrin activation is integral to the successful

spread of Shigella. To determine the signaling pathway through which VirA acts, we need to find the initial target. Currently, there is no known direct binding partner of VirA. Determining the identity of this molecular target is an essential step in further understanding of VirA's role in virulence.

Ezrin activation plays an important role in the promotion of cell-to-cell spread by *Shigella*. It is our belief that ezrin activation plays an important role in protrusion formation during cell-to-cell spread. Pedestal formation is similar to protrusion formation in that it requires a localization of actin at the point of attachment or spread. It is critical to determine if ezrin activation occurs during pedestal formation, and if it is EspG dependent.

We have established a role for VirA in the importance of spread of the bacteria, but VirA may play a role beyond this phenotype. Recent studies suggest VirA is involved in inhibiting membrane trafficking, much like EspG [289]. EspG acts as a scaffold to target Arf and PAK proteins to the golgi [54]. By blocking the active sites of Arf, EspG may prevent signaling for normal membrane trafficking. Further studies suggest this process inhibits the secretion of cytokines for an immune response to EPEC [289]. We are interested to see if inhibition of membrane trafficking by VirA is an important or secondary role during infection and during over expression of VirA inside the cell.

While EspG overexpression is known to target ARF and PAK to the golgi, which results in altered membrane trafficking, the importance of this function and of EspG for EPEC infection is unknown [54]. ARF6 plays a role in both endosome

recycling and membrane ruffling due to Rac induced actin rearrangement [290, 291]. EspG or VirA dependent inhibition of protein secretion has not been shown in an infection model and may be due to overexpression of EspG. This needs to be further evaluated. To understand this process, protein secretion needs to be evaluated using wild type and an EspG null strain. If EspG does inhibit secretion during infection, presumably under conditions where EspG levels are quite low, this would imply a specific PAK target that is critical for protein secretion. To our knowledge no such PAK substrate has been identified; PAK's role in regulating protein secretion has not yet been noted. If inhibition of protein secretion results in the loss of cytokine secretion, we will study how PMN recruitment is affected using a mouse model, to determine if EspG is important for prevention of inflammation and clearance of the bacteria.

Long Term Goals

While progress towards identifying new effectors and their roles in infection is steady, this process is slow. Many experiments lead to non-relevant and misleading data. It is necessary to establish more effective experiments to elucidate the role of virulence factors in different life cycle stages and host environment. Bacteria infection requires several successful steps to successfully colonize host tissues-extracellular immune system evasion, colonization, intracellular survival and dissemination. The virulence factors have evolved to perform different functions during these steps, which makes it difficult to successfully determine the

functions of the proteins. Experiments must allow for differences in host cell type and host environment. A long-term goal for this project is to be able to establish biologically relevant experiments to determine the function of virulence factors that address individual steps of infection.

Understanding how virulence factors interact with their host cell targets not only allows us to recognize their function during infection, but provides a better understanding in how signaling occurs within the cells. A broad goal for our lab is to use what we know about how virulence factors function to identify novel signaling pathways in eukaryotic cells. Eukaryotic cell signaling pathways are extensive and complex. A single pathway can be involved in many normal cell functions, which can obscure some subtle signaling events. Virulence factors target different parts of the pathway and by understanding how the factors manage to usurp these pathways we can determine the roles of these signaling pathways in normal host cell function. Due to the nature by which virulence factors usurp host cell pathways, we can ue their functions as a tool to further on-going work to study diseases.

LIST OF PUBLICATIONS

Germane K.L., Ohi R., Goldberg M.B., Spiller B.W. *Structural and Functional Studies Indicate that Shigella VirA is not a Protease and does not Directly Destabilize Microtubules.* Biochemistry,2008. **47** (39):10241-3.

Germane K.L., Spiller B.W. *Structural and Functional Studies Indicate that the EPEC Effector, EspG, Directly Binds p21-Activated Kinase*. Biochemistry, 2011. **50**(6):917-9.

LeNoue-Newton M., Watkins G.R., Zou P., Germane K.L., McCorvey L.R., Wadzinski B.E., Spiller B.W. *The E3 ubiquitin ligase- and protein phosphatase 2A (PP2A)-binding domains of the Alpha4 protein are both required for Alpha4 to inhibit PP2A degradation.* Journal of Biological Chemistry, 2011. **286**(20):17665-71.

BIBLIOGRAPHY

1. Dean, P., *Functional domains and motifs of bacterial type III effector proteins and their roles in infection.* FEMS microbiology reviews, 2011.

2. Ghosh, P., *Process of protein transport by the type III secretion system.* Microbiology and molecular biology reviews : MMBR, 2004. **68**(4): p. 771-95.

3. Troisfontaines, P. and G.R. Cornelis, *Type III secretion: more systems than you think.* Physiology, 2005. **20**: p. 326-39.

4. Coburn, B., I. Sekirov, and B.B. Finlay, *Type III secretion systems and disease.* Clinical microbiology reviews, 2007. **20**(4): p. 535-49.

5. Hueck, C.J., *Type III protein secretion systems in bacterial pathogens of animals and plants.* Microbiology and molecular biology reviews : MMBR, 1998. **62**(2): p. 379-433.

6. Galan, J.E., *Common themes in the design and function of bacterial effectors.* Cell host & microbe, 2009. **5**(6): p. 571-9.

7. Tanida, I., *Autophagy basics.* Microbiology and immunology, 2011. **55**(1): p. 1-11.

8. Flannagan, R.S., G. Cosio, and S. Grinstein, *Antimicrobial mechanisms of phagocytes and bacterial evasion strategies.* Nature Reviews Microbiology, 2009. **7**(5): p. 355-366.

9. Barz, C., et al., *The Yersinia Ser/Thr protein kinase YpkA/YopO directly interacts with the small GTPases RhoA and Rac-1.* FEBS letters, 2000. **482**(1-2): p. 139-43.

10. Grosdent, N., et al., *Role of Yops and adhesins in resistance of Yersinia enterocolitica to phagocytosis.* Infection and immunity, 2002. **70**(8): p. 4165-76.

11. Mogemark, L., et al., *Disruption of target cell adhesion structures by the Yersinia effector YopH requires interaction with the substrate domain of p130Cas.* European journal of cell biology, 2005. **84**(4): p. 477-89.

12. Phillips, R.M., et al., *In vivo phospholipase activity of the Pseudomonas aeruginosa cytotoxin ExoU and protection of mammalian cells with phospholipase A2 inhibitors.* The Journal of biological chemistry, 2003. **278**(42): p. 41326-32.

13. Iwai, H., et al., *A bacterial effector targets Mad2L2, an APC inhibitor, to modulate host cell cycling.* Cell, 2007. **130**(4): p. 611-23.

14. Hersh, D., et al., *The Salmonella invasin SipB induces macrophage apoptosis by binding to caspase-1.* Proceedings of the National Academy of Sciences of the United States of America, 1999. **96**(5): p. 2396-401.

15. Schnoor, M. and C.A. Parkos, *Disassembly of endothelial and epithelial junctions during leukocyte transmigration.* Frontiers in bioscience : a journal and virtual library, 2008. **13**: p. 6638-52.

16. Sansonetti, P.J., *Molecular and cellular mechanisms of invasion of the intestinal barrier by enteric pathogens. The paradigm of Shigella.* Folia microbiologica, 1998. **43**(3): p. 239-46.

17. Sansonetti PJ, A.J., Huerre M, Harada A, Matsushima K, *Interleukin-8 Controls Bacterial Transepithelial Translocation at the Cost of Epithelial Destruction in Experimental Shigellosis.* Infection and immunity, 1999. **67**(3): p. 1471-1480.

18. Shames, S.R., et al., *The pathogenic E. coli type III effector EspZ interacts with host CD98 and facilitates host cell prosurvival signalling.* Cellular microbiology, 2010. **12**(9): p. 1322-39.

19. Dong, N., L. Liu, and F. Shao, *A bacterial effector targets host DH-PH domain RhoGEFs and antagonizes macrophage phagocytosis.* The EMBO journal, 2010. **29**(8): p. 1363-76.

20. Tu, X., et al., *EspH, a new cytoskeleton-modulating effector of enterohaemorrhagic and enteropathogenic Escherichia coli.* Molecular microbiology, 2003. **47**(3): p. 595-606.

21. Brugirard-Ricaud, K., et al., *Site-specific antiphagocytic function of the Photorhabdus luminescens type III secretion system during insect colonization.* Cellular microbiology, 2005. **7**(3): p. 363-71.

22. Rosenshine, I., et al., *A pathogenic bacterium triggers epithelial signals to form a functional bacterial receptor that mediates actin pseudopod formation.* The EMBO journal, 1996. **15**(11): p. 2613-24.

23. Cambronne, E.D. and O. Schneewind, *Bacterial invasins: molecular systems dedicated to the invasion of host tissues.* Contributions to microbiology, 2005. **12**: p. 181-209.

24. Ridley, A.J., *Rho GTPases and actin dynamics in membrane protrusions and vesicle trafficking.* Trends in cell biology, 2006. **16**(10): p. 522-9.

25. Jaffe, A.B. and A. Hall, *Rho GTPases: biochemistry and biology.* Annual review of cell and developmental biology, 2005. **21**: p. 247-69.

26. Van Aelst, L. and C. D'Souza-Schorey, *Rho GTPases and signaling networks.* Genes & development, 1997. **11**(18): p. 2295-322.

27. Buss, C., et al., *Identification and characterization of Ibe, a novel type III effector protein of A/E pathogens targeting human IQGAP1.* Cellular microbiology, 2009. **11**(4): p. 661-77.

28. Alto, N.M., et al., *Identification of a bacterial type III effector family with G protein mimicry functions.* Cell, 2006. **124**(1): p. 133-45.

29. Friebel, A., et al., *SopE and SopE2 from Salmonella typhimurium activate different sets of RhoGTPases of the host cell.* The Journal of biological chemistry, 2001. **276**(36): p. 34035-40.

30. Hardt, W.D., et al., *S-typhimurium encodes an activator of Rho GTPases that induces membrane ruffling and nuclear responses in host cells.* Cell, 1998. **93**(5): p. 815-826.

31. Demali, K.A., A.L. Jue, and K. Burridge, *IpaA targets beta1 integrins and rho to promote actin cytoskeleton rearrangements necessary for Shigella entry.* The Journal of biological chemistry, 2006. **281**(51): p. 39534-41.

32. Hamiaux, C., et al., *Structural mimicry for vinculin activation by IpaA, a virulence factor of Shigella flexneri.* EMBO reports, 2006. **7**(8): p. 794-9.

33. Clifton, D.R., et al., *A chlamydial type III translocated protein is tyrosine-phosphorylated at the site of entry and associated with recruitment of actin.* Proceedings of the National Academy of Sciences of the United States of America, 2004. **101**(27): p. 10166-10171.

34. Upadhyay, A., et al., *The guanine-nucleotide-exchange factor BopE from Burkholderia pseudomallei adopts a compact version of the Salmonella SopE/SopE2 fold and undergoes a closed-to-open conformational change upon interaction with Cdc42.* The Biochemical journal, 2008. **411**(3): p. 485-93.

35. Stevens, M.P., et al., *A Burkholderia pseudomallei type III secreted protein, BopE, facilitates bacterial invasion of epithelial cells and exhibits guanine nucleotide exchange factor activity.* Journal of bacteriology, 2003. **185**(16): p. 4992-6.

36. Ma, C.X., et al., *Citrobacter rodentium infection causes both mitochondrial dysfunction and intestinal epithelial barrier disruption in vivo: role of*

mitochondrial associated protein (Map). Cellular Microbiology, 2006. **8**(10): p. 1669-1686.

37. Martinez, E., et al., *Binding to Na(+) /H(+) exchanger regulatory factor 2 (NHERF2) affects trafficking and function of the enteropathogenic Escherichia coli type III secretion system effectors Map, EspI and NleH.* Cellular microbiology, 2010. **12**(12): p. 1718-31.

38. Arbeloa, A., et al., *Subversion of actin dynamics by EspM effectors of attaching and effacing bacterial pathogens.* Cellular microbiology, 2008. **10**(7): p. 1429-41.

39. Cheng, H.C., et al., *Structural mechanism of WASP activation by the enterohaemorrhagic E-coli effector EspF(U).* Nature, 2008. **454**(7207): p. 1009-U54.

40. Campellone KG, R.D., Leong JM, *EspFU is a translocated EHEC effector that interacts with Tir and N-WASP and promotes Nck-independent actin assembly.* Development Cell, 2004. **7**(2): p. 217-28.

41. Mitra, K., D.G. Zhou, and J.E. Galan, *Biophysical characterization of SipA, an actin-binding protein from Salmonella enterica.* Febs Letters, 2000. **482**(1-2): p. 81-84.

42. McGhie, E.J., R.D. Hayward, and V. Koronakis, *Cooperation between actin-binding proteins of invasive Salmonella: SipA potentiates SipC nucleation and bundling of actin.* Embo Journal, 2001. **20**(9): p. 2131-2139.

43. Mounier, J., et al., *The IpaC carboxyterminal effector domain mediates Src-dependent actin polymerization during Shigella invasion of epithelial cells.* Plos Pathogens, 2009. **5**(1): p. e1000271.

44. Poh, J., et al., *SteC is a Salmonella kinase required for SPI-2-dependent F-actin remodelling.* Cellular Microbiology, 2008. **10**(1): p. 20-30.

45. Shaikh, N., J. Terajima, and H. Watanabe, *IpaC of Shigella binds to the C-terminal domain of beta-catenin.* Microbial Pathogenesis, 2003. **35**(3): p. 107-117.

46. Crepin, V.F., et al., *Dissecting the role of the Tir:Nck and Tir:IRTKS/IRSp53 signalling pathways in vivo.* Molecular Microbiology, 2010. **75**(2): p. 308-323.

47. Brown, M.D., et al., *Actin Pedestal Formation by Enteropathogenic Escherichia coli Is Regulated by IQGAP1, Calcium, and Calmodulin.* Journal of Biological Chemistry, 2008. **283**(50): p. 35212-35222.

48. Cantarelli, V.V., et al., *Talin, a host cell protein, interacts directly with the translocated intimin receptor, Tir, of enteropathogenic Escherichia coli, and is essential for pedestal formation.* Cellular Microbiology, 2001. **3**(11): p. 745-751.

49. Smith, K., et al., *Enteropathogenic Escherichia coli Recruits the Cellular Inositol Phosphatase SHIP2 to Regulate Actin-Pedestal Formation.* Cell host & microbe, 2010. **7**(1): p. 13-24.

50. Brandt, S., et al., *Dual infection system identifies a crucial role for PKA-mediated serine phosphorylation of the EPEC-Tir-injected effector protein in regulating Rac1 function.* Cellular Microbiology, 2009. **11**(8): p. 1254-1271.

51. Bommarius, B., et al., *Enteropathogenic Escherichia coli Tir is an SH2/3 ligand that recruits and activates tyrosine kinases required for pedestal formation.* Molecular Microbiology, 2007. **63**(6): p. 1748-1768.

52. Freeman, N.L., et al., *Interaction of the enteropathogenic Escherichia coli protein, translocated intimin receptor (Tir), with focal adhesion proteins.* Cell Motility and the Cytoskeleton, 2000. **47**(4): p. 307-318.

53. Germane, K.L. and B.W. Spiller, *Structural and Functional Studies Indicate That the EPEC Effector, EspG, Directly Binds p21-Activated Kinase.* Biochemistry, 2011. **50**(6): p. 917-9.

54. Selyunin, A.S., et al., *The assembly of a GTPase-kinase signalling complex by a bacterial catalytic scaffold.* Nature, 2011. **469**(7328): p. 107-11.

55. Bulgin, R., et al., *The T3SS Effector EspT Defines a New Category of Invasive Enteropathogenic E. coli (EPEC) Which Form Intracellular Actin Pedestals.* Plos Pathogens, 2009. **5**(12): p. -.

56. Kim, M., et al., *Bacteria hijack integrin-linked kinase to stabilize focal adhesions and block cell detachment.* Nature, 2009. **459**(7246): p. 578-U109.

57. Scidmore, M.A., E.R. Fischer, and T. Hackstadt, *Restricted fusion of Chlamydia trachomatis vesicles with endocytic compartments during the initial stages of infection.* Infection and immunity, 2003. **71**(2): p. 973-84.

58. Buchmeier, N.A. and F. Heffron, *Inhibition of macrophage phagosome-lysosome fusion by Salmonella typhimurium.* Infection and immunity, 1991. **59**(7): p. 2232-8.

59. Delevoye, C., et al., *Conservation of the biochemical properties of IncA from Chlamydia trachomatis and Chlamydia caviae - Oligomerization of IncA*

mediates interaction between facing membranes. Journal of Biological Chemistry, 2004. **279**(45): p. 46896-46906.

60. Delevoye, C., et al., *SNARE protein mimicry by an intracellular bacterium.* Plos Pathogens, 2008. **4**(3): p. e1000022.

61. Scidmore, M.A. and T. Hackstadt, *Mammalian 14-3-3beta associates with the Chlamydia trachomatis inclusion membrane via its interaction with IncG.* Molecular microbiology, 2001. **39**(6): p. 1638-50.

62. Geddes, K., et al., *Identification of new secreted effectors in Salmonella enterica serovar Typhimurium.* Infection and immunity, 2005. **73**(10): p. 6260-71.

63. Knodler, L.A., et al., *Salmonella type III effectors PipB and PipB2 are targeted to detergent-resistant microdomains on internal host cell membranes.* Molecular microbiology, 2003. **49**(3): p. 685-704.

64. Knodler, L.A. and O. Steele-Mortimer, *The Salmonella effector PipB2 affects late endosome/lysosome distribution to mediate Sif extension.* Molecular biology of the cell, 2005. **16**(9): p. 4108-23.

65. Shotland, Y., H. Kramer, and E.A. Groisman, *The Salmonella SpiC protein targets the mammalian Hook3 protein function to alter cellular trafficking.* Molecular microbiology, 2003. **49**(6): p. 1565-76.

66. Salcedo, S.P. and D.W. Holden, *SseG, a virulence protein that targets Salmonella to the Golgi network.* Embo Journal, 2003. **22**(19): p. 5003-5014.

67. Birmingham, C.L., et al., *Autophagy controls Salmonella infection in response to damage to the Salmonella-containing vacuole.* The Journal of biological chemistry, 2006. **281**(16): p. 11374-83.

68. Pachikara, N., et al., *Productive Chlamydia trachomatis lymphogranuloma venereum 434 infection in cells with augmented or inactivated autophagic activities.* FEMS microbiology letters, 2009. **292**(2): p. 240-9.

69. Ogawa, M., et al., *Escape of intracellular Shigella from autophagy.* Science, 2005. **307**(5710): p. 727-31.

70. Kayath, C.A., et al., *Escape of intracellular Shigella from autophagy requires binding to cholesterol through the type III effector, IcsB.* Microbes and Infection, 2010. **12**(12-13): p. 956-966.

71. Yao, Q., et al., *A bacterial type III effector family uses the papain-like hydrolytic activity to arrest the host cell cycle.* Proceedings of the National Academy of Sciences of the United States of America, 2009. **106**(10): p. 3716-3721.

72. Chellas-Gery, B., C.N. Linton, and K.A. Fields, *Human GCIP interacts with CT847, a novel Chlamydia trachomatis type III secretion substrate, and is degraded in a tissue-culture infection model.* Cellular Microbiology, 2007. **9**(10): p. 2417-2430.

73. Ye, Z., et al., *Salmonella effector AvrA regulation of colonic epithelial cell inflammation by deubiquitination.* The American journal of pathology, 2007. **171**(3): p. 882-92.

74. Jones, R.M., et al., *Salmonella AvrA Coordinates Suppression of Host Immune and Apoptotic Defenses via JNK Pathway Blockade.* Cell host & microbe, 2008. **3**(4): p. 233-44.

75. Bakowski, M.A., et al., *The phosphoinositide phosphatase SopB manipulates membrane surface charge and trafficking of the Salmonella-containing vacuole.* Cell host & microbe, 2010. **7**(6): p. 453-62.

76. Bernal-Bayard, J. and F. Ramos-Morales, *Salmonella Type III Secretion Effector SlrP Is an E3 Ubiquitin Ligase for Mammalian Thioredoxin.* Journal of Biological Chemistry, 2009. **284**(40): p. 27587-27595.

77. Bernal-Bayard, J., E. Cardenal-Munoz, and F. Ramos-Morales, *The Salmonella type III secretion effector, salmonella leucine-rich repeat protein (SlrP), targets the human chaperone ERdj3.* The Journal of biological chemistry, 2010. **285**(21): p. 16360-8.

78. Ungewickell, A., et al., *The identification and characterization of two phosphatidylinositol-4,5-bisphosphate 4-phosphatases.* Proceedings of the National Academy of Sciences of the United States of America, 2005. **102**(52): p. 18854-18859.

79. Collier-Hyams, L.S., et al., *Cutting edge: Salmonella AvrA effector inhibits the key proinflammatory, anti-apoptotic NF-kappa B pathway.* Journal of immunology, 2002. **169**(6): p. 2846-50.

80. Orth, K., et al., *Disruption of signaling by Yersinia effector YopJ, a ubiquitin-like protein protease.* Science, 2000. **290**(5496): p. 1594-1597.

81. Mittal, R., et al., *The Acetyltransferase Activity of the Bacterial Toxin YopJ of Yersinia Is Activated by Eukaryotic Host Cell Inositol Hexakisphosphate.* Journal of Biological Chemistry, 2010. **285**(26): p. 19927-19934.

82. Le Negrate, G., et al., *Salmonella secreted factor L deubiquitinase of Salmonella typhimurium inhibits NF-kappaB, suppresses IkappaBalpha ubiquitination and modulates innate immune responses.* Journal of immunology, 2008. **180**(7): p. 5045-56.

83. Matsumoto, H. and G.M. Young, *Proteomic and functional analysis of the suite of Ysp proteins exported by the Ysa type III secretion system of Yersinia enterocolitica Biovar 1B.* Molecular Microbiology, 2006. **59**(2): p. 689-706.

84. Kim, D.W., et al., *The Shigella flexneri effector OspG interferes with innate immune responses by targeting ubiquitin-conjugating enzymes.* Proceedings of the National Academy of Sciences of the United States of America, 2005. **102**(39): p. 14046-51.

85. Arbibe, L., et al., *An injected bacterial effector targets chromatin access for transcription factor NF-kappaB to alter transcription of host genes involved in immune responses.* Nature immunology, 2007. **8**(1): p. 47-56.

86. Smith, G.K., et al., *Active-site dynamics of SpvC virulence factor from Salmonella typhimurium and density functional theory study of phosphothreonine lyase catalysis.* The journal of physical chemistry. B, 2009. **113**(46): p. 15327-33.

87. Trosky, J.E., et al., *VopA inhibits ATP binding by acetylating the catalytic loop of MAPK kinases.* Journal of Biological Chemistry, 2007. **282**(47): p. 34299-34305.

88. Newton, H.J., et al., *The type III effectors NleE and NleB from enteropathogenic E. coli and OspZ from Shigella block nuclear translocation of NF-kappaB p65.* Plos Pathogens, 2010. **6**(5): p. e1000898.

89. Yen, H., et al., *NleC, a type III secretion protease, compromises NF-kappaB activation by targeting p65/RelA.* Plos Pathogens, 2010. **6**(12): p. e1001231.

90. Nagamatsu, K., et al., *Bordetella evades the host immune system by inducing IL-10 through a type III effector, BopN.* Journal of Experimental Medicine, 2009. **206**(13): p. 3073-3088.

91. Fehr, D., et al., *AopP, a type III effector protein of Aeromonas salmonicida, inhibits the NF-kappaB signalling pathway.* Microbiology, 2006. **152**(Pt 9): p. 2809-18.

92. Reis, R.S. and F. Horn, *Enteropathogenic Escherichia coli, Samonella, Shigella and Yersinia: cellular aspects of host-bacteria interactions in enteric diseases.* Gut pathogens, 2010. **2**(1): p. 8.

93. Rzomp, K.A., A.R. Moorhead, and M.A. Scidmore, *The GTPase Rab4 interacts with Chlamydia trachomatis inclusion membrane protein CT229.* Infection and immunity, 2006. **74**(9): p. 5362-73.

94. Cortes, C., et al., *Chlamydia pneumoniae inclusion membrane protein Cpn0585 interacts with multiple Rab GTPases.* Infection and immunity, 2007. **75**(12): p. 5586-96.

95. Wang, X., et al., *Involvement of TIP60 acetyltransferase in intracellular Salmonella replication.* BMC microbiology, 2010. **10**: p. 228.

96. Hemrajani, C., et al., *NleH effectors interact with Bax inhibitor-1 to block apoptosis during enteropathogenic Escherichia coli infection.* Proceedings of the National Academy of Sciences of the United States of America, 2010. **107**(7): p. 3129-3134.

97. Martinez E, S.G., Berger CN, Lee SF, Robinson KS, Badea L, Simpson N, Hall RA, Hartland EL, Crepin VF, Frankel G., *Binding to Na(+) /H(+) exchanger regulatory factor 2 (NHERF2) affects trafficking and function of the enteropathogenic Escherichia coli type III secretion system effectors Map, EspI and NleH.* Cell Microbiol, 2010 Dec. **12**(12): p. 1718-31.

98. Nadler, C., et al., *The type III secretion effector NleE inhibits NF-kappaB activation.* Plos Pathogens, 2010. **6**(1): p. e1000743.

99. Wu, B., et al., *NleG Type 3 effectors from enterohaemorrhagic Escherichia coli are U-Box E3 ubiquitin ligases.* Plos Pathogens, 2010. **6**(6): p. e1000960.

100. Gao, X., et al., *Bacterial effector binding to ribosomal protein s3 subverts NF-kappaB function.* Plos Pathogens, 2009. **5**(12): p. e1000708.

101. Wan, F., et al., *IKKbeta phosphorylation regulates RPS3 nuclear translocation and NF-kappaB function during infection with Escherichia coli strain O157:H7.* Nature immunology, 2011. **12**(4): p. 335-43.

102. Rohde, J.R., et al., *Type III secretion effectors of the IpaH family are E3 ubiquitin ligases.* Cell host & microbe, 2007. **1**(1): p. 77-83.

103. Ashida, H., et al., *A bacterial E3 ubiquitin ligase IpaH9.8 targets NEMO/IKKgamma to dampen the host NF-kappaB-mediated inflammatory response.* Nature cell biology, 2010. **12**(1): p. 66-73; sup pp 1-9.

104. Zhu, Y.Q., et al., *Structure of a Shigella effector reveals a new class of ubiquitin ligases.* Nature structural & molecular biology, 2008. **15**(12): p. 1302-1308.

105. McPhee, J.B., P. Mena, and J.B. Bliska, *Delineation of Regions of the Yersinia YopM Protein Required for Interaction with the RSK1 and PRK2 Host Kinases and Their Requirement for Interleukin-10 Production and Virulence.* Infection and Immunity, 2010. **78**(8): p. 3529-3539.

106. Hentschke, M., et al., *Yersinia Virulence Factor YopM Induces Sustained RSK Activation by Interfering with Dephosphorylation.* PLoS One, 2010. **5**(10): p. -.

107. Tam, V.C., et al., *Functional Analysis of VopF Activity Required for Colonization in Vibrio cholerae.* Mbio, 2010. **1**(5): p. -.

108. Baruch, K., et al., *Metalloprotease type III effectors that specifically cleave JNK and NF-kappa B.* Embo Journal, 2011. **30**(1): p. 221-231.

109. Zhang, Y., et al., *The inflammation-associated Salmonella SopA is a HECT-like E3 ubiquitin ligase.* Molecular Microbiology, 2006. **62**(3): p. 786-793.

110. Braun, M., et al., *Characterization of an ADP-ribosyltransferase toxin (AexT) from Aeromonas salmonicida subsp salmonicida.* Journal of Bacteriology, 2002. **184**(7): p. 1851-1858.

111. Fehr, D., et al., *Aeromonas exoenzyme T of Aeromonas salmonicida is a bifunctional protein that targets the host cytoskeleton.* Journal of Biological Chemistry, 2007. **282**(39): p. 28843-28852.

112. Henriksson, M.L., et al., *Exoenzyme S shows selective ADP-ribosylation and GTPase-activating protein (GAP) activities towards small GTPases in vivo.* Biochemical Journal, 2002. **367**: p. 617-628.

113. Kazmierczak, B.I. and J.N. Engel, *Pseudomonas aeruginosa ExoT acts in vivo as a GTPase-activating protein for RhoA, Rac1, and Cdc42.* Infection and Immunity, 2002. **70**(4): p. 2198-2205.

114. Sierra, J.C., et al., *Unraveling the mechanism of action of a new type III secretion system effector AexU from Aeromonas hydrophila.* Microbial Pathogenesis, 2010. **49**(3): p. 122-34.

115. Vlahou, G., et al., *Yersinia outer protein YopE affects the actin cytoskeleton in Dictyostelium discoideum through targeting of multiple Rho family GTPases.* Bmc Microbiology, 2009. **9**: p. -.

116. Shao, F. and J.E. Dixon, *YopT is a cysteine protease cleaving Rho family GTPases.* Genus Yersinia: Entering the Functional Genomic Era, 2003. **529**: p. 79-84.

117. Kodama, T., et al., *Identification and characterization of VopT, a novel ADP-ribosyltransferase effector protein secreted via the Vibrio parahaemolyticus type III secretion system 2.* Cellular Microbiology, 2007. **9**(11): p. 2598-2609.

118. Tezcan-Merdol, D., L. Engstrand, and M. Rhen, *Salmonella enterica SpvB-mediated ADP-ribosylation as an activator for host cell actin degradation.* International Journal of Medical Microbiology, 2005. **295**(4): p. 201-212.

119. Yarbrough, M.L., et al., *AMPylation of Rho GTPases by Vibrio VopS Disrupts Effector Binding and Downstream Signaling.* Science, 2009. **323**(5911): p. 269-272.

120. Broberg, C.A., et al., *A Vibrio Effector Protein Is an Inositol Phosphatase and Disrupts Host Cell Membrane Integrity.* Science, 2010. **329**(5999): p. 1660-1662.

121. Stenner-Liewen, F., et al., *CADD, a Chlamydia protein that interacts with death receptors.* Journal of Biological Chemistry, 2002. **277**(12): p. 9633-9636.

122. Burdette, D.L., J. Seemann, and K. Orth, *Vibrio VopQ induces PI3-kinase-independent autophagy and antagonizes phagocytosis.* Molecular Microbiology, 2009. **73**(4): p. 639-649.

123. French, C.T., et al., *The Bordetella type III secretion system effector BteA contains a conserved N-terminal motif that guides bacterial virulence factors to lipid rafts.* Cellular Microbiology, 2009. **11**(12): p. 1735-1749.

124. Kuwae, A., et al., *BopC is a novel type III effector secreted by Bordetella bronchiseptica and has a critical role in type III-dependent necrotic cell death.* Journal of Biological Chemistry, 2006. **281**(10): p. 6589-6600.

125. Kim, M., et al., *Bacterial interactions with the host epithelium.* Cell host & microbe, 2010. **8**(1): p. 20-35.

126. Peralta-Ramirez, J., et al., *EspF interacts with nucleation-promoting factors to recruit junctional proteins into pedestals for pedestal maturation and*

disruption of paracellular permeability. Infection and Immunity, 2008. **76**(9): p. 3854-3868.

127. Hodges, K., et al., *The enteropathogenic Escherichia coli effector protein EspF decreases sodium hydrogen exchanger 3 activity.* Cellular microbiology, 2008. **10**(8): p. 1735-45.

128. Marches, O., et al., *EspF of enteropathogenic Escherichia coli binds sorting nexin 9.* Journal of bacteriology, 2006. **188**(8): p. 3110-5.

129. Guttman, J.A., et al., *Attaching and effacing pathogen-induced tight junction disruption in vivo.* Cellular microbiology, 2006. **8**(4): p. 634-45.

130. Nougayrede, J.P. and M.S. Donnenberg, *Enteropathogenic Escherichia coli EspF is targeted to mitochondria and is required to initiate the mitochondrial death pathway.* Cellular Microbiology, 2004. **6**(11): p. 1097-1111.

131. Holmes, A., et al., *The EspF Effector, a Bacterial Pathogen's Swiss Army Knife.* Infection and Immunity, 2010. **78**(11): p. 4445-4453.

132. Thanabalasuriar, A., et al., *The bacterial virulence factor NleA is required for the disruption of intestinal tight junctions by enteropathogenic Escherichia coli.* Cellular Microbiology, 2010. **12**(1): p. 31-41.

133. Lee, S.F., et al., *A C-terminal class I PDZ binding motif of EspI/NleA modulates the virulence of attaching and effacing Escherichia coli and Citrobacter rodentium.* Cellular microbiology, 2008. **10**(2): p. 499-513.

134. Kim, J., et al., *The bacterial virulence factor NleA inhibits cellular protein secretion by disrupting mammalian COPII function.* Cell host & microbe, 2007. **2**(3): p. 160-171.

135. Lizumi, Y., et al., *The enteropathogenic E-coli effector EspB facilitates microvillus effacing and antiphagocytosis by inhibiting myosin function.* Cell host & microbe, 2007. **2**(6): p. 383-392.

136. Puthenedam, M., et al., *Modulation of tight junction barrier function by outer membrane proteins of enteropathogenic Escherichia coli: Role of F-actin and junctional adhesion molecule-1.* Cell Biology International, 2007. **31**(8): p. 836-844.

137. Knappstein, S., et al., *alpha(1)-antitrypsin binds to and interferes with functionality of EspB from atypical and typical enteropathogenic Escherichia coli strains.* Infection and Immunity, 2004. **72**(8): p. 4344-4350.

138. Levin, I., et al., *Identification of an unconventional E3 binding surface on the UbcH5 similar to Ub conjugate recognized by a pathogenic bacterial E3 ligase.* Proceedings of the National Academy of Sciences of the United States of America, 2010. **107**(7): p. 2848-2853.

139. Broberg, C.A., *A Vibrio effector protein is an inositol phosphatase and disrupts host cell membrane integrity (September, pg 1660, 2010).* Science, 2011. **331**(6013): p. -.

140. Yahr, T.L., et al., *ExoY, an adenylate cyclase secreted by the Pseudomonas aeruginosa type III system.* Proceedings of the National Academy of Sciences of the United States of America, 1998. **95**(23): p. 13899-13904.

141. Kotloff, K.L., J.P. Winickoff, B. Ivanoff, J.D. Clemens, D.L. Swerdlow, P.J. Sansonetti, G.K. Adak, M.M. Levine, *Global burden of Shigella infections: implications for vaccine develompment and implementation of control strategies*, in *Bulletin W.H.O.*1999. p. 651-666.

142. DuPont, H.L., et al., *Inoculum size in shigellosis and implications for expected mode of transmission.* J Infect Dis, 1989. **159**(6): p. 1126-8.

143. van den Broek, J.M., et al., *Risk factors for mortality due to shigellosis: a case-control study among severely-malnourished children in Bangladesh.* J Health Popul Nutr, 2005. **23**(3): p. 259-65.

144. Flores, A., M. Araque, and L. Vizcaya, *Multiresistant Shigella species isolated from pediatric patients with acute diarrheal disease.* The American journal of the medical sciences, 1998. **316**(6): p. 379-84.

145. Sansonetti, P.J., et al., *Infection of rabbit Peyer's patches by Shigella flexneri: effect of adhesive or invasive bacterial phenotypes on follicle-associated epithelium.* Infect Immun, 1996. **64**(7): p. 2752-64.

146. Wassef, J.S., D.F. Keren, and J.L. Mailloux, *Role of M cells in initial antigen uptake and in ulcer formation in the rabbit intestinal loop model of shigellosis.* Infect Immun, 1989. **57**(3): p. 858-63.

147. Schroeder, G.N. and H. Hilbi, *Molecular pathogenesis of Shigella spp.: controlling host cell signaling, invasion, and death by type III secretion.* Clin Microbiol Rev, 2008. **21**(1): p. 134-56.

148. Mounier, J., et al., *Shigella flexneri enters human colonic Caco-2 epithelial cells through the basolateral pole.* Infect Immun, 1992. **60**(1): p. 237-48.

149. Zychlinsky, A., et al., *In vivo apoptosis in Shigella flexneri infections.* Infect Immun, 1996. **64**(12): p. 5357-65.

150. Zychlinsky, A., M.C. Prevost, and P.J. Sansonetti, *Shigella flexneri induces apoptosis in infected macrophages.* Nature, 1992. **358**(6382): p. 167-9.

151. Fernandez-Prada, C.M., et al., *Shigella flexneri IpaH(7.8) facilitates escape of virulent bacteria from the endocytic vacuoles of mouse and human macrophages.* Infection and Immunity, 2000. **68**(6): p. 3608-3619.

152. Mounier, J., et al., *The IpaC Carboxyterminal Effector Domain Mediates Src-Dependent Actin Polymerization during Shigella Invasion of Epithelial Cells.* Plos Pathogens, 2009. **5**(1): p. -.

153. Sansonetti, P.J., et al., *Caspase-1 activation of IL-1beta and IL-18 are essential for Shigella flexneri-induced inflammation.* Immunity, 2000. **12**(5): p. 581-90.

154. Cornelis, G.R., *The type III secretion injectisome.* Nat Rev Microbiol, 2006. **4**(11): p. 811-25.

155. Watarai, M., S. Funato, and C. Sasakawa, *Interaction of ipa proteins of Shigella flexneri with alpha(5)beta(1) integrin promotes entry of the bacteria into mammalian cells.* Journal of Experimental Medicine, 1996. **183**(3): p. 991-999.

156. Skoudy, A., et al., *CD44 binds to the Shigella IpaB protein and participates in bacterial invasion of epithelial cells.* Cellular Microbiology, 2000. **2**(1): p. 19-33.

157. Yoshida, S., et al., *Shigella deliver an effector protein to trigger host microtubule destabilization, which promotes Rac1 activity and efficient bacterial internalization.* The EMBO journal, 2002. **21**(12): p. 2923-35.

158. Yoshida, S., et al., *Microtubule-severing activity of Shigella is pivotal for intercellular spreading.* Science, 2006. **314**(5801): p. 985-9.

159. Germane, K.L., et al., *Structural and functional studies indicate that Shigella VirA is not a protease and does not directly destabilize microtubules.* Biochemistry, 2008. **47**(39): p. 10241-3.

160. Davis, J., et al., *Novel fold of VirA, a type III secretion system effector protein from Shigella flexneri.* Protein Sci, 2008. **17**(12): p. 2167-73.

161. De Geyter, C., et al., *Characterization of the interaction of IpaB and IpaD, proteins required for entry of Shigella flexneri into epithelial cells, with a lipid membrane.* European Journal of Biochemistry, 2000. **267**(18): p. 5769-5776.

162. Sansonetti, P.J., et al., *Multiplication of Shigella flexneri within HeLa cells: lysis of the phagocytic vacuole and plasmid-mediated contact hemolysis.* Infect Immun, 1986. **51**(2): p. 461-9.

163. Bernardini, M.L., et al., *Identification of icsA, a plasmid locus of Shigella flexneri that governs bacterial intra- and intercellular spread through interaction with F-actin.* Proc Natl Acad Sci U S A, 1989. **86**(10): p. 3867-71.

164. Monack, D.M. and J.A. Theriot, *Actin-based motility is sufficient for bacterial membrane protrusion formation and host cell uptake.* Cell Microbiol, 2001. **3**(9): p. 633-47.

165. Hale, T.L., *Genetic basis of virulence in Shigella species.* Microbiological reviews, 1991. **55**(2): p. 206-24.

166. Parsot, C., *Shigella flexneri: genetics of entry and intercellular dissemination in epithelial cells.* Current topics in microbiology and immunology, 1994. **192**: p. 217-41.

167. Buchrieser, C., et al., *The virulence plasmid pWR100 and the repertoire of proteins secreted by the type III secretion apparatus of Shigella flexneri.* Molecular microbiology, 2000. **38**(4): p. 760-71.

168. Jiang, Y., et al., *The complete sequence and analysis of the large virulence plasmid pSS of Shigella sonnei.* Plasmid, 2005. **54**(2): p. 149-59.

169. Venkatesan, M.M., et al., *Complete DNA sequence and analysis of the large virulence plasmid of Shigella flexneri.* Infection and immunity, 2001. **69**(5): p. 3271-85.

170. Yang, F., et al., *Genome dynamics and diversity of Shigella species, the etiologic agents of bacillary dysentery.* Nucleic acids research, 2005. **33**(19): p. 6445-58.

171. Kane, C.D., et al., *MxiE regulates intracellular expression of factors secreted by the Shigella flexneri 2a type III secretion system.* Journal of bacteriology, 2002. **184**(16): p. 4409-19.

172. Le Gall, T., et al., *Analysis of virulence plasmid gene expression defines three classes of effectors in the type III secretion system of Shigella flexneri.* Microbiology, 2005. **151**(Pt 3): p. 951-62.

173. Parsot, C., *Shigella type III secretion effectors: how, where, when, for what purposes?* Current opinion in microbiology, 2009. **12**(1): p. 110-6.

174. LaBrec, E.H., H. Schneider, T. J. Magnani, and S. B. Formal, *Epithelial cel penetration as an essential step in the pathogenesis of bacillary dysentery.* J.Bacteriol., 1964. **88**: p. 1503-1518.

175. Nataro, J.P. and J.B. Kaper, *Diarrheagenic Escherichia coli.* Clinical microbiology reviews, 1998. **11**(1): p. 142-201.

176. Robins-Browne, R.M. and E.L. Hartland, *Escherichia coli as a cause of diarrhea.* Journal of gastroenterology and hepatology, 2002. **17**(4): p. 467-75.

177. Frankel, G., et al., *Enteropathogenic and enterohaemorrhagic Escherichia coli: more subversive elements.* Molecular microbiology, 1998. **30**(5): p. 911-21.

178. Bray, *Isolation of antigenically homogeneous strains of Bact. coli neapolitanum from summer diarrhoea of infants.* J. pathol. bacteriol. , 1945. **57**: p. 239-247.

179. Giles C., S.G., and Smith J. , *Epidemic gastroenteritis of infants in Aberdeen during 1947.* Arch. Dis. Child., 1949. **24**: p. 45-53.

180. Taylor, j., Powell, B.W., Wright, J. , *Infantile diarrhea and vomiting: a clinical and bacteriological investigation.* Br. Med. J., 1949. **2**: p. 117-141.

181. Senerwa, D., et al., *Enteropathogenic Escherichia-Coli Serotype O111-Hnt Isolated from Preterm Neonates in Nairobi, Kenya.* Journal of Clinical Microbiology, 1989. **27**(6): p. 1307-1311.

182. Gomes, T.A.T., Rassi, V., Macdonald, K.L., Ramos, S.R.T.S., Trabulsi, L.R., Vieira, M.A.M., Guth, B.E.C., Candeias, J.A.N., Ivey, C., Toledo, M.R.F. and Blake, P.A., *Enteropathogens associated with acute diarrhoeal disease in urban infants in Sao Paulo, Brazil.* Journal of infectious disease, 1991. **164**: p. 331-337.

183. Cravioto, A., et al., *Prospective study of diarrhoeal disease in a cohort of rural Mexican children: incidence and isolated pathogens during the first two years of life.* Epidemiology and infection, 1988. **101**(1): p. 123-34.

184. Cravioto, A., Reyes, R.E., Trujillo, F., Uribe, F., Navarro, A., de la Roca, J.M., Hernandez, J.M., Perez, G. and Vazquez, V., *Risk of diarrhoea during the first year of life associated with initial and subsequent colonization by specific enteropathogens.* Am. J. Epidemiol., 1990. **131**: p. 886-904.

185. Cravioto, A., et al., *Enteropathogenic Escherichia coli: The Mexican experience.* Revista De Microbiologia, 1996. **27**: p. 21-24.

186. Robinsbrowne, R.M., et al., *Failure to Detect Conventional Enterotoxins in Classical Enteropathogenic (Serotyped) Escherichia-Coli Strains of Proven Pathogenicity.* Infection and Immunity, 1982. **38**(2): p. 798-801.

187. Levine, M.M., *Escherichia-Coli That Cause Diarrhea - Enterotoxigenic, Enteropathogenic, Enteroinvasive, Enterohemorrhagic, and Enteroadherent.* Journal of Infectious Diseases, 1987. **155**(3): p. 377-389.

188. Rowe, B., *Role of Escherichia-Coli in Gastroenteritis.* Clinics in Gastroenterology, 1979. **8**(3): p. 625-644.

189. Albert, M.J., *Epidemiology of enteropathogenic Escher- ichia coli infection in Bangladesh.* Rev. Microbiol., 1996. **Sa˜o Paulo 27**((suppl.1)): p. 17-20.

190. Robins-Browne, R.M., *Traditional enteropathogenic Escherichia coli of infantile diarrhea.* Reviews of infectious diseases, 1987. **9**(1): p. 28-53.

191. McDaniel, T.K., Jarvis, K.G., Donnenberg, M.S. and Kaper, J.B., *A genetic locus of enterocyte effacement conserved among diverse enterobacterial pathogens.* Proc. Natl. Acad. Scie, 1995. **92**: p. 1664-1668.

192. McDaniel, T.K. and J.B. Kaper, *A cloned pathogenicity island from enteropathogenic Escherichia coli confers the attaching and effacing phenotype on E. coli K-12.* Molecular microbiology, 1997. **23**(2): p. 399-407.

193. Wong, A.R., et al., *Enteropathogenic and enterohaemorrhagic Escherichia coli: even more subversive elements.* Molecular microbiology, 2011. **80**(6): p. 1420-38.

194. Donnenberg, M.S., *Interactions between Enteropathogenic Escherichia coli and Epithelial Cells.* Clinical Infectious Diseases, 1999. **28**(3): p. 451-455.

195. Warawa, J., B.B. Finlay, and B. Kenny, *Type III secretion-dependent hemolytic activity of enteropathogenic Escherichia coli.* Infection and immunity, 1999. **67**(10): p. 5538-40.

196. Donnenberg, M.S. and J.B. Kaper, *Enteropathogenic Escherichia coli.* Infection and immunity, 1992. **60**(10): p. 3953-61.

197. Khan, M.A., et al., *Flagellin-dependent and -independent inflammatory responses following infection by enteropathogenic Escherichia coli and Citrobacter rodentium.* Infection and immunity, 2008. **76**(4): p. 1410-22.

198. Schuller, S., et al., *The ex vivo response of human intestinal mucosa to enteropathogenic Escherichia coli infection.* Cellular microbiology, 2009. **11**(3): p. 521-30.

199. Iizumi, Y., et al., *The enteropathogenic E. coli effector EspB facilitates microvillus effacing and antiphagocytosis by inhibiting myosin function.* Cell host & microbe, 2007. **2**(6): p. 383-92.

200. Holmes, A., et al., *The EspF effector, a bacterial pathogen's Swiss army knife.* Infection and immunity, 2010. **78**(11): p. 4445-53.

201. Marches, O., et al., *EspJ of enteropathogenic and enterohaemorrhagic Escherichia coli inhibits opsono-phagocytosis.* Cellular microbiology, 2008. **10**(5): p. 1104-15.

202. Salazar-Gonzalez, H. and F. Navarro-Garcia, *Intimate adherence by enteropathogenic Escherichia coli modulates TLR5 localization and proinflammatory host response in intestinal epithelial cells.* Scandinavian journal of immunology, 2011. **73**(4): p. 268-83.

203. Pearson, J.S., et al., *A type III effector protease NleC from enteropathogenic Escherichia coli targets NF-kappaB for degradation.* Molecular microbiology, 2011. **80**(1): p. 219-30.

204. Schonthaler, H.B., J. Guinea-Viniegra, and E.F. Wagner, *Targeting inflammation by modulating the Jun/AP-1 pathway.* Annals of the rheumatic diseases, 2011. **70 Suppl 1**: p. i109-12.

205. Matsuzawa, T., et al., *Enteropathogenic Escherichia coli activates the RhoA signaling pathway via the stimulation of GEF-H1.* EMBO J, 2004. **23**(17): p. 3570-82.

206. Elliott, S.J., et al., *EspG, a novel type III system-secreted protein from enteropathogenic Escherichia coli with similarities to VirA of Shigella flexneri.* Infect Immun, 2001. **69**(6): p. 4027-33.

207. Uchiya, K., et al., *Identification of a novel virulence gene, virA, on the large plasmid of Shigella, involved in invasion and intercellular spreading.* Mol Microbiol, 1995. **17**(2): p. 241-50.

208. Mavris, M., P.J. Sansonetti, and C. Parsot, *Identification of the cis-acting site involved in activation of promoters regulated by activity of the type III secretion apparatus in Shigella flexneri.* J Bacteriol, 2002. **184**(24): p. 6751-9.

209. Demers, B., P.J. Sansonetti, and C. Parsot, *Induction of type III secretion in Shigella flexneri is associated with differential control of transcription of genes encoding secreted proteins.* Embo Journal, 1998. **17**(10): p. 2894-2903.

210. Germane, K.L., et al., *Structural and Functional Studies Indicate That Shigella VirA Is Not a Protease and Does Not Directly Destabilize Microtubules.* Biochemistry, 2008.

211. Shaw, R.K., et al., *Enteropathogenic Escherichia coli type III effectors EspG and EspG2 disrupt the microtubule network of intestinal epithelial cells.* Infect Immun, 2005. **73**(7): p. 4385-90.

212. Smollett, K., et al., *Function and distribution of EspG2, a type III secretion system effector of enteropathogenic Escherichia coli.* Microbes Infect, 2006. **8**(8): p. 2220-7.

213. Hardwidge, P.R., et al., *Modulation of host cytoskeleton function by the enteropathogenic Escherichia coli and Citrobacter rodentium effector protein EspG.* Infect Immun, 2005. **73**(5): p. 2586-94.

214. Campellone, K.G. and J.M. Leong, *Tails of two Tirs: actin pedestal formation by enteropathogenic E. coli and enterohemorrhagic E. coli O157:H7.* Curr Opin Microbiol, 2003. **6**(1): p. 82-90.

215. Tomson, F.L., et al., *Enteropathogenic Escherichia coli EspG disrupts microtubules and in conjunction with Orf3 enhances perturbation of the tight junction barrier.* Mol Microbiol, 2005. **56**(2): p. 447-64.

216. Van Duyne, G.D., et al., *Atomic structures of the human immunophilin FKBP-12 complexes with FK506 and rapamycin.* Journal of molecular biology, 1993. **229**(1): p. 105-24.

217. Elsinghorst, E.A., *Measurement of invasion by gentamicin resistance.* Methods in enzymology, 1994. **236**: p. 405-20.

218. Leung, Y., S. Ally, and M.B. Goldberg, *Bacterial actin assembly requires toca-1 to relieve N-wasp autoinhibition.* Cell host & microbe, 2008. **3**(1): p. 39-47.

219. Hyman, A., et al., *Preparation of modified tubulins.* Methods in enzymology, 1991. **196**: p. 478-85.

220. Varga, V., et al., *Yeast kinesin-8 depolymerizes microtubules in a length-dependent manner.* Nature cell biology, 2006. **8**(9): p. 957-62.

221. Belmont, L.D. and T.J. Mitchison, *Identification of a protein that interacts with tubulin dimers and increases the catastrophe rate of microtubules.* Cell, 1996. **84**(4): p. 623-31.

222. Desai, A., et al., *Kin I kinesins are microtubule-destabilizing enzymes.* Cell, 1999. **96**(1): p. 69-78.

223. Sawin, K.E. and T.J. Mitchison, *Poleward microtubule flux mitotic spindles assembled in vitro.* The Journal of cell biology, 1991. **112**(5): p. 941-54.

224. Sawin, K.E. and T.J. Mitchison, *Mitotic spindle assembly by two different pathways in vitro.* The Journal of cell biology, 1991. **112**(5): p. 925-40.

225. Otwinowski, Z.a.M., W. , *Processing of X-ray Diffraction Data Collected in Oscillation Mode.* Methods in Enzymology, 1997(267A): p. 307-326.

226. Sheldrick, G.M., *A short history of SHELX.* Acta crystallographica. Section A, Foundations of crystallography, 2008. **64**(Pt 1): p. 112-22.

227. Vonrhein, C., et al., *Automated structure solution with autoSHARP.* Methods in molecular biology, 2007. **364**: p. 215-30.

228. Abrahams JP, L.A., *Methods used in the structure determination of bovine mitochondrial F1 ATPase.* Acta Crystallogr D Biol Crystallogr., 1996. **52**(Pt 1): p. 30-42.

229. Jones, T.A., et al., *Improved methods for building protein models in electron density maps and the location of errors in these models.* Acta crystallographica. Section A, Foundations of crystallography, 1991. **47 (Pt 2)**: p. 110-9.

230. Emsley, P. and K. Cowtan, *Coot: model-building tools for molecular graphics.* Acta crystallographica. Section D, Biological crystallography, 2004. **60**(Pt 12 Pt 1): p. 2126-32.

231. Brunger, A.T., et al., *Crystallography & NMR system: A new software suite for macromolecular structure determination.* Acta crystallographica. Section D, Biological crystallography, 1998. **54**(Pt 5): p. 905-21.

232. Adams, P.D., et al., *PHENIX: building new software for automated crystallographic structure determination.* Acta crystallographica. Section D, Biological crystallography, 2002. **58**(Pt 11): p. 1948-54.

233. Painter, J. and E.A. Merritt, *A molecular viewer for the analysis of TLS rigid-body motion in macromolecules.* Acta crystallographica. Section D, Biological crystallography, 2005. **61**(Pt 4): p. 465-71.

234. Painter, J. and E.A. Merritt, *Optimal description of a protein structure in terms of multiple groups undergoing TLS motion.* Acta crystallographica. Section D, Biological crystallography, 2006. **62**(Pt 4): p. 439-50.

235. Novotny, M., D. Madsen, and G.J. Kleywegt, *Evaluation of protein fold comparison servers.* Proteins, 2004. **54**(2): p. 260-70.

236. Krissinel, E.B., et al., *The new CCP4 Coordinate Library as a toolkit for the design of coordinate-related applications in protein crystallography.* Acta crystallographica. Section D, Biological crystallography, 2004. **60**(Pt 12 Pt 1): p. 2250-5.

237. Gibrat, J.F., T. Madej, and S.H. Bryant, *Surprising similarities in structure comparison.* Current opinion in structural biology, 1996. **6**(3): p. 377-85.

238. Madej, T., J.F. Gibrat, and S.H. Bryant, *Threading a database of protein cores.* Proteins, 1995. **23**(3): p. 356-69.

239. DeLano, W.L., 2002.

240. Thompson, J.D., D.G. Higgins, and T.J. Gibson, *CLUSTAL W: improving the sensitivity of progressive multiple sequence alignment through sequence weighting, position-specific gap penalties and weight matrix choice.* Nucleic acids research, 1994. **22**(22): p. 4673-80.

241. Gouet, P., et al., *ESPript: analysis of multiple sequence alignments in PostScript.* Bioinformatics, 1999. **15**(4): p. 305-8.

242. Bond, C., *TopDraw: a sketchpad for protein structure topology cartoons.* Bioinformatics. , 2003. **19**(2): p. 311-2.

243. Panchenko, A.R. and S.H. Bryant, *A comparison of position-specific score matrices based on sequence and structure alignments.* Protein science : a publication of the Protein Society, 2002. **11**(2): p. 361-70.

244. Holm, L. and C. Sander, *Mapping the protein universe.* Science, 1996. **273**(5275): p. 595-603.

245. Malet, H., et al., *Crystal structure of the RNA polymerase domain of the West Nile virus non-structural protein 5.* The Journal of biological chemistry, 2007. **282**(14): p. 10678-89.

246. Richardson, J.S., *The anatomy and taxonomy of protein structure.* Advances in protein chemistry, 1981. **34**: p. 167-339.

247. Murzin, A.G., et al., *SCOP: a structural classification of proteins database for the investigation of sequences and structures.* Journal of molecular biology, 1995. **247**(4): p. 536-40.

248. Donnenberg, M.S., J.B. Kaper, and B.B. Finlay, *Interactions between enteropathogenic Escherichia coli and host epithelial cells.* Trends Microbiol, 1997. **5**(3): p. 109-14.

249. Benard, V. and G.M. Bokoch, *Assay of Cdc42, Rac, and Rho GTPase activation by affinity methods.* Methods in enzymology, 2002. **345**: p. 349-59.

250. Ashkenazy, H., et al., *ConSurf 2010: calculating evolutionary conservation in sequence and structure of proteins and nucleic acids.* Nucleic acids research, 2010. **38**(Web Server issue): p. W529-33.

251. Ghosh, P., *Process of protein transport by the type III secretion system.* Microbiol Mol Biol Rev, 2004. **68**(4): p. 771-95.

252. Rice, L.M., T.N. Earnest, and A.T. Brunger, *Single-wavelength anomalous diffraction phasing revisited.* Acta Crystallogr D Biol Crystallogr, 2000. **56**(Pt 11): p. 1413-20.

253. Armstrong, D.S., et al., *Detection of a widespread clone of Pseudomonas aeruginosa in a pediatric cystic fibrosis clinic.* American journal of respiratory and critical care medicine, 2002. **166**(7): p. 983-7.

254. Ladwein, M. and K. Rottner, *On the Rho'd: the regulation of membrane protrusions by Rho-GTPases.* FEBS Lett, 2008. **582**(14): p. 2066-74.

255. Yoshida, S., et al., *Shigella deliver an effector protein to trigger host microtubule destabilization, which promotes Rac1 activity and efficient bacterial internalization.* EMBO J, 2002. **21**(12): p. 2923-35.

256. Benard, V. and G.M. Bokoch, *Assay of Cdc42, Rac, and Rho GTPase activation by affinity methods.* Methods Enzymol, 2002. **345**: p. 349-59.

257. Ren, X.D., W.B. Kiosses, and M.A. Schwartz, *Regulation of the small GTP-binding protein Rho by cell adhesion and the cytoskeleton.* EMBO J, 1999. **18**(3): p. 578-85.

258. Lei, M., et al., *Structure of PAK1 in an autoinhibited conformation reveals a multistage activation switch.* Cell, 2000. **102**(3): p. 387-97.

259. Nolen, B., S. Taylor, and G. Ghosh, *Regulation of protein kinases; controlling activity through activation segment conformation.* Mol Cell, 2004. **15**(5): p. 661-75.

260. Sells, M.A., et al., *Human p21-activated kinase (Pak1) regulates actin organization in mammalian cells.* Curr Biol, 1997. **7**(3): p. 202-10.

261. Manser, E., et al., *Expression of constitutively active alpha-PAK reveals effects of the kinase on actin and focal complexes.* Mol Cell Biol, 1997. **17**(3): p. 1129-43.

262. Dummler, B., et al., *Pak protein kinases and their role in cancer.* Cancer and Metastasis Reviews, 2009. **28**(1-2): p. 51-63.

263. Ben-Ami, G., et al., *Agents that inhibit Rho, Rac, and Cdc42 do not block formation of actin pedestals in HeLa cells infected with enteropathogenic Escherichia coli.* Infect Immun, 1998. **66**(4): p. 1755-8.

264. Demers, B., P.J. Sansonetti, and C. Parsot, *Induction of type III secretion in Shigella flexneri is associated with differential control of transcription of genes encoding secreted proteins.* EMBO J, 1998. **17**(10): p. 2894-903.

265. Oaks, E.V., M.E. Wingfield, and S.B. Formal, *Plaque formation by virulent Shigella flexneri.* Infection and immunity, 1985. **48**(1): p. 124-9.

266. Skoudy, A., et al., *A functional role for ezrin during Shigella flexneri entry into epithelial cells.* Journal of Cell Science, 1999. **112**(13): p. 2059-2068.

267. Simonovic, I., et al., *Enteropathogenic Escherichia coli activates ezrin, which participates in disruption of tight junction barrier function.* Infection and Immunity, 2001. **69**(9): p. 5679-5688.

268. Gould, K.L., et al., *Cdna Cloning and Sequencing of the Protein-Tyrosine Kinase Substrate, Ezrin, Reveals Homology to Band-4.1.* Embo Journal, 1989. **8**(13): p. 4133-4142.

269. Bretscher, A., K. Edwards, and R.G. Fehon, *ERM proteins and merlin: Integrators at the cell cortex.* Nature Reviews Molecular Cell Biology, 2002. **3**(8): p. 586-599.

270. Ivetic, A. and A.J. Ridley, *Ezrin/radixin/moesin proteins and Rho GTPase signalling in leucocytes.* Immunology, 2004. **112**(2): p. 165-176.

271. Loebrich, S., et al., *Activated radixin is essential for GABA(A) receptor alpha 5 subunit anchoring at the actin cytoskeleton.* Embo Journal, 2006. **25**(5): p. 987-999.

272. Forte, J.G., et al., *Comparative study of ezrin phosphorylation among different tissues: more is good; too much is bad.* American Journal of Physiology-Cell Physiology, 2008. **295**(1): p. C192-C202.

273. Forte, J.G., et al., *High turnover of ezrin T567 phosphorylation: conformation, activity, and cellular function.* American Journal of Physiology-Cell Physiology, 2007. **293**(3): p. C874-C884.

274. Yonemura, S., T. Matsui, and S. Tsukita, *Rho-dependent and -independent activation mechanisms of ezrin/radixin/moesin proteins: an essential role for polyphosphoinositides in vivo.* Journal of Cell Science, 2002. **115**(12): p. 2569-2580.

275. Niggli, V., et al., *Identification of a Phosphatidylinositol-4,5-Bisphosphate-Binding Domain in the N-Terminal Region of Ezrin.* Febs Letters, 1995. **376**(3): p. 172-176.

276. Algrain, M., et al., *Ezrin Contains Cytoskeleton and Membrane-Binding Domains Accounting for Its Proposed Role as a Membrane-Cytoskeletal Linker.* Journal of Cell Biology, 1993. **120**(1): p. 129-139.

277. Bretscher, A., *Rapid Phosphorylation and Reorganization of Ezrin and Spectrin Accompany Morphological-Changes Induced in a-431 Cells by Epidermal Growth-Factor.* Journal of Cell Biology, 1989. **108**(3): p. 921-930.

278. Hanzel, D.K., et al., *Immunological Localization of an 80-Kda Phosphoprotein to the Apical Membrane of Gastric Parietal-Cells.* American Journal of Physiology, 1989. **256**(6): p. G1082-G1089.

279. Thuillier, L., et al., *Ligation of Cd4 Surface-Antigen Induces Rapid Tyrosine Phosphorylation of the Cytoskeletal Protein Ezrin.* Cellular Immunology, 1994. **156**(2): p. 322-331.

280. Gary, R. and A. Bretscher, *Ezrin Self-Association Involves Binding of an N-Terminal Domain to a Normally Masked C-Terminal Domain That Includes the F-Actin Binding-Site.* Molecular biology of the cell, 1995. **6**(8): p. 1061-1075.

281. Turunen, O., T. Wahlstrom, and A. Vaheri, *Ezrin Has a Cooh-Terminal Actin-Binding Site That Is Conserved in the Ezrin Protein Family.* Journal of Cell Biology, 1994. **126**(6): p. 1445-1453.

282. Pearson, M.A., et al., *Structure of the ERM protein moesin reveals the FERM domain fold masked by an extended actin binding tail domain.* Cell, 2000. **101**(3): p. 259-70.

283. Gautreau, A., D. Louvard, and M. Arpin, *Morphogenic effects of ezrin require a phosphorylation-induced transition from oligomers to monomers at the plasma membrane.* Journal of Cell Biology, 2000. **150**(1): p. 193-203.

284. Zhou, R.H., et al., *Phosphorylation of ezrin on threonine 567 produces a change in secretory phenotype and repolarizes the gastric parietal cell.* Journal of Cell Science, 2005. **118**(19): p. 4381-4391.

285. Kotloff, K.L., et al., *Global burden of Shigella infections: implications for vaccine development and implementation of control strategies.* Bulletin of the World Health Organization, 1999. **77**(8): p. 651-666.

286. DuPont HL, L.M., Hornick RB and . Formal SB, *Inoculum size in shigellosis and implications for expected mode of transmission.* The Journal of Infectious Diseases 1989. **159**(6): p. 1126-8.

287. Nataro, J.P. and J.B. Kaper, *Diarrheagenic Escherichia coli.* Clin Microbiol Rev, 1998. **11**(1): p. 142-201.

288. Campellone, K.G. and J.M. Leong, *Tails of two Tirs: actin pedestal formation by enteropathogenic E-coli and enterohemorrhagic E-coli O157 : H7.* Current Opinion in Microbiology, 2003. **6**(1): p. 82-90.

289. Clements, A., et al., *EspG of enteropathogenic and enterohemorrhagic E. coli binds the Golgi matrix protein GM130 and disrupts the Golgi structure and function.* Cellular microbiology, 2011.

290. Radhakrishna, H., et al., *ARF6 requirement for Rac ruffling suggests a role for membrane trafficking in cortical actin rearrangements.* Journal of Cell Science, 1999. **112 (Pt 6)**: p. 855-66.

291. Hiroyama, M. and J.H. Exton, *Studies of the roles of ADP-ribosylation factors and phospholipase D in phorbol ester-induced membrane ruffling.* Journal of cellular physiology, 2005. **202**(2): p. 608-22.